2012-04-26

Mangroves on the Move: Predictions of Storm Surge Effects on Coastal Vegetation

Jiang Jiang
University of Miami, jjiang@bio.miami.edu

UNIVERSITY OF MIAMI

MANGROVES ON THE MOVE: PREDICTIONS OF STORM SURGE EFFECTS ON COASTAL VEGETATION

By

Jiang Jiang

A DISSERTATION

Submitted to the Faculty
of the University of Miami
in partial fulfillment of the requirements for
the degree of Doctor of Philosophy

Coral Gables, Florida

May 2012

UNIVERSITY OF MIAMI

A dissertation submitted in partial fulfillment of
the requirements for the degree of
Doctor of Philosophy

MANGROVES ON THE MOVE: PREDICTIONS OF STORM SURGE EFFECTS ON COASTAL VEGETATION

Jiang Jiang

Approved:

_____ Donald DeAngelis, Ph.D. Professor of Biology	_____ Terri A. Scandura, Ph.D. Dean of the Graduate School
_____ Leonel Sternberg, Ph.D. Professor of Biology	_____ Carol Horvitz, Ph.D. Professor of Biology
_____ Shigui Ruan, Ph.D. Professor of Mathematics	_____ Fernando Miralles-Wilhelm, Ph.D. Professor of Earth and Environment Florida International University

JIANG, JIANG (Ph.D., Biology)

Mangroves on the Move: Predictions of Storm Surge Effects on Coastal Vegetation (May 2012)

Abstract of a dissertation at the University of Miami.

Dissertation supervised by Professor Donald DeAngelis.
No. of pages in text. (133)

The landward coastal zones of the low-lying habitats are characterized by sharp ecotones between salinity-tolerant (halophytic) vegetation types, such as mangroves, and salinity-intolerant (glycophytic) vegetation types, such as freshwater marsh and hardwood hammocks. Empirical studies show a gradual landward migration of these ecotones in some areas, due to sea level rise (SLR), and evidence in some areas of rapid change from glycophytic to halophytic vegetation, possibly as regime shifts resulting from salinity overwash from storm surges. In this dissertation work, the plausibility of storm surge related regime shifts of glycophytic vegetation was investigated using a coupled hydrological and ecological simulation model, and the resilience of the ecotone was studied using a mathematical model.

In view of potential effects of storm surge associate with SLR on Everglades ecosystems, particularly the consequences these pose for the Comprehensive Everglades Restoration Plan, both empirical and modeling studies on coastal vegetation are underway. In this dissertation work, the Spatially Explicit Hammock/Mangrove (SEHM) computer simulation model of the ecotone between those vegetation types was used to show the influence of both abiotic (elevation gradient, groundwater salinity, tidal amplitude, precipitation, freshwater flow) and biotic factors (plant physiology, competitive abilities, dispersal, positive feedbacks between plants and soil salinity) on the

mechanisms of ecotone formation. The model simulation results indicate that an environmental gradient of salinity, caused by tidal flux, is the key factor separating vegetation communities, while positive feedback involving the interactions of vegetation types with the vadose zone salinity increases the sharpness of boundaries, and maintains the ecological resilience of mangrove/ hammock ecotones against minor disturbances. The model also shows that the dry season, with its low precipitation, has a strong effect on the position of the mangrove/hammock ecotone.

Using a mathematical model of an ecotone vulnerable to possible future changes, I estimated the resilience of the ecotone to disturbances. The specific ecotone is that between two different vegetation types, salinity-tolerant and salinity-intolerant, along a gradient in groundwater salinity. In the case studied, each vegetation type, through soil feedback loops, promoted local soil salinity levels that favor itself in competition with the other type. Alternative stable equilibria, one for salinity-tolerant and one for salinity intolerant vegetation, were shown to exist over a region of the groundwater salinity gradient, bounded by two bifurcation points. This region was shown to depend sensitively on parameters such as the rate of upward infiltration of salinity from groundwater into the soil due to evaporation. I showed also that increasing diffusion rates of vegetation can lead to shrinkage of the range between the two bifurcation points. Sharp ecotones are typical of salt-tolerant vegetation (mangroves) near the coastline and salt-intolerant vegetation inland, even though the underlying elevation and groundwater salinity change very gradually. A disturbance such as an input of salinity to the soil from a storm surge could upset this stable boundary, leading to a regime shift of salinity-tolerant vegetation inland. I showed, however, that, for my model as least, a simple pulse disturbance would

not be sufficient; the salinity would have to be held at a high level, as a 'press,' for some time. The approach used here should be generalizable to study the resilience of a variety of ecotones to disturbances.

The SEHM model has been modified to simulate the mangrove-freshwater marsh ecotone. This model is based on intensive field studies by USGS across a mangrove-marsh ecotone on the Harney River in Everglades National Park. The model indicates that two factors are closely related to storm surge effect on vegetation. One of these is salinity intrusion, which has been proposed as a major disturbance to freshwater wetlands. The other is invasion of mangrove seedlings, which have rarely been reported as drivers for ecotone position changes. The model simulation results indicate that, at least for the cases studied, the regime shift of vegetation from freshwater marsh to mangroves was more sensitive to the density of mangrove seedlings passively transported by the storm surge than to the magnitudes of the salinity intrusion. The observed high salinities after regime shifts in the model are the result of more than simply the salinity overwash from the storm surge. Once mangrove prapagules establish successfully, high salinity can be maintained via evapotranspiration of the invading halophytic vegetation, which leaves salt in the soil. While initial salinity intrusion helps mangrove prapagules compete with dense freshwater marsh, the mangroves, once established, continue to hold the concentration of soil salinity high.

Acknowledgements

I have many people to thank who contributed in substantial ways to this work. First, I would like to thank my advisor, Donald L. DeAngelis, for his excellent guidance, caring, patience, and providing me with an excellent atmosphere for doing research. Don was extremely patient and understanding when I was experiencing fear and depression. I also want to thank Don and his wife Lee for taking me in like family.

I would like to thank my committee members for guiding my research for the past several years. I would like to thank Professor Leo Sternberg for his intellectual input and nice help with my research. I thank Dr. Carol Horvitz, who taught me a lot from both field and theoretical modeling. I had a very nice experience joining her lab meeting. Dr. Shigui Ruan provided insightful comments during all the stages of my project. I really appreciate his help. A special thanks goes to Dr. Fernando Miralles-Wilhelm, who was willing to participate in my final defense committee at the last moment. I gained experience collaborating with him on the NASA WaterSCAPES project. In addition, I want to thank Professor Dave Janos for all the Friday afternoon Mycorrhiza Group meetings where I learned about scientific writing skills and improved my statistic skills.

This work cannot be done without support from USGS South Florida Integrated Science Center. I would like to thank Dr. Catherine Langtimm, overall PI of FISCHS project I participated. She is a great leader and provided lots of help and comments on my dissertation. I want to thank other FISCHS team members, Thomas J. Smith, Eric Swain, Dennis Krohn, Brad Stith, Melinda Lohmann, Ann M. Foster, Zuzanna Zajac for their comments.

Being a teaching assistant has been one of the most unforgettable experiences I've had as a graduate student. I want to thank Dr. Dana Krempels for her help with teaching the general biology lab. I appreciate the support of the staff in the Department of Biology, especially Beth Goad, Marisa Hightower, Marilyn Morejon and Rob Burgess.

I want to thank my labmate, Shu Ju, for her help especially at beginning of my graduated studies. I also want to thank my labmate and friend, Bo Zhang, for her encouragement during last stage of my dissertation work. In addition, I want to thank the supports from all the friends I met during my stay at the University of Miami.

Last but not least, I would like to thank my parents and my wife, Ying Fang, for their continuous support and love.

TABLE OF CONTENTS

LIST OF TABLES

Chapter 2

Chapter 3

LIST OF FIGURES

Chapter 1

Chapter 2

Chapter 3

Chapter 4

CHAPTER 1

INTRODUCTION

Background of study

Climate Change and Storm Surge Threat of Coastal Vegetation Changes

Storm surges associated with sea level rise (SLR) are important predicted consequences of global climate change and have the potential for severe effects on the vegetation of low-lying coastal areas, islands and atoll islands (Nicholls and Cazenave, 2010). Rising sea level would also mean higher storm surges, even if the intensity and frequency of the storm do not change. A calculation made by Najjar et al. (2000) indicates that the current 100-year flood levels will occur 3 to 4 times more frequently by the end of 21st century in the mid-Atlantic coastal region. The impact of mean SLR will be a gradual effect on shoreline retreat and subsequent loss of ecosystem area in these locations.

However, large scale ocean water intrusion through storm surges may affect large areas on a short time scale, including the inundation of whole low-lying atolls. The immediate effect will be on the freshwater lenses that sit on top of saline ground water in these areas. Such effects on available fresh water may have negative consequences for the populations of coastal areas and, particularly, atoll islands, as they depend critically on fresh water stored in the lenses (Anderson, 2007; White and Falkland, 2010). Whether such short-term pulses will lead to long-term effects on vegetation depends on many factors; the physiological and competitive properties of local vegetation, precipitation,

overland freshwater flow, elevation gradient, and depth and salinity of groundwater (White and Falkland, 2010).

In tropical and subtropical coastal areas increase in salinities of the vadose zone induced by these events might reduce or eradicate the salinity intolerant species and promote landward migration of mangroves. Inland expansion of mangroves at the expense of freshwater vegetation has been the subject of much literature on coastal ecosystems. Stratigraphic evidence indicates that mangroves have replaced freshwater marsh along coastal southern Florida throughout the Holocene (Willard and Bernhardt, 2011; Williams et al., 2003). Alexander and Crook (1974) attributed the spread of mangroves into former pineland on Key Largo as a result of sea level rise. Lara et al. (2002) reported the progression of the black mangroves (*Avicennia germinans*) into the higher elevation plain dominated by grasses (*Sporobulus virginicus*) and herbs (*Sesuvium portulacastrum*) at the central part of the Bragança peninsula, Brazil for the study period of 1972 to 1992. From 8.8 km^2 in 1972, the areas dominated by grasses and herbs have shrunk to 5.6 km^2 in 1997.

However, to my knowledge, there is no detailed model explaining coastal vegetation ecotone pattern formation including all the factors and mechanisms involved (see below). Most vegetation models simplify hydrologic factors. Hydrology models, such as USGS's Saturated-Unsaturated TRAnsport (SUTRA) model (Voss and Provost, 2010), do not model vegetation, and therefore give no information on possible changes in plant communities resulting from interactions with hydrology and vadose zone salinity. Having models that couple vegetation and hydrology in detail would be of practical

importance for forecasting long-term effects of storm surges on coastal areas and small islands and atolls.

Mechanisms of Ecotone Boundaries

Coastal vegetation usually forms spatial patterns with abrupt transition zones, or ecotones, between salinity-tolerant (halophytic) and salinity-intolerant (glycophytic) vegetations. Stability of ecotones maintains ecological resilience of vegetation against small disturbances. Frequently, this stability can be attributed to environmental gradients, with enhancement due to competition. An example of the sharpening of ecotones between two vegetation types in coastal areas involves salinity-tolerant (halophytic) vegetation (mangrove vegetation in tropical and sub-tropical regions) and salinity intolerant (glycophytic) vegetation (hardwood trees or freshwater marsh) in southern Florida coastal areas. Typically, mangrove and hardwood hammock trees are not interspersed. Sharp 'ecotones' (transition zones) typically separate the salinity tolerant mangroves from the salinity intolerant hardwood hammock species, which occupy the similar geographical areas of southern Florida (Snyder et al., 1990; Sternberg et al., 2007). In this case, although hammocks tend to be at slightly higher elevations, the primary environmental factor that affects their competition is soil salinity.

The following mechanisms underlie the normal stability of the ecotone. Both mangroves (*Rhizophora mangle*, *Avicennia germinans*, *Laguncularia racemosa*) and hammock species (e.g., *Bursera simaruba*, *Coccoloba diversifolia*, *Eugenia axillaris*, *Sideroxylon foetissimum*, *Simarauba glauca*) obtain their water from the vadose zone (unsaturated soil zone). In coastal areas this vadose zone is underlain by highly brackish ground water, so that evapotranspiration, by depleting water in the vadose zone during

the dry season, can lead to infiltration by more saline ground water. Although hardwood hammock trees tend to decrease their evapotranspiration when vadose zone salinities begin to increase, thus limiting the salinization of the vadose zone, mangroves can continue to transpire at relatively high salinities. Thus, each vegetation type, through positive feedback, tends to promote local salinity conditions that favor itself in competition, which helps explain the stability of sharp boundaries between the types, despite a very gradual elevation gradient.

Field investigations and comparative studies have shown a correlation of intertidal salinity gradient with the mangrove/ hammock transition pattern (Ball, 2002; Schmitz et al., 2006; Ukpong, 1991), yet few mechanistic models describe such spatial interactions and its stability. For simplicity, the original version of MANHAM did not simulate propagule dispersal in a realistic way, but assumed dispersal could occur uniformly across locations. Modeling of intra specific competition with MANHAM also was simplified by assuming a homogeneous distribution of vegetation within each spatial pixel. Recent studies have found that intertidal dispersal mechanisms and the effects of environmental heterogeneity at the individual level are critical for understanding spatial patterns of coastal communities (Levine and Murrell, 2003; Sousa et al., 2007). For these reasons, studies of vegetation dynamics in response to environmental gradients at the individual level have major implications for our understanding of coastal spatial patterns in general. Furthermore, it is still unclear how these ecological hydrological processes interact to make habitats more vulnerable or resilience to change.

Possibility of Regime Shift

The mechanisms of positive feedback described above are important in maintaining the ecotone between halophytic and glycophytic vegetation types. However, if a large enough disturbance in soil salinity overwhelms the feedback maintaining the favorable conditions for glycophytic vegetation, even for a short period of time, the ecotone may no longer be maintained; that is, a regime shift can occur (Scheffer and Carpenter, 2003), moving the ecotone. Large areas of freshwater vegetation may be replaced by halophytic vegetation following storm surge overwash, which may lead to permanent salinization of the vadose zone. For example, Baldwin and Mendelssohn (1998) studied the effects of salinity and inundation coupled with clipping of aboveground vegetation on two adjoining plant communities, *Spartina patens* and *Sagittaria lancifolia*. The study concluded that the vegetation might shift to a salt-tolerant or flood-tolerant species, depending on the level of flooding and salinity at the time of disturbance. As another example, Hurricanes Katrina and Rita (2005), which affected the coastal areas of Louisiana, created large storm surges. Subsequent changes in the vegetation have been identified in both freshwater and brackish communities, as studied by Steyer et al. (2010). They noted that in the central region of their study area, marsh composition changed to a more saline classification, which was consistent with fall 2006 high mean salinities that exceeded mean pore-water salinity levels tolerated by the dominant species, as identified by Chabreck (1970). More generally, shifts in vegetation types in otherwise stable ecosystems due to disturbances like grazing, anthropogenic causes, fire suppression and precipitation redistribution have been widely reported

(Clymo and Hayward, 1982; Eppinga et al., 2009; Mutch, 1970; Scholes and Archer, 1997)

To understand how Florida's coastal forests respond to sea level rise, I extended the MANHAM model to include buttonwoods (Saha et al., 2011). The basic assumptions and model structure are similar to MANHAM model. I extend this model to include a third community, buttonwood forests, with salinity tolerance intermediate to mangroves and hammocks. The relationship between transpiration and salinity of buttonwoods is less sensitive to salinity compared to hammocks, but more sensitive compared to mangroves. Buttonwood is dominant in brackish water areas, whereas few coexist with mangrove at higher salinity levels (Urrego et al., 2009). In my simulations, under stable environmental conditions, hardwood hammocks occupied the higher elevation cells, mangroves occupied the lower elevation cells, and buttonwood woodland occupied the landscape between hammocks and mangroves (Figure. 1.1a). There exists a clear, sharp boundary between buttonwoods and mangroves, except for some mangroves scattered in the buttonwood woodland, which is similar to the hammock/mangrove ecotone described in Sternberg et al. (2007). The presence of mangroves in a more glycophytic community can be explained by observations that mangroves have a greater tolerance to salinity and are able to utilize low salinity water as well as the high salinity water lethal to both buttonwoods and hammock species (Sternberg and Swart, 1987). Buttonwood and hammock species can coexist in certain areas, with hammock aggregates in buttonwood woodland or vice versa (Figure. 1.1a). As sea level rises at a rate of 3 mm/year for about 33.3 years, the original buttonwood dominated areas are replaced by mangroves (Figure. 1.1b). This invasion does not occur as a solid front, but rather by fragmentation of the

original buttonwood stand. Similarly, buttonwood invades the hammock area as individuals and small aggregates, not as a solid front. Overall, during sea level rise the buttonwood forest is squeezed out of the intermediate salinity niche between mangroves and hammocks. Buttonwood frequency decreases from 26.3% before sea-level rise to 19.9% after an increase in sea level of 100 mm.

MANHAM model was also used to investigate the possibility of regime shift caused by salinity overwash (Teh et al. 2008). The model simulates the competition of these glycophytic and halophytic vegetation on a 100 x 100 grid of 1 m spatial cells. It simulates interaction of vegetation with hydrology and salinity dynamics in the vadose zone. The environmental factors of precipitation, groundwater salinity, and tides are included using data in daily time steps. Simulations by the model indicated that a significant 1-day storm surge event can initiate a vegetation shift to mangroves from hardwood hammocks in areas initially dominated by the latter. Mangroves will take over more than half of the higher elevation cells if the storm surge saturates the vadose zone at more than 15 ppt. It is observed that the shift occurs decades after the storm surge. A light storm surge that saturates the vadose zone by less than 7 ppt will not cause a vegetation shift. The rate of domination by mangroves in the high elevation cells after a storm surge was found to depend on the thickness or depth of the vadose zone. A thicker vadose zone will have a larger volume of high salinity which takes longer to be flushed out by precipitation. Thus, for an extended period of time, the growth of hardwood hammocks will be suppressed while mangroves will continue to grow. This will promote a faster rate of mangroves takeover. On the other hand, a smaller volume of high salinity will be washed out quickly by precipitation and therefore, allowing the hardwood

hammocks to recover. However, the study of Teh et al (2008) uses fairly simple assumptions on vegetation growth and hydrology, and connot capture detail regime shift processes.

Research objectives

The main objective of my dissertation research is to develop a suite of models of coupled hydrology and coastal vegetation communities that are able to simulate vegetation dynamics of coastal habitat. In my dissertation, I used both a mathematic analytical model and a coupled ecological-hydrological simulation model to test hypotheses and address issues of ecological and economic importance. My main work components are followings:

In Chapter 2, I investigated spatial pattern formation of coastal vegetation in response to external gradients and positive feedbacks affecting soil porewater salinity. I aimed to find out how the hypothesized 'vegetation switch' interacts with underlying environmental gradients to form sharp ecotones between mangroves and hardwood hammock vegetation. More specifically, I ask the following questions: Will the sharp boundary still exist if the self reinforcing feedback is taken out of the model? Could the self-reinforcing feedback alone cause sharp boundaries between vegetation types under completely uniform environmental conditions?

In Chapter 3, I estimated the resilience of the ecotone of coastal vegetation to disturbances. My objective was to build a model of an appropriate degree of complexity to capture the mechanisms discussed in Chapter 2, but to also allow mathematical analysis. I derived the model from classic competitive Lotka–Volterra equations, with a third equation describing salinity dynamics. I first examined the dynamics of the two

competing coastal plant species, along with the inhibitor, salinity, which is explicitly considered as a variable. Second, I extend the model to the case in which there is a slight gradient in an environmental condition, specifically groundwater salinity along one dimension, in order to investigate the effect of the gradient on potential large-scale regime shifts. I calculated the resilience of the ecotone; that is, the characteristics of the disturbance needed to cause a large spatial shift in the ecotone.

In Chapter 4, I applied the coupled hydrological-ecological simulation model to test mangrove-freshwater marsh ecotone changes at a coastal edge of Florida Everglades. I analyzed how long-term changes in the mangrove-marsh ecotone could occur after storm surge events, and whether, on the basis of empirical data, they are likely to have occurred in a region of the Everglades affected by a hurricane. First, hydrology and salinity dynamics were investigated from 2000-2010, a period during which Hurricane Wilma passed northwest of Everglades (2005). Second, vegetation dynamics were simulated based on hydrology data from Hurricane Wilma. Finally, long-term vegetation changes under given scenarios of salinity intrusion and amount of mangrove dispersal to freshwater marsh sites by hypothetical storm surge were simulated.

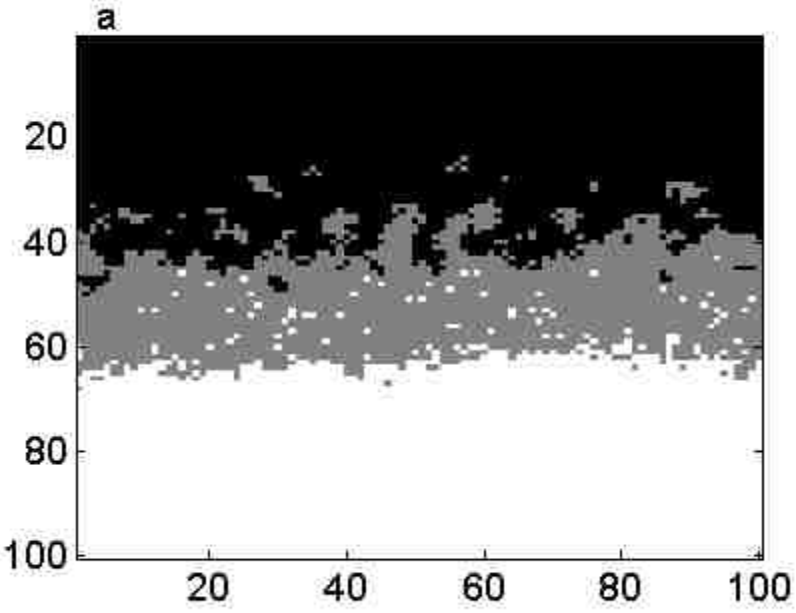
a
20
40
60
80
100
20
40
60
80
100

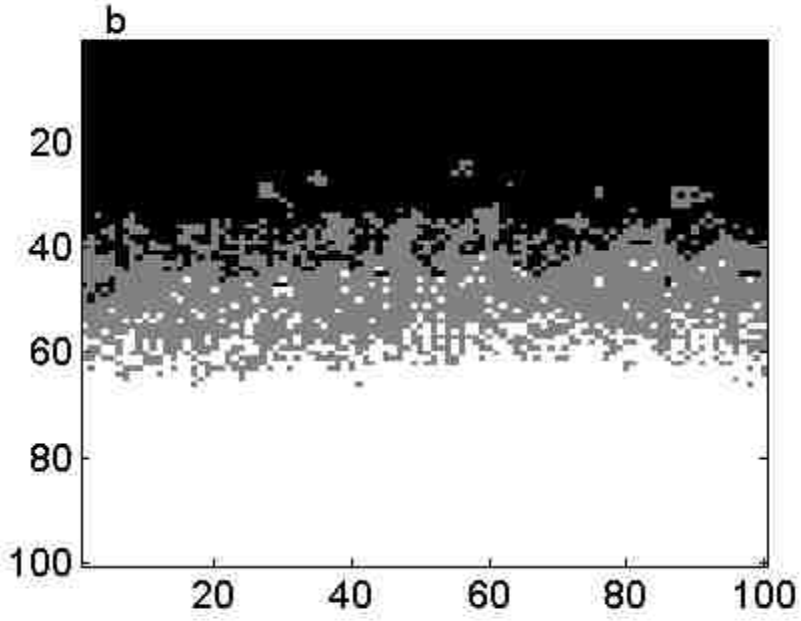

Figure 1.1: (a) Horizontal view 100 × 100 m^2 grid cells showing distribution of mangrove (white), buttonwood (grey) and hammock (black) 33.3 years after stable pattern formed without sea level rise, and (b) subject to sea level rise 3 mm/year. In these two graphs, upper x axis depicts inland side while lower x axis the seaward side.

Chapter 2

SPATIAL PATTERN FORMATION OF COASTAL VEGETATION[1]

Summary

The coastal vegetation of South Florida typically comprises salinity-tolerant mangroves bordering salinity-intolerant hardwood hammocks and fresh water marshes. Two primary ecological factors appear to influence the maintenance of mangrove/ hammock ecotones against changes that might occur due to disturbances. One of these is a gradient in one or more environmental factors. The other is the action of positive feedback mechanisms, in which each vegetation community influences its local environment to favor itself, reinforcing the boundary between communities. The relative contributions of these two factors, however, can be hard to discern. A spatially explicit individual-based model of vegetation, coupled with a model of soil hydrology and salinity dynamics is presented here to simulate mangrove/ hammock ecotones in the coastal margin habitats of South Florida. The model simulation results indicate that an environmental gradient of salinity, caused by tidal flux, is the key factor separating vegetation communities, while positive feedback involving the different interaction of each vegetation type with the vadose zone salinity increases the sharpness of boundaries, and maintains the ecological resilience of mangrove/ hammock ecotones against small disturbances. Investigation of effects of precipitation on positive feedback indicates that the dry season, with its low precipitation, is the period of strongest positive feedback.

[1] Landscape Ecology. 27, 109-119

Background

Ecotones, or the abrupt transitions between vegetation types, have long been a focus of study in ecology (e.g., Clements, 1907; Transeau, 1935). While many transition zones, or ecotones, between floristic types are broad and diffuse, some are remarkable narrow (e.g., Oosting, 1955; Walker et al., 2003). Frequently, this can be attributed to the steep environmental gradients, with further enhancement due to competition. For example, the sharp altitudinal boundary between hardwood and boreal forest at about 792 m in the Green Mountains of Vermont (and other elevations elsewhere) is attributed by Siccama (1974) in part to a climatic discontinuity near that elevation (see also Shugart et al., 1980). The boundary is reinforced by modifications of the local environment on the boreal side by the spruce and fir trees, which make conditions inhospitable for hardwoods. Similar sharp ecotones have been found in tropical montane forest (e.g., Martin et al., 2011).

The mechanism by which plants can modify their local environment to create a sharp boundary between them has been termed a 'vegetation switch' (Wilson and Agnew, 1992). According to this concept, two vegetation types are each capable of occupying a particular area, and each capable of altering the local environment in its own favor. Examples of ecotones shaped by such feedbacks of vegetation on the environment include boundaries between fire-dependent (e.g., savannah) and non-fire-dependent communities, in which the former have been hypothesized to have evolved to be more flammable (e.g., Mutch, 1970); treeline ecotones along smooth environmental gradients in alpine ecosystems (Wiegand et al., 2006), where modeling indicates that abrupt changes in tree density were due to positive feedback involving both facilitation and

growth inhibition; the 'ridge and slough' landscape in the Everglades, in which sawgrass creates slightly higher elevations through soil accretion that separates it from more aquatic vegetation like water lily, bladderwort, and spike rush (Larsen et al., 2007); and bog habitats, in which mediation of light availability(Clymo and Hayward, 1982), acidity (van Breemen, 1995), temperature (Eppinga et al., 2009), and nutrient availability (Eppinga et al., 2009) have all been hypothesized to play a role in sharpening boundaries between Sphagnum and vascular plants.

Another example of the sharpening of ecotones between two vegetation types through their different effects on the environment involves mangrove vegetation and hardwood hammock vegetation (tropical hardwood trees) in southern Florida coastal areas. Typically, mangrove and hardwood hammock trees are not interspersed. Sharp 'ecotones' (transition zones) typically separate the salinity tolerant mangroves from the salinity intolerant hardwood hammock species, which occupy the similar geographical areas of southern Florida (Snyder et al., 1990; Sternberg et al., 2007). In this case, although hammocks tend to be at slightly higher elevations, the primary environmental factor that affects their competition is soil salinity. The following mechanisms underlie the normal stability of the ecotone. Both mangroves (*Rhizophora mangle*, *Avicennia germinans*, *Laguncularia racemosa*) and hammock species (e.g., *Bursera simaruba*, *Coccoloba diversifolia*, *Eugenia axillaris*, *Sideroxylon foetissimum*, *Simarauba glauca*) obtain their water from the vadose zone (unsaturated soil zone). In coastal areas this vadose zone is underlain by highly brackish ground water, so that evapotranspiration, by depleting water in the vadose zone during the dry season, can lead to infiltration by more saline ground water. Although hardwood hammock trees tend to decrease their

evapotranspiration when vadose zone salinities begin to increase, thus limiting the salinization of the vadose zone, mangroves can continue to transpire at relatively high salinities. Thus, each vegetation type tends to promote local salinity conditions that favor itself in competition, which helps explain the stability of sharp boundaries between the types, despite a very gradual elevation gradient.

A number of IBMs (Individual Based Models) have been developed for mangrove forest dynamics (Berger and Hildenbrandt, 2000; Chen and Twilley, 1998; Doyle and Girod, 1997; Doyle et al., 2003), and their applications to aspects of forecasting potential effects of global climate change have been reviewed (Berger et al., 2008). In particular, Doyle and Girod (1997) used computer simulations of their SELVA-MANGRO model of mangroves to project possible inland migration of mangroves in along the southern Florida coastline in response to projections of sea level rise. This was done using projections of the changing locations of tidal influence, given the topography of southern Florida and the assumption of a continuation of the current rate of sea level rise. However, despite this and numerous other contributions to understanding of mangrove dynamics that have come from these IBMs, I know of no applications that focus strongly on the development and maintenance of ecotones between the mangroves and other vegetation, particularly the type of hardwood hammock vegetation typical of southern Florida.

The overall aim of my study is to find out how the hypothesized 'vegetation switch' interacts with underlying environmental gradients to form sharp ecotones between mangroves and hardwood hammock vegetation. More specifically, I ask the following questions: Will the sharp boundary still exist if the self-reinforcing feedback is taken out of the model? Could the self-reinforcing feedback alone cause sharp boundaries

between vegetation types under completely uniform environmental conditions? This is in the spirit of using modeling to understand the causes for patterns observed in nature (Grimm et al., 2005).

Method

To address these issues, I built SEHM (Spatially Explicit Hammocks and Mangroves) model, an individual-based model that simulates the spatial pattern of the ecotone between mangrove and hammock vegetation. SEHM omits many details that more comprehensive tree dynamics models include, such as community dynamics and competition for nutrients, in order to focus on the effects of salinity on competition between two vegetation types. I use the Overview, Design Concepts, and Details protocol (Grimm et al., 2006; 2010) to describe my model. A complete description of the model is available in appendix A. Here, I provide an overview of SEHM.

I simulated intra- and inter- specific competition between mangroves and hammocks, including the effects of the underlying hydrodynamics of tides, soil porewater and ground water. The model links two main components, an individual-based vegetation dynamics submodel and a grid-based hydrodynamics submodel, which operate on different computational time steps, a daily time scale for physiological processes of water uptake by plants, which changes soil salinity, and a monthly time scale for vegetation dynamics. During each monthly time step, every tree can have a growth increment that is a function of neighborhood competition, and the salinity of the particular spatial cell or cells occupied by the tree's roots. Then, after a tree reaches maturity, new recruits are produced at monthly intervals by the tree. The appearance of successful new recruits depends, in part, on the salinity of the soil porewater and also on neighborhood

competition. At the end of the monthly time step, death may occur due to size-dependent factors (low d.b.h., diameter at breast height of tree) and also from reduced growth rate caused by competition or salinity. Information on the total amount of root biomass distributed in each cell is passed to the hydrodynamics, which updates water and salinity on daily time steps. Monthly average values of salinity in each cell, which affect tree growth and seedling establishment, are then returned to the submodels for vegetation dynamics.

All parameters are shown in Table 2.1. No data from specific locations were available to us. So I calibrated the model based on parameters that could generate a sharp boundary similar to what I observed from southern Florida mangrove/ hardwood hammock ecotones. The model simplified the system to a standard species for each vegetation type and that the mangroves are represented by *Rhizophora mangle* when data are available from literatures. Since the model was meant to study possible mechanisms of ecotone formation between mangroves and hardwood hammock vegetation, I focused on the aspects of model structure that affect spatial pattern. I examined the effects of completely removing positive feedback to see changes of spatial pattern (see *Simulation experiment* section for details), but did not perform a complete sensitivity analysis of the parameters involved in feedback due to simulation time constraints.

Simulation experiments

Vegetation simulations were performed in a square area that represents 1 ha, with an initially random distribution of an equal number of mangroves and hammock trees across the area. Salinity dynamics were simulated in a grid-based system with 100×100 cells. Each cell represents a 1×1 m^2 segment within a landscape typical of Florida's

coastal topography, which is assumed in the model to increase locally in elevation from the coast at an average of 10 mm per meter, following (Sternberg et al., 2007; Teh et al., 2008). Although this elevation gradient is much greater than the large-scale regional gradient from the coast inland, it might not be atypical of local elevation gradients.

To investigate the relative contributions of the positive feedback mechanism and external environmental factors to the sharp ecotone between mangroves and hardwood hammocks, I used SEHM to perform two experiments.

Experiment 1

The first simulation experiment included simulations to distinguish the relative effects of the internal positive feedback mechanisms and external environmental factors. Four different trials were performed within Experiment 1. In the first trial, I used SEHM with all components of the model active, to examine whether patterns similar to field observations emerged from an initially random distribution of trees, as was done with MANHAM (Sternberg et al., 2007; Teh et al., 2008). In this full model simulation of mangroves and hardwood hammock trees gradually segregated into two homogeneous stands, with a sharp boundary between them. I measured the degrees of sharpness (*SI*) by means of technique borrowed from the entropy of mixing. Mangroves and hardwood hammocks were considered as analogous to two substances mixing on a surface. Maximum entropy (E_{max}) represents perfectly random mixing of two vegetation types (Macchiato et al., 1992). The degree of sharpness (*SI*) was calculated by,

$$SI = \omega(1 - E / E_{\max})$$

where, E is entropy of the system, which is calculated by $E = -\sum p_i \log p_i$, and p_i is probability of trees in single cell. and ω is a normalization coefficient based on an

optimally sharp ecotone, which corresponds to mangroves being evenly distributed below mean tidal height and hardwood hammocks evenly distributed above mean tidal height.

In the second trial, I removed the feedback between vegetation and soil porewater salinity. Vegetation growth rate and regeneration rate still were able to be affected by soil porewater salinity. But soil porewater salinity was not able to be affected by changes in vegetation; in particular, a constant water uptake of 2.1 mm/day was assumed uniformly across the model landscape. I explain the choice of why choosing 2.1 mm/day in more detail in the Results and Discussion. Other values of water uptake ranging from 1.0 to 3.0 mm/day were also simulated. A sign test was used to quantify the difference in the degree of sharpness of the ecotone for the first two trials.

In the third trial, I kept only the self-reinforcing feedback, and made the underlying environmental conditions completely uniform across space, such that there was the same elevation for all the cells and there was no tidal effect. If self-reinforcing feedback alone can maintain a sharp boundary, I would expect aggregation patterns of the two vegetation types to emerge; that is, a pattern of homogeneous clumps of vegetation of each type. I measured the degree of clumpedness of overall landscape patterns by focusing on the aggregation of the rarer vegetation (whether mangrove or hammock) on the model landscape in any given simulation. In this technique, the dominant vegetation type was considered as background habitat, and the trees of the rare vegetation type were the test objects. Simulations leading to fewer than 5 individuals of the rare type on the landscape were considered as monospecific and not used to calculate aggregation indices. For simulations leading to coexistence of the two types on the model landscape, each individual tree of the rare type was identified as either the same as or different from each

of its neighbors within 3 meters. The aggregation index was computed by dividing the links between trees of the same vegetation type by the total number of links. Since the third trial required the assumption of a constant water table salinity and distance to water table, I also chose other higher and lower constant water table salinities and distance to water table, separately. Nine sets of constant values were simulated. A Kruskal-Wallis test, followed by an all-pairwise comparison of Dwass-Steel-Critchlow-Fligner test, was used to test the effects of the two factors.

In the fourth trial, similar to the use of a control group in field experiments, I removed positive feedback and simulated the model under uniform environmental conditions. In this completely uniform spatial area, without feedbacks, I expected a relatively intermixed distribution between the two vegetation types for this trial. All the trials are repeated 20 times, estimated by power analysis.

Experiment 2

In the field, soil porewater salinity differs between the wet season and dry season, although the spatial pattern of mangrove/ hardwood hammock does not respond to salinity changes on such a short time scale (Semeniuk, 1983). I predicted that it is primarily high salinity during the dry season that defines the long-term ecotones between the hardwood hammock community and the mangroves, as salinity stress should be the highest then and as there is insufficient time for vegetation to shift back towards the hardwood hammock community during the following wet season.

To investigate seasonality of precipitation on the distribution of mangroves and hardwood hammock I first tested the effect of precipitation on spatial pattern. All components of the SEHM model were working the same as in the third trial in

experiment 1, which removed environmental gradients, except for experimental control of the precipitation amount. I also tested the effect of precipitation under the full version of SEHM, to completely understand the interaction between positive feedback and precipitation effect on spatial pattern. Finally, I investigated the monthly variation of soil porewater salinity after the vegetation distribution reached equilibrium.

Results

Comparison of mechanisms (Experiment 1)

The combined mechanisms of positive feedback and an environmental gradient (first trial) resulted in a clear boundary between hammocks and mangroves (Figure 2.1a), and showed a strong resemblance to typical patterns of coastal vegetation distribution. The model contains both tidal effects, which directly influence soil porewater, and the positive feedback mechanism discussed earlier, in which each vegetation type has a self-reinforcing effect on itself by influencing soil porewater salinity in its favor. Starting from an initially random distribution of the two tree types across the landscape, a vegetation pattern emerged with full mangrove coverage within 30 m of the seaward end of the landscape to full hammock coverage at higher elevations. This is shown by the circles and the solid line fit in Figure 2.2, where the relative percentage of hammock basal area is plotted versus distance from the seaward edge of the transition.

For the second trial, positive feedback was removed from the model by not allowing the vegetation to have any effect on the soil porewater salinity, so porewater salinity was determined by abiotic effects alone; i.e., tides, precipitation, and salinity diffusion between cells. Nevertheless, salinity still was able to affect vegetation growth. Specifically, plant effects on salinity in the previous trial were removed by assuming a

constant water uptake rate (evapotranspiration) by plants across the landscape, regardless of vegetation type and soil salinity. With the feedback removed, the simulation output still produced a boundary (Figure 2.1b), corroborating the idea that the tidal effect alone can maintain the boundary. Notice that with the assumption of constant water uptake of 2.1 mm/day, there is some shifting upward of the elevation boundary, with mangroves moving a few meters inland to higher elevations that were initially fully covered by hammock vegetation (Figure 2.2). I compared Trial 1 and Trial 2 near the seaward end and near the inland edge separately (Figure 2.1a, 2.1b). At the seaward end, which is affected by tidal flux, salinity was too high for hammocks to persist, so I found no difference there between Trial 1 and Trial 2; in both trials vegetation was dominated by mangroves near the seaward end. Near the inland end, with positive feedback in Trial 1, hammock trees reduced their evapotranspiration and kept the soil porewater in that area at a low salinity level.

To determine if the difference in sharpness observed between the first and second trials represents a general rule, 20 simulations were performed for each case, and a sign test of degrees of sharpness (*SI*) showed a significant difference ($p<0.01$), with a mean difference of degree of sharpness of 0.57 versus 0.37 for the first and second trials, respectively. When water uptake of only 1.8 mm/day was assumed, however, the sharpness index of Trial 2 was not significantly different from that of Trial 1 ($p=0.12$). To examine the effects of other values of water uptake, a range from 1.0 to 3.0 mm/day was used and degree of sharpness was plotted against water uptake (Figure 2.3). With an extremely low constant rate of water uptake, which reduced the capillary rise of saline water, the external tidal effect played an important role, and a sharp ecotone continued to

be maintained. But the relative effect of tidal flux diminished as water uptake increased (Figure 2.3), showing the importance of the magnitude of evapotranspiration on the salinity and vegetation dynamics.

Positive feedback alone (Trial 3), resulted in an aggregation pattern (Figure 2.1c), with a mean value of aggregation index of 0.65. This is significantly higher than that of the null model (Trial 4; Figure 2.1d), in which both positive feedback and environmental gradient were removed, which showed a weak aggregation pattern, with a mean value of 0.46. In Trial 3, the distance to the water table and the water table salinity were assumed to be the same for all cells across the area and there was no tidal effect, so there was no preferential ecotone along the transect from seaward to inland. The different vegetation types adjusted evapotranspiration response to soil porewater salinity, and evapotranspiration in turn changed the soil porewater salinity through capillary rising of the saline water. Two factors, distance to water table and water table salinity, combined with evapotranspiration, can affect soil porewater salinity. In the real world, greater distance from the soil surface to water table is related to higher elevation at the inland end of the elevation gradient, so I used a series of different values of distance of soil surface to water table. Significant differences were found for the aggregation index depending on the values of distance to water table and water table salinity (Figure 2.4). The aggregation index was high when water table salinity was high, such that the positive feedback between vegetation and soil porewater salinity was strong. I found a significantly lower aggregation index at high elevations for which distance to the water table also was large. At high elevations, soil porewater salinity dynamics slowed because of the thickness of the soil layer. Thus, soil porewater salinity increased less at high

elevations than at low elevations, when mangroves were present in hammock habitats. This also means that only weak positive feedback occurred at high elevation. Interaction effects also were significant; for example, extremely high water table salinity could overcome stagnancy of soil porewater salinity dynamics at high elevation (Figure 2.4).

Effect of precipitation on ecotones (Experiment 2)

At permanent extremely high or low precipitation levels, hammock trees or mangroves, respectively, outcompeted the other species type. Aggregation indices on a uniform landscape, with no environmental gradient effects, were high over a range of low precipitation values, and declined as precipitation increased (Figure 2.5). At relatively high precipitation, hammocks dominated the whole habitat, and mangroves were scattered in gaps among the hammock trees instead of occurring a distinct mangrove habitats.

I also used a full version of SEHM, which included both positive feedback and environmental gradient, to simulate the effect of precipitation on ecotone pattern. A clear ecotone line did not emerge along the elevation gradient, however, when the precipitation was permanently low, which created conditions in which the positive feedback was strong. In that case, positive feedback maintained clumping of mangroves within inland hammock habitats, and tidal flux created mangrove-dominate habitats at the seaward edge. However, an ecotone line was clear at a constant high precipitation, because high precipitation favored hammocks at all points without tidal effects, while the intertidal zone was dominated by mangroves because of periodic saline ocean water inundation.

The salinity pattern varied seasonally, as shown in monthly snapshots (Figure 2.6), even though the vegetation aggregation pattern persisted during a specific year (Figure

2.1c). The spatial pattern of salinity was relatively homogeneous at the end of December (Figure 2.6 Dec), but highly heterogeneous at the end of June (Figure 2.6 Jun), although the vegetation pattern was the same. Mangrove habitats maintained high salinities, while hammock habitats still maintained low salinities. Temporal variation of spatial salinity pattern of soil porewater followed the shape of the precipitation pattern, but with a delay of about two months. The dry season in the model ended at the end of April, while salinity of mangrove habitats reached their highest levels at the end of June. This is similar to field observations at the Harney River estuary, Everglades National Park(Anderson et al., 2003). The lag probably results from delayed capillary rise of salinity depending upon soil layer depth.

Discussion

Some studies investigating ecotones have focused on the mechanism of positive feedback alone (Cutini et al., 2010; Zeng and Malanson, 2006), but gradients of external environmental conditions are also important. My results suggest that mechanisms of spatial pattern formation of coastal vegetation are more complex than previously suggested, and patterns may not be simply the outcome of either effects of positive feedback or environmental gradients alone.

Relative contribution of positive feedback to sharp ecotones

A combination of positive feedback and environmental gradients is likely responsible for the sharp boundary between mangrove and hammock vegetation types in coastal habitats. My first simulations supported this (Figure 2.1a). The pattern is similar to earlier simulations using MANHAM (see Sternberg et al. 2007, Teh et al. 2008), and is consistent with environmental gradients being important in establishing vegetation

ecotones. However, it was difficult to determine the contribution of positive feedback on this boundary from simulation of MANHAM alone. My Trial 3 (Figure 2.1c) simulation showed that positive feedback between plants and soil porewater salinity contributed to the sharp ecotone between hammock and mangroves. The strength of the positive feedback is represented by how fast the salinity of soil porewater changes due to the alternating processes of capillary rising from the saline water table versus infiltration of precipitation. As shown in Figure 2.4, a combination of a high water table and high salinity of the water table created a strong positive feedback and resulted in a relatively high aggregation index. In nature, high water table salinity is usually associated with low elevation at the intertidal zone. This implies strong positive feedback at intertidal zone, while weak positive feedback occurs at high elevations associated with low water table salinity where hammocks dominate.

My results indicate that positive feedback may not necessarily be essential to boundary formation, at least for the elevation gradient that I used. The effects of positive feedback relative to environmental gradient were evidenced by Trial 2 in which positive feedback was removed. In Trial 2, when I fixed water uptake at a constant value of 2.1 mm/day across the whole landscape (the average water uptake in Trial 1), salinity increased and benefitted mangroves. There exists a certain level of soil porewater salinity at which there is a balance in the competitive relationship between hammock trees and mangroves. This is because hammock vegetation is competitively dominant over mangroves under low salinity conditions, while mangrove vegetation is dominant under high salinities. Therefore, one may expect a salinity level at which the two vegetation types are approximately equal competitively, which prevails at the boundaries of these

two vegetation types. In my simulation experiments, if a high level of water uptake was assumed (e.g. >2.3 mm/day in Figure 2.3), the balance was destroyed and mangroves dominated the whole area. If an extremely low level of water uptake was assumed, the balance was destroyed in the opposite direction and much of the area should be dominated by hammock. But in that case, because the seaward end of the area was frequently inundated by saline tides, a sharp boundary between hammocks and mangroves near the mean tide level occurred in the simulation, even sharper than outputs of Trial 1. This implies that positive feedback would not be a necessary mechanism for sharpness of the boundary, if water uptake was permanently low. However, water uptake typically varies between 2.0~2.5 mm/day when salinity is low, and at this level, the boundary became vague in Trial 2, with the positive feedback removed. This indicates that under certain conditions positive feedback is an essential mechanism for maintaining a sharp ecotone, and that an environmental gradient alone only determines that a diffuse boundary exists.

Dry seasons are the major determinant of the vegetation distribution pattern

I studied the aggregation pattern when the environmental gradient was removed and different levels of precipitation were assumed, and found that aggregations of two coexisting vegetation types occurred over a certain range of low precipitation, but not at extremely low precipitation, at which level positive feedback predominated and mangroves dominated the whole region. At somewhat higher levels of precipitation, positive feedback still favors mangroves in the dry season, during which salt, rising through capillary action, accumulates in the soil porewater and stresses hammock trees.

But it is possible that local aggregations of hardwood hammock trees could occur and prevent invasion of mangroves.

Temporal variation in soil porewater salinity resulting from fluctuations in precipitation, coupled with positive feedback between vegetation and salinity, resulted in spatio-temporal variation of the salinity pattern (Figure 2.6). Nevertheless, vegetation distributions were relatively stable and coincided with the salinity pattern at the end of June, a 1-2 month time lag following the end of the dry season. This implies that strong positive feedback during the periodic dry season resulted in a highly heterogeneous aggregation of salinity and vegetation pattern. The following wet season prevented mangroves from continuously invading hardwood hammock habitats, but was not enough for dominance to shift back to hammock.

These theoretical results need empirical support. Cases of sharp ecotones between mangroves and hardwood hammocks are well documented in southern Florida, i.e. Florida Keys (Ross et al., 1992; Sternberg et al., 1991), Waccasassa Bay on the west coast of Florida(Williams et al., 2003), Turkey Point on the southeast coast of Florida (Pool et al., 1977), et al. But my simulation results suggest that there could be patchiness of mangroves in more inland habitats, where there is no tidal effects, but occasional storm surge inundations occur. Inland isolated mangroves have been reported on the island of Inagua in the Bahamas(Lugo, 1981), island of Barbuda, West Indies (Stoddart et al., 1973), and southwest of Moreton Island at Australia (Manson et al., 2003), et al. But there are no reports of this pattern of southern Florida hardwood hammocks stands. This could be due to high precipitation of southern Florida during wet season, and less extreme droughts during dry season.

Implications for coastal ecosystem pattern with Climate change

The objective of SEHM is to improve the projections of possible changes in coastal vegetation patterns in southern Florida that may result from both the rise of mean sea level and from saline overwash resulting from storm surges. Simulations of a simpler forerunner of SEHM, MANHAM, indicated that broad areas of freshwater vegetation (hardwood hammocks) could theoretically undergo regime shift to halophytic (mangrove) vegetation under a sufficiently large storm surge. Using SEHM, I have attempted to study the environmental and autogenic factors maintaining the ecotone between freshwater and halophytic vegetation more carefully. SEHM is still making a number of simplifications of the actual coastal hydrology. For example, the subsurface advection of freshwater (e.g. see Wilson, 2005), and other aspects of groundwater dynamics are ignored. I will take these into account in future versions of SEHM. It is also relevant to note that the expected increase in freshwater sheet flow from the implementation of the CERP (Comprehensive Everglades Restoration Plan), which will affect both surface and groundwater flow. This may have similar effect to increased precipitation (Perry, 2004), although I have not explicitly simulated this effect here. The potential effects of CERP on future water flows is currently being simulated (Swain et al., 2003) and will be taken into in SEHM.

Table 2.1 Parameters for mangroves and hammocks used in the SEHM model. Most of parameters of mangroves are from literatures. Parameters of hammocks are assumed to have same values as mangroves if they are not sensitive, and to have values changed in reasonable ways otherwise. Sensitive parameters, which have different value between mangroves and hammocks, are in bold.

Parameters	Description	Hammocks	Mangroves
G	**Growth constant**	437	267[a]
D_{max}	**Maximum DBH (cm)**	122	100[a]
H_{max}	**Maximum height (cm)**	4267	4000[a]
b_2	**Constant in height to DBH relationship**	67.75	77.26[a]
b_3	**Constant in height to DBH relationship**	0.278	0.396[a]
k	Light attenuation coefficient	0.4	0.4
c_{LA}	Constant in LAI to DBH relationship	2.01	2.01
b_{LA}	Constant in LAI to DBH relationship	0.228	0.228
K_{FA}	Half saturated coefficient for competition effect on growth	0.5	0.5
α_{HH}	Strength of the effect of hammock on itself	1.0	-
α_{MH}	Strength of the effect of mangrove on hammock	0.2	-
α_{MM}	Strength of the effect of mangrove on itself	-	1.0
α_{HM}	Strength of the effect of hammock on mangrove	-	5.0
FON_{Min}	Minimum field strength	0.01	0.01[b]
η	**Below-ground to above-ground biomass ratio**	0.1	0.2
c_{AB}	Constant in root biomass to DBH relationship	0.251	0.251[c]
b_{AB}	Constant in root biomass to DBH relationship	2.46	2.46[c]
β	Attenuation rate of root density	0.776	0.776[d]
a_{HL}	Constant in maximum root extension to DBH relationship	41.143	41.143 [d]
b_{HL}	**Constant in maximum root extension to DBH relationship**	0.15789	0.11789 [d]
m_c	Constant background mortality	0.0015	0.0015
m_s	Coefficient of stress on mortality	0.001	0.001

Table 2.1 Continue

u	Coefficient of DBH to mortality relationship	0.05	0.05
v	Coefficient of growth rate to mortality relationship	5	5
P_{max}	Maximum fecundity	10	10
ε	Baseline survivalship	0.001	0.001
θ	**Coefficient for salinity effect on birth rate**	1.625	0.25
K_{sv}	**Half saturated coefficient for salinity effect on birth rate**	10	35
K_{FS}	Half saturated coefficient for field strength on birth rate	0.5	0.5
f_L	Coefficient of dispersal probability with distance	0.2	0.2
Max_d	**Maximum local dispersal distance (m)**	30	10

[a] Chen and Twilley (1998)
[b] Berger and Hildenbrandt (2000)
[c] Komiyama et al. (2008)
[d] Komiyama et al. (1987)

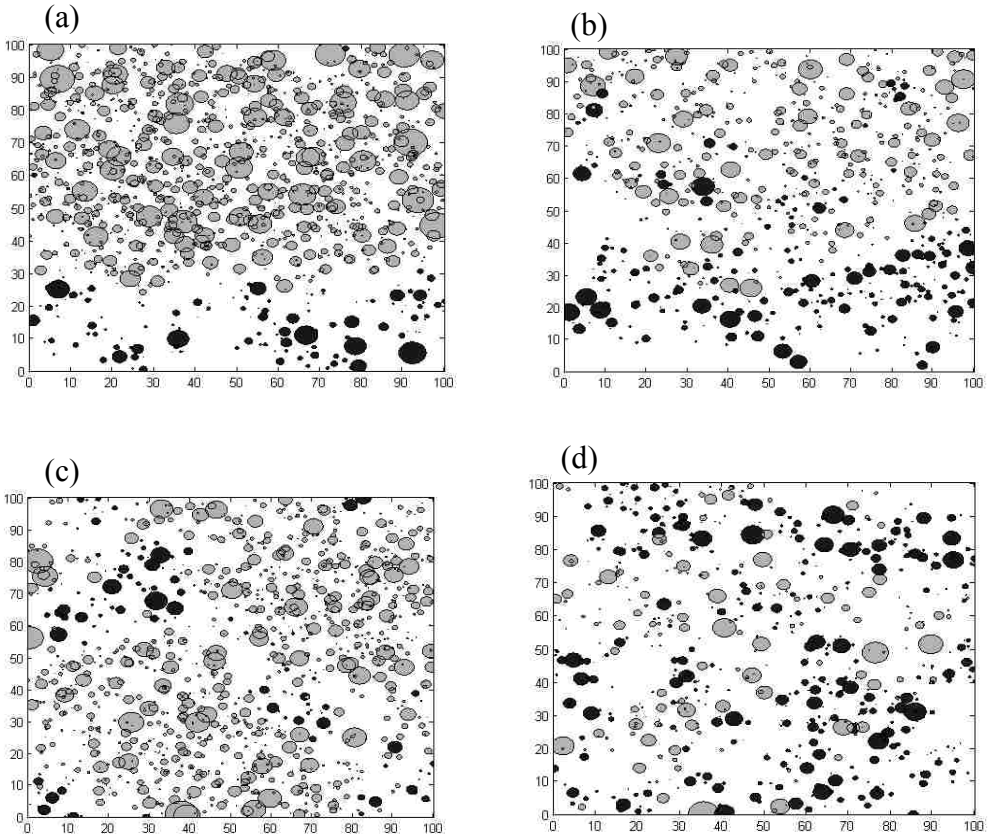

Figure 2.1 Simulation output showing distribution of mangrove (dark) and hardwood hammocks (gray) in 100 X 100 m2 landscape, from (a) Trial 1, complete SEHM model, (b) Trial 2, removing only positive feedback between vegetation and soil porewater salinity, (c) Trial 3, removing only environmental gradient of salinity, (d) Trial 4, removing both mechanisms. Diameter of each circle is four times d.b.h.

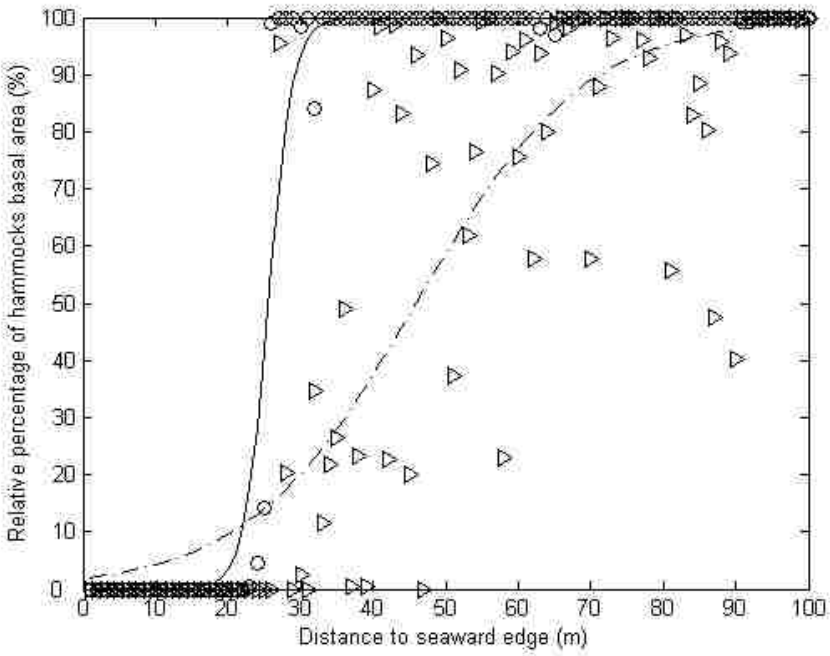

Figure 2.2: Relative percentage of hammock basal area is plotted versus distance from the seaward end of the transect. The circles and solid line represent Trial 1 output and a logistic regression fit, respectively. The triangles and dashed line represent Trial 2 output with constant water uptake 2.1 mm/day and a logistic regression fit, respectively.

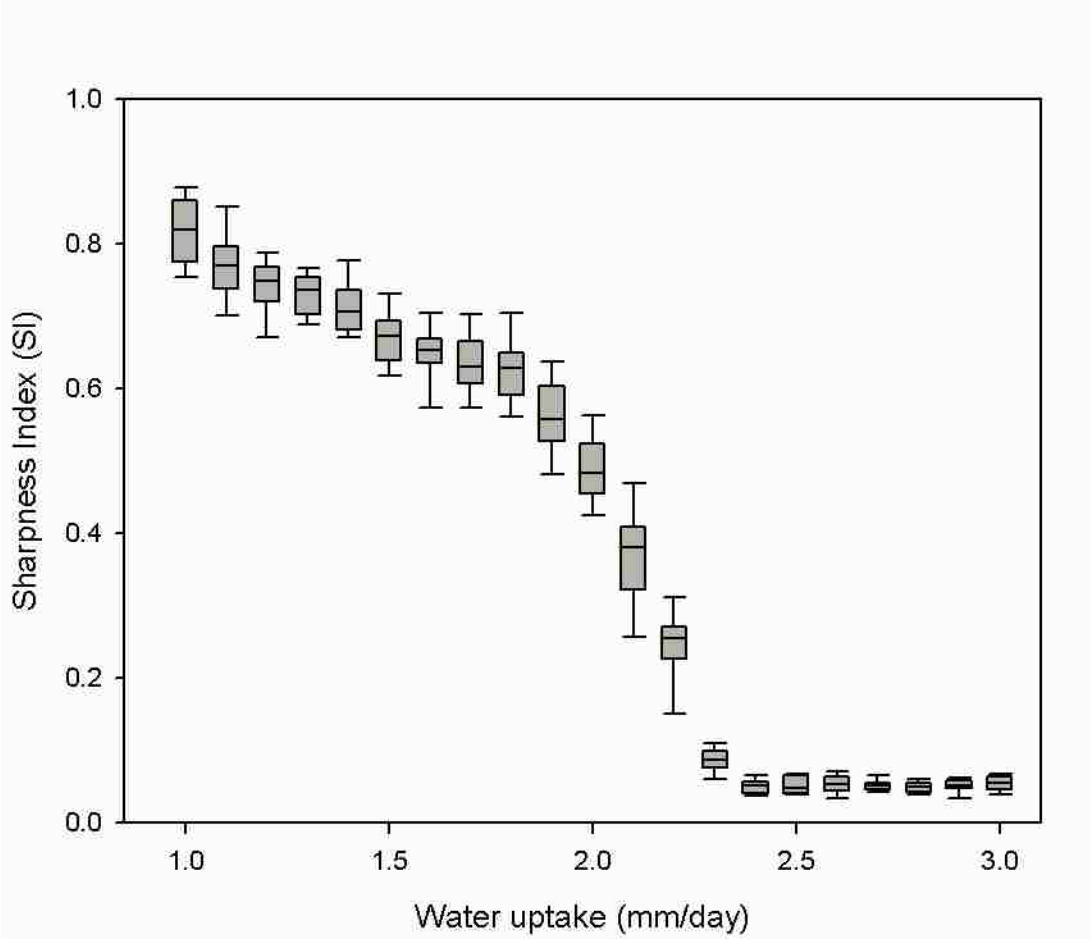

Figure 2.3: Box-and-Whisker plot of sharpness index versus water uptake (evapotranspiration) of plants in Trial 2, which removed the positive feedback between plants and salinity dynamics. The boundary of the box indicates the 25th and 75th percentile. The line within the box marks the median. Whiskers (error bars) above and below the box indicate the 90th and 10th percentiles.

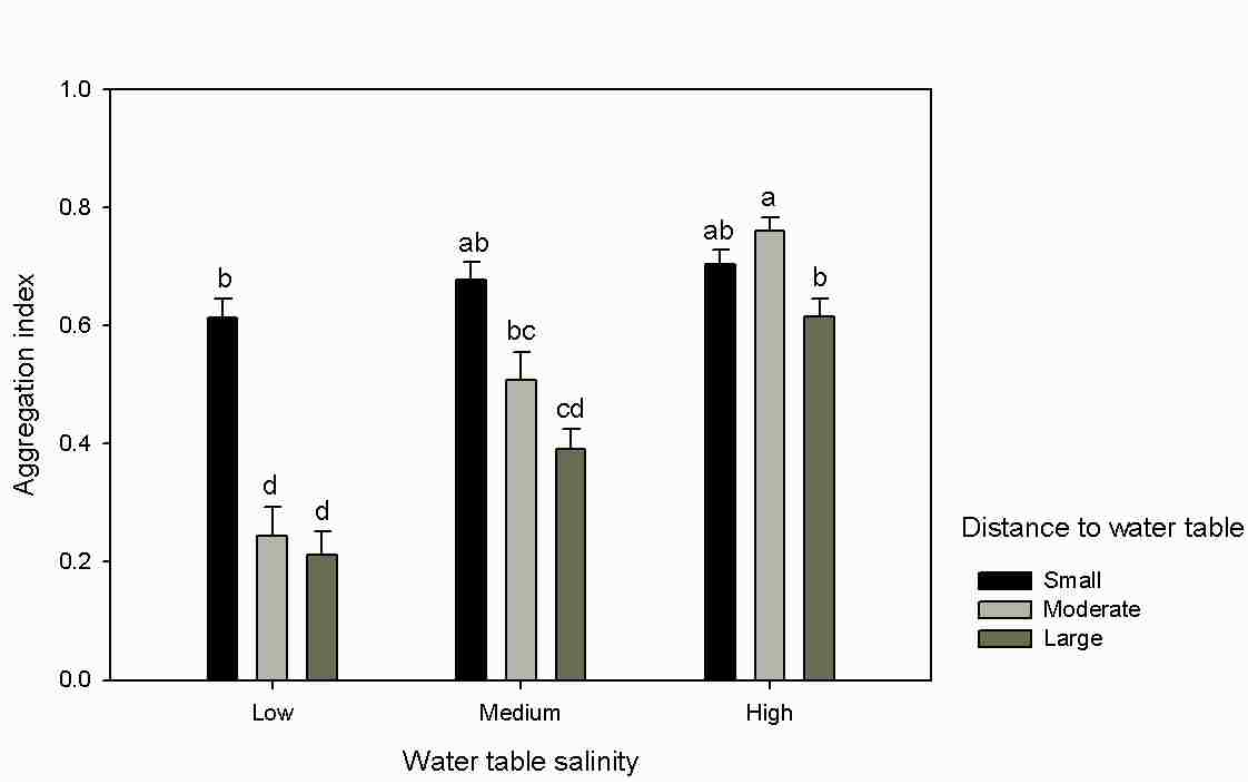

Figure 2.4: The aggregation index in Trial 3, in which the environmental gradient was removed, at different levels of water table salinity and distance to water table. Error bars show the standard error of the mean (SEM). Bars marked with same letters do not differ statistically by all-pairwise comparisons Dwass-Steel-Critchlow-Fligner test following the Kruskal-Wallis test.

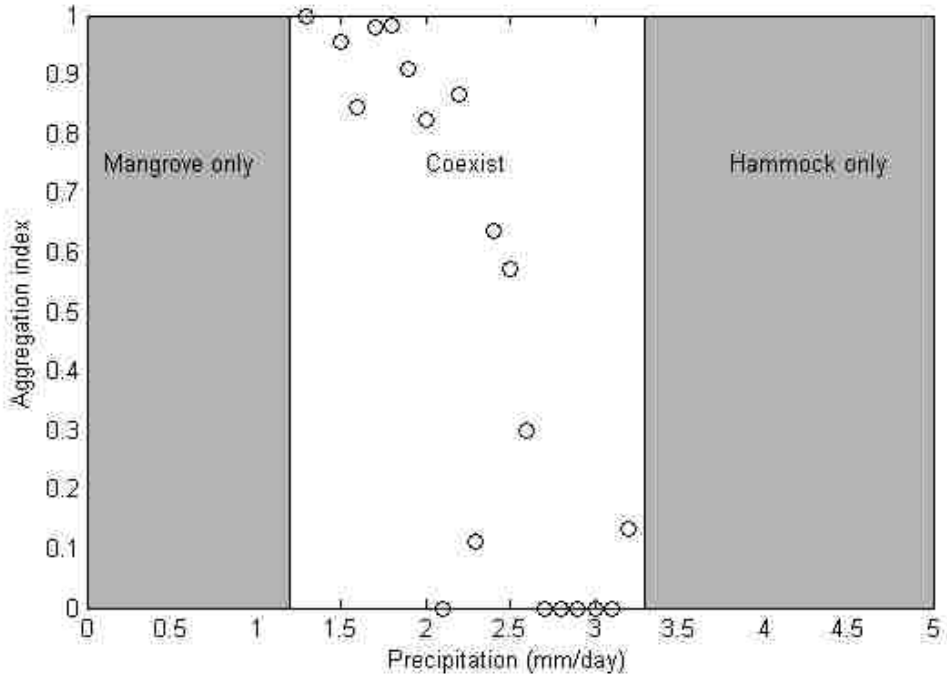

Figure 2.5: Aggregation index versus precipitation when environmental gradients were removed. Gray areas show one species type outcompetes another type, so that an aggregation index cannot be calculated.

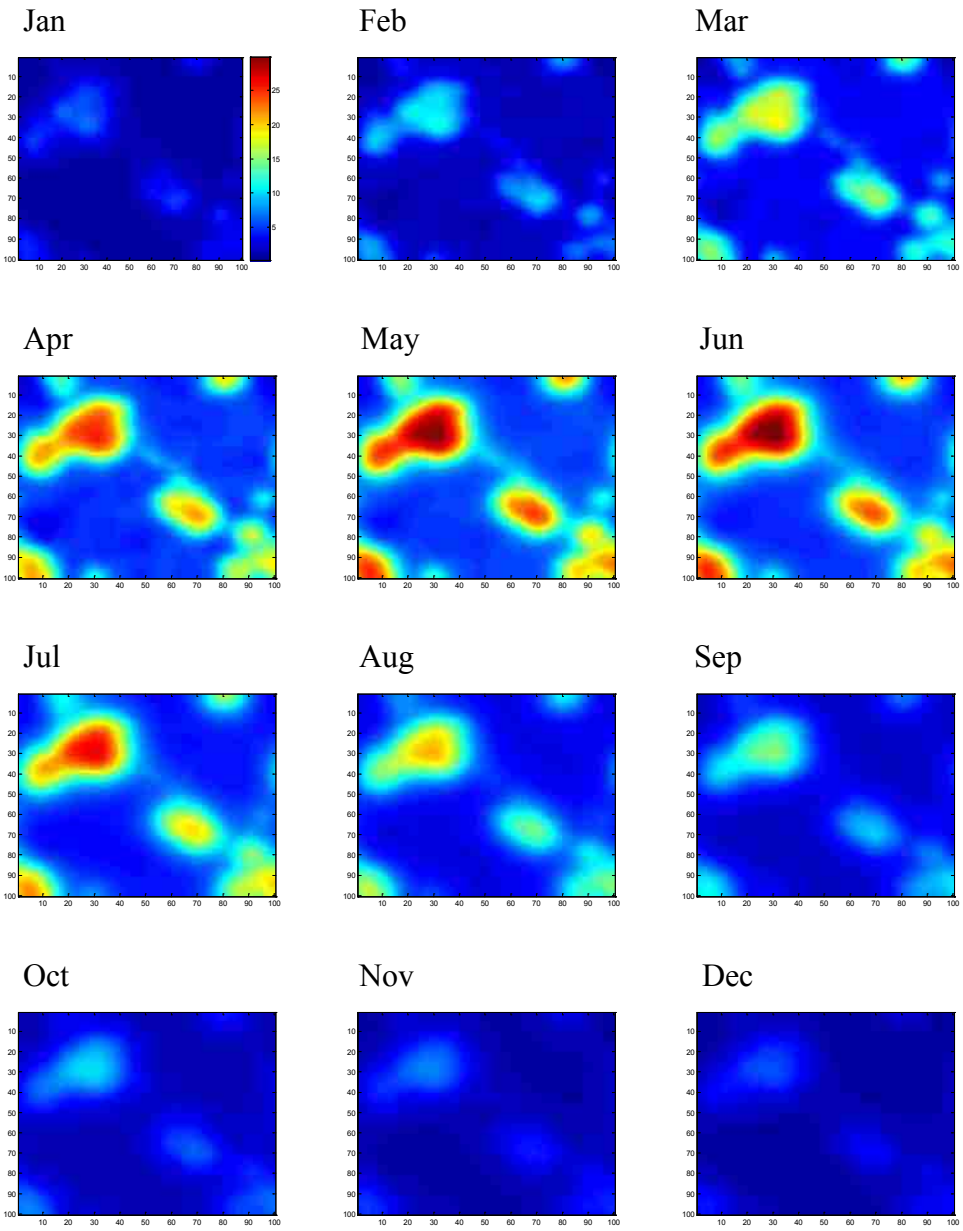

Figure 2.6: Snapshot of soil porewater salinity along the 100 X 100 landscape at each month during the simulation over a year after steady state conditions have been achieved. Color changes from dark blue to red represent salinity values increasing from 0 ppt to 30 ppt. Corresponding vegetation distribution from Figure 2.1c.

Chapter 3

TOWARDS A THEORY OF ECOTONE RESILIENCE[2]

Summary

Ecotones represent locations where vegetation change is likely to occur as a result of climate and other environmental changes. Using a model of an ecotone vulnerable to such future changes, I estimated the resilience of the ecotone to disturbances. In the case studied, each vegetation type, through soil feedback loops, promoted local soil salinity levels that favor itself in competition with the other type. Bifurcation analysis was used to study the system of equations for the two vegetation types and soil salinity. Alternative stable equilibria, one for salinity-tolerant and one for salinity intolerant vegetation, were shown to exist over a region of the groundwater salinity gradient, bounded by two bifurcation points. This region was shown to depend sensitively on parameters such as the rate of upward infiltration of salinity from groundwater into the soil due to evaporation. I showed also that increasing diffusion rates of vegetation can lead to shrinkage of the range between the two bifurcation points. Sharp ecotones are typical of salt-tolerant vegetation (mangroves) near the coastline and salt-intolerant vegetation inland, even though the underlying elevation and groundwater salinity change very gradually. A disturbance such as an input of salinity to the soil from a storm surge could upset this stable boundary, leading to a regime shift of salinity-tolerant vegetation inland. I showed, however, that, for my model as least, a simple pulse disturbance would not be sufficient; the salinity would have to be held at a high level, as a 'press,' for some time. The approach used here should be generalizable to study the resilience of a variety of ecotones to disturbances.

[2] Theoretical Population Biology.In press

Background

Ecological resilience and regime shifts have been major topics in the study of ecosystem dynamics during the last two decades (Briske et al., 2010; Scheffer et al., 2001). These concepts are particularly important to the study of ecotones, or zones over which there is a rapid transition between adjacent types of vegetation. Ecotones are zones where changes in vegetation type are likely to occur when environmental conditions change. Ecotones usually occur along externally imposed environmental gradients; that is, such as changes in edaphic characteristics or climatic variables, such as temperature or precipitation. In some cases, these environmental gradients are strong enough that they determine a boundary that rigidly separates the vegetation types, such as occurs at the shore of a lake. In other cases the gradients are weak enough, or the vegetation types are plastic enough in their tolerances, that there is large potential range of overlap between the vegetation types. In such cases, the ecotone might occur as a gradual change from dominance of one vegetation type to the other. However, situations also exist where even relatively weak environmental gradients are characterized by ecotones so sharp that they almost resemble edges. These can result from what has been termed a positive feedback 'switch', in which each vegetation type alters the local environment through positive feedback in a way that favors itself (Lloyd et al., 2000; Wilson and Agnew, 1992), such that it excludes the other type.

When different vegetation types can each potentially occupy the same sites along some region of a gradient, and also exhibit this switch behavior, then alternative stable states, or bistability, can exist in this region. Alternative stable states and their mechanisms have been identified for some ecotones that have been studied in detail.

Among these are grass-tree ecotones (e.g., Accatino et al., 2010; Boughton et al., 2006; Sternberg, 2001; Vilà et al., 2001), alpine tree lines (e.g., Bekker, 2005; Malanson, 1997; Nishimura and Kohyama, 2002; Wiegand et al., 2006), tropical alpine treelines (Bader et al., 2008; Martin et al., 2011) rush-mangrove ecotones (Walker et al., 2003), Sphagnum bog-vascular plant ecotones (Ehrenfeld et al., 2005; Hotes et al., 2010), forest-mire ecotones (Agnew et al., 1993), ecotones between different vegetation successional stages in a calcareous dune slack (Adema and Grootjans, 2003), sclerophyllous shrub–forest ecotones (Odion et al., 2010), and ecotones around allelopathic plants (Gentle and Duggin, 1997). These systems all involve a switch mechanism (Wilson and Agnew, 1992) of some sort, in which vegetation types alter the environment to favor themselves and exclude other types

Some of the mechanisms that maintain ecotones act continuously in time, but others are episodic. Fire is an episodic mechanism that favors pyrogenic vegetation such as grass over forest in such ecotones as Mediterranean Basin woodlands (Vilà et al., 2001), higher elevation pines over lower elevation cloud forest in tropical mountains (Martin et al., 2011), and sclerophyllous shrub vegetation over forest in mountains such as the Klamath Mountains of California (Odion et al., 2010). In the absence of fire, the non-pyrogenic vegetation is superior to the pyrogenic vegetation is superior (e.g., forest shades out grass), so the ecotone could move shift in favor of the former during intervals between fires, but occasional fire events will burn back the young growth of non-pyrogenic vegetation, setting back the ecotone. The forest-mire ecotone is an example of continuous mechanism of enforcement of a sharp ecotone. Tree seedlings cannot establish in the mire, but they can establish on fallen tree boles, maintaining the boundary

(Agnew et al., 1993). In both of these examples, the vegetation types show this switch mechanism.

In all of the examples there are zones along the environmental gradient where the fundamental conditions are such that either of two alternative vegetation types could exist. The ecotone merely represents the current position of the sharp boundary within this area of overlap, inflenced by the positive feedbacks of each vegetation type favoring itself and excluding the other. Because this overlap area is a zone of bistability, it is possible that either changing environmental conditions or disturbances could lead to regime shifts; that is, sudden, spatially extensive changes in favor of one of the vegetation types that shifts the position of the ecotone. The reason that regime shifts can be sudden and extensive stems from the positive feedbacks that maintain the ecotone between the two vegetation types. Because of these self-reinforcing positive feedbacks, the ecotone resists change until the change in the environment is great enough to overcome the feedbacks. That is termed 'resilience'. But once the resilience of the self-reinforcing feedbacks is overcome, feedbacks operate to promote change to the alternative vegetation type. Two types of environmental change can trigger regime shift (e.g., Beisner et al., 2003; Briske et al., 2008). One is gradual change in some environmental variable that eventually reaches a threshold past which the shift occurs (e.g., Carpenter et al., 1999; Folke et al., 2004; Petersen et al., 2008; Scheffer et al., 2001). The second type of change is a large disturbance that pushes the system beyond the threshold, such that it cannot return to the original vegetation state, but moves to the alternative state (e.g., May, 1977; Stringham et al., 2003). If the disturbance is not so large that it pushes the system outside its domain of

ecological resilience, the ecosystem can return to its original state following a disturbance (Holling, 1973).

Areas on which gradients are slight may be vulnerable to regime shifts covering large areas, The Everglades in southern Florida, which is very flat in elevation, is one such place, and thus is of special concern with respect to the potential effects of climate change. Regime shifts from one stable state to alternative stable state due to disturbance have been hypothesized to be possible in both the coastal margin and freshwater marshes of the Everglades (D'Odorico et al., 2011; Larsen and Harvey, 2010; Sternberg et al., 2007).

Because ecotones are places along which regime shifts are most likely to occur, ways of estimating the resilience of these ecotones are needed (Briske et al., 2008). This chapter examines an ecotone in the coastal Everglades that has been the object of recent study (Sternberg et al., 2007; Teh et al., 2008), the case of competition between salt-tolerant (halophytic) mangroves and salt-intolerant (glycophytic) hardwood hammock or freshwater marsh vegetation types that can coexist in coastal areas, such as the southern coast of Florida. I use this as a specific case of an ecotone that is vulnerable to a regime shift. I analyze a model of this system and estimate the resilience of the system against the most likely cause of regime shift, a storm surge. Although the model is applied to the specific case of an ecotone between halophytic and glycophytic vegetation, it is generic in nature.

Empirical research shows that mangrove and hardwood hammock vegetation types are spatially separated by sharp ecotones, such that salt-tolerant mangroves line the coastal areas, and salt-intolerant species, hardwood hammocks or freshwater marsh,

occupy slightly higher elevations where salinity is lower (Ross et al., 1992). The soil salinity level decreases sharply across the boundary from salt-tolerant to salt-intolerant vegetation. The differences in elevation may be so slight that it is not clear why the sharp ecotones exist precisely where they do. This led Sternberg et al. (2007) to propose that feedback effects of the two vegetation types on local soil salinity maintain the sharp ecotone. The ecohydrology of the salt-tolerant vegetation (mangroves) promotes high local soil salinity by maintaining high transpiration even when soil salinity is high, while the salt-intolerant vegetation tends to promote low levels of local soil salinity, by decreasing transpiration when soil salinity is high (Lin and Sternberg, 1992; Passioura et al., 1992; Volkmar et al., 1998). But it has also been suggested that a sufficiently large pulse of salinity, due to a storm surge, could cause a regime shift, moving the location of the ecotone inland from the coast (Teh et al., 2008).

My objective was to build a model of an appropriate degree of complexity to capture the mechanisms in the mangrove-hammock ecotone, but to also allow analysis. Models built by theoretical ecologists to describe regime shifts can, for convenience, be classified into three general categories of increasing complexity; (1) systems with a single variable (e.g., a species population) with multiple equilibria (May, 1977), (2) systems with two or more variables (e.g., competing species populations) interacting through positive feedback loops (Accatino et al., 2010; Churkina and Svirezhev, 1995; Genkai-Kato and Carpenter, 2005; Gilad et al., 2007), but still analytically tractable, and (3) large network simulation models, which can only be studied numerically (Shannon et al., 2004). Systems of two competing vegetation types, each of which tends to create a local environment (e.g., abiotic conditions) favorable to itself, can often be described with

models that fall into the second category; that is, they are simple enough that some mathematical analysis is possible. Such systems can be described fairly simply in terms of feedback loops between each vegetation type and its local environment. I take this approach to consider the case in which the one vegetation type can create changes in the local environmental conditions that inhibit the other vegetation type, while the other vegetation type is a better competitor in the absence of those high levels of the inhibitor. Together, these mechanisms maintain a stable spatial boundary or ecotone between the vegetation types. I hypothesize, however, that a sufficiently strong external disturbance, by influencing the inhibitor concentration over parts of the spatial domain of the competing species, might cause a regime shift involving the two vegetation types, in which one vegetation type expands in space at the expense of the other. The inhibitor in my case is salinity and storm surges are such disturbances, as they can push large volumes of sea water far inland, carrying salinity far up the usual gradient from marine to freshwater conditions (Krauss et al., 2009)

Theoretical studies have shown that spatial heterogeneity may weaken the tendency for large-scale catastrophic regime shifts in ecosystems if local environmental characteristics vary along a smooth gradient (van Nes and Scheffer, 2005). This is a situation that applies to my case of coastal vegetation, as groundwater salinity, which plays a role in soil salinity dynamics, decreases gradually as the distance inland from the coastline increases. Here, I first examine the dynamics of two competing coastal plant species, along with the inhibitor, salinity, which is explicitly considered as a variable. Second, I extend the model to the case in which there is a slight gradient in an environmental condition, specifically groundwater salinity along one dimension, in order

to investigate the effect of the gradient on potential large-scale regime shifts. I calculate the resilience of the ecotone; that is, the characteristics of the disturbance needed to cause a large spatial shift in the ecotone.

Method

I consider a very simple model in order to obtain results that are easily comprehended in an analytic framework and that can be compared with analogous models of competing vegetation types. My model combines two-species Lotka-Volterra (LV) competition with the effects of a growth inhibitor, salinity. The model equations for the competing vegetation types are,

$$\frac{dN_1}{dt} = N_1(\rho_1 f(S) - \alpha_{11}N_1 - \alpha_{12}N_2) \tag{3.1}$$

$$\frac{dN_2}{dt} = N_2\left(\rho_2 h(S) - \alpha_{21}N_1 - \alpha_{22}N_2\right) \tag{3.2}$$

where N_1 and N_2 are the biomasses (kg/m^2) of salt-intolerant and salt-tolerant species, respectively. All parameters are positive; ρ_i is the intrinsic growth rate for species i, α_{ij} is the competition coefficient of species j on species i, and $f(S)$ and $h(S)$ are growth rate reduction functions for salt-intolerant (SI) (i.e., freshwater) species and salt-tolerant (ST) (halophytic) species, respectively, as a function of the salinity level in the soil, S. It is well known that in the traditional LV competition model, coexistence occurs only if both

$$\frac{\alpha_{21}}{\alpha_{11}} < \frac{\rho_2 h(S)}{\rho_1 f(S)} \text{ and } \frac{\alpha_{12}}{\alpha_{22}} < \frac{\rho_1 f(S)}{\rho_2 h(S)} \tag{3.3a,b}$$

hold. It is also clear that S affects this relationship. The salinity inhibits growth of the SI species more than the ST species, so $f(S) < h(S)$ for all values of $S > 0$. When salinity increases above about 2 ppt, $f(S)$ decreases dramatically, while $h(S)$ shows little decline

within salinity levels below about 30 ppt (Sternberg et al., 2007). For mathematical convenience, I assume $h(S)$ =1, and $f(S) = \mu/(\mu + S)$, μ is half attenuation coefficient; $f(S)=0.5$, when $S= \mu$. For a list of the parameters and their values, estimated to be consistent with conditions of a coastal Florida ecosystem, see Table 3.1.

Salt-intolerant species are usually superior competitors to salt-tolerant species under low salinity conditions (Kenkel et al., 1991). I assumed SI species can outcompete the ST species under low salinity circumstances (i.e., $\alpha_{21} > \alpha_{12}$). When salinity is very low, $f(S)$ approaches its maximum, 1.0, and criterion (3.3a) is the one that is likely to be violated. This implies that species 1 (SI) has a relatively strong effect on species 2 (ST) and species 2 has a relatively weak effect on species 1, allowing species 1 to exclude species 2. At high salinity, the situation is reversed due to the decreased growth rate of species 1; i.e., $f(S)$ approaches 0, in which case species 2 outcompetes species 1, so that criterion (3.3b) is more likely to be violated, allowing species 2 to exclude species 1. Because the zero-growth isoclines of N_1 and N_2 can intersect when salinity is at intermediate levels, a positive equilibrium can feasibly exist, with coexistence of the two species. Under conditions in which the product of interspecific competition coefficients is larger than the product of intraspecific competition coefficients in equation 3 (or $\alpha_{12}\alpha_{21} > \alpha_{11}\alpha_{22}$), however, both criteria 3a and 3b are violated; that is, the equilibrium point is unstable, and one of the two species will go to extinction, depending on initial population densities. I made this assumption in my model. Figure 1 shows the zero-growth isoclines of the two species. Coexistence is impossible at all three salinity levels shown in the figure.

I make soil salinity, *S*, a variable and introduce an equation to describe the dynamics of salinity. Soil salinity is assumed to be positively affected by salt-tolerant species, following the fact that salt-tolerant plants continuously transpire, even under highly saline circumstances, tending to cause infiltration of salt from saline groundwater (Passioura et al., 1992; Sternberg et al., 2007). I describe salinity dynamics by the following equation,

$$\frac{dS}{dt} = \beta_0 g + \frac{\beta_1 N_2}{k + N_2} g - \varepsilon S \,. \tag{3.4}$$

Here *g* is groundwater salinity and β_0 is coefficient that describes the rate at which salinity infiltrates upwards into the soil from saline groundwater through capillary action, replacing soil water that is lost through evaporation. The second term in (3.4) describes the increase in soil salinity due to the same infiltration process, except that the loss of water from the soil is through evapotranspiration of the salt-tolerant mangroves (for simplicity I ignore the smaller evapotranspiration from the SI species, which does not change my results qualitatively). The final term describes the loss of salinity from the soil, where ε is the washout rate of salinity due to precipitation or other freshwater input.

To extend the model to spatial dynamics along a one-dimensional gradient, I assume that the densities of both vegetation types can vary spatially as distance, *z*, inland from the coast increases. I assume also that groundwater salinity, *g(z)*, decreases monotonically from the coastline, and I add diffusion terms to all equations.

$$\frac{\partial N_1}{\partial t} = N_1(\rho_1 f(S) - \alpha_{11} N_1 - \alpha_{12} N_2) + D_1 \frac{\partial^2 N_1}{\partial z^2} \tag{3.5}$$

$$\frac{\partial N_2}{\partial t} = N_2\left(\rho_2 h(S) - \alpha_{21} N_1 - \alpha_{22} N_2\right) + D_2 \frac{\partial^2 N_2}{\partial z^2} \tag{3.6}$$

$$\frac{\partial S}{\partial t} = \beta_0 g(z) + \frac{\beta_1 N_2}{k + N_2} g(z) - \varepsilon S + D_s \frac{\partial^2 S}{\partial z^2}. \qquad (3.7)$$

The diffusion terms assume that both vegetation types can spread horizontally due to vegetation growth and propagule dispersal and that salinity can also diffuse horizontally. D_1, D_2 and D_s are diffusion rate of species 1, species 2 and salinity, respectively.

The above model is studied using a combination of mathematical and numerical analysis. First I study the equilibrium spatial vegetation patterns that emerge in this model, and then I study the effects of external disturbances on this pattern.

Results

Groundwater salinity g as a bifurcation parameter

I first study the system of equations (3.5, 3.6, and 3.7), without diffusion, by using the groundwater salinity value, g, as a bifurcation parameter. Equations (3.1, 3.2 and 3.4) imply the existence of a positive feedback loop; that is, species 2 has positive effect on soil salinity, while increasing soil salinity inhibits species 1, which benefits species 2 by reducing its direct competition effects. Bifurcation analysis shows that an unstable positive equilibrium occurs over a certain range of groundwater salinity values, g; that is, between the bifurcation points, $g_1^* < g < g_2^*$ (Figure 3.2). Other equilibria include an unstable trivial equilibrium E_0 ($N_1=0$, $N_2=0$, $S>0$), and two boundary equilibria, E_1 ($N_1 = \frac{\rho_1 f(S)}{\alpha_{11}}$, $N_2=0$, $S>0$) and E_2 ($N_1=0$, $N_2 = \frac{\rho_2}{\alpha_{22}}$, $S>0$). These two boundary equilibria represent two alternative steady states, both of which are stable over the range $g_1^* < g < g_2^*$ (Figure 3.2, Appendix B). Outside of this range, only one of these equilibrium points is stable.

Solutions for the values of g_1^* and g_2^* for this system is presented in Appendix A, and the values are shown below:

$$g_1^* = \frac{\varepsilon\mu\left(\frac{\rho_1\alpha_{22}}{\rho_2\alpha_{12}} - 1\right)(k\alpha_{22} + \rho_2)}{k\beta_0\alpha_{22} + (\beta_0 + \beta_1)\rho_2}, \quad g_2^* = \frac{\varepsilon\mu}{\beta_0}\left(\frac{\rho_1\alpha_{21}}{\rho_2\alpha_{11}} - 1\right).$$

The interval (g_1^*, g_2^*) represents the spatial zone along the gradient in which a regime shift from one vegetation type to the other could be caused by a sufficiently large external stress or disturbance. The size of the interval, $\Delta g = g_2^* - g_1^*$, is sensitive to β_0, the coefficient related to the effect of groundwater salinity on soil salinity through upward capillary movement due to evaporation (Figure 3.3). When β_0 is small, the increase in soil salinity due to direct salinity infiltration from groundwater into the soil due to evaporation is likely to be negligible compared with the effect on infiltration due to vegetative evapotranspiration, which makes upward movement of saline groundwater sensitive to the type of vegetation; therefore, g_1^* changes very little with changes in β_0. However, g_2^* is sensitive to changes in β_0. In the range of small β_0, decreasing β_0 causes a rapid increase in g_2^*, so the zone where regime shifts could occur becomes large. In contrast, if the groundwater salinity coefficient, β_0, is relatively large (i.e., larger than the effect of evapotranspiration), g_1^*, along with g_2^*, decreases with increasing values of β_0, so the size interval between them, $\Delta g = g_2^* - g_1^*$, shrinks to relatively small values.

Spatial boundary formation under a groundwater salinity gradient

From the bifurcation analysis above, I know that two alternative stable states exist over a range of groundwater salinities, $g_1^* < g < g_2^*$. It can be shown that, along a gradient of groundwater salinities, when there is no diffusion, there is the possibility of a

discontinuous transition from complete dominance by one species to complete dominance by the other at any point along the gradient, with the location depending on the initial biomasses of each species.

When horizontal spatial diffusion of the three variables is non-zero but small, a stationary solution of the system exists, and it still shows a sharp transition from one species to another species along the gradient (this is a result similar to that of Levin 1974, see Appendix B) . In the following I ignored horizontal diffusion of salinity, because measurements of salinity diffusion in relevant soils (Hollins et al., 2000; Passioura et al., 1992) showed it to be small ($D_s < 0.0003$ m^2/day). As a result, vertical movements of salinity due to evapotranspiration are much faster than horizontal diffusion. I also studied the sensitivity of my simulations to somewhat larger values of the salinity diffusion rate and found that they do not change the position of the sharp transition (results not shown). However, when I increased the non-zero diffusion coefficients of vegetation, D_1 and D_2, I found that the interval over which there are two alternative equilibria is no longer the same as the original interval without diffusion, (g_1^*, g_2^*), but it shrinks as the diffusion coefficient of vegetation increases in size. I was not able to derive expressions for the new bifurcation points, g_1 and g_2, as analytic functions of the D_1 and D_2. Instead, extensive numerical evaluations were used to determine the behavior of the bifurcation points in response to a gradual increase of D_1 and D_2. To calculate these, the diffusion coefficients were incremented together stepwise from zero. After each increment of the diffusion rates, the model was initialized with a large value of one vegetation type and a small amount of the other type, and then simulated to determine the attractors of the new trajectory. Each set of simulations was stopped when a bifurcation point was detected.

Figure 3.4 shows the bifurcation points as a function of the diffusion coefficients. Only diffusion coefficients less than 0.015 were used, because higher diffusion rates led to mixing of the species and a very diffuse boundary, such that no bifurcation point could be detected. As the diffusion rates increase, the bifurcation points converge on each other.

Simulating the effects of size and duration of disturbance on potential regime shifts.

Case 1: Without diffusion.

Regime shifts may occur at any point on the range from g_1^* to g_2^*, over which each of the two boundary equilibria, E_1 and E_2, has its own basin of attraction. Any disturbances that cause N_1 and N_2 to cross over the separatrix from one basin of attraction to the other one will result in a regime shift. I numerically studied many different initial points to identify the basin to which each belongs, enabling us to construct the boundary between basins. First, I investigated the uniform system without diffusion. Figure 3.5 shows the basin boundary, or separatrix, for the special case of g=5.0 ppt. For the parameter values listed in Table 1, the initial biomasses of N_1 and N_2 determine that trajectories stay within the basin of attraction of either E_1 or E_2 (Figure 3.5a). The initial salinities have virtually no influence on the basin of attraction. Even a very high initial value of salinity would not shift the domain of attraction from E_1 to E_2, because the salinity dynamics are much faster than vegetation dynamics, and salinity tends to wash out of the soil before it appreciably affects the biomasses of SI vegetation. Only if I slow down the speed of the salinity dynamics relative to the vegetation dynamics is the basin location of the initial point sensitive to initial salinity (for example, see Figure 3.5b, in which salinity dynamics are slowed down 20-fold). The basins for the equilibria E_1 and E_2 are located on opposite sides of the boundary.

Ecological resilience here is defined to embody the range of disturbance magnitudes that cannot push the system from one basin of attraction into another basin. For example, I investigated whether pulses of salinity, with the vegetation densities unperturbed, would result in a regime shift, if the vegetation state was initially near E_1 (SI dominant). It can be shown, with reference to Figure 3.5a (in which g=5.0 ppt), that a salinity pulse of 20ppt, without any accompanying change in N_1 and N_2, except for a tiny increment in N_2 away from zero (i.e., initially, N_1=2.53, N_2=0.01), will result in trajectories that always remain within the initial basin of attraction of E_1. As g increases, the basin of E_1 will decrease in size. As long as $g<g_2$, however, an instantaneous pulse of salinity alone will not push the system into the basin of E_2. But if the salinity pulse is turned into a 'press', that is, if it is held at about 20 ppt for a sufficiently long period, this can result in a regime shift (Figure 3.6). When salinity S is held at a high level, N_1 starts to decline dramatically, while N_2 stays close to zero for some time due to its low initial value. When S is held to 20 ppt for enough time (8 years, in this case), the trajectory moves from the basin of attraction of E_1 to the basin of attraction of E_2, and then approaches E_2, even though the press on S had been released (T=8 years in Figure 3.6). For shorter press durations, the system will still go back to E_1, after the press on S is released, allowing it to follow the dynamics prescribed by equation (4) (T=7 years in Figure 3.6). Thus, a critical disturbance duration, T, is needed for a regime shift to occur, when the disturbance involves only changing salinity.

Case 2: With diffusion.

Next I investigated the critical disturbance duration, T, when a groundwater salinity gradient, $g(z)$, was included, for a few different levels of the vegetation diffusion

rate. The disturbance was set at S=20 ppt for duration of T years. I used simulations to determine the value of T needed for a regime shift, by incrementing the duration over which S was held at 20 ppp from 0 to larger values of time. After each increment of disturbance duration (T) by 0.1, the simulation was run for initial conditions of N_1 set at equilibrium values along the salinity gradient, and N_2=0.01, S=20, and then run until there was no detectable movement from the new stable state for at least 1000 years. The spatial gradient of salinity along a transect inland from the coast was modeled on a one-dimensional spatial grid of discrete spatial cells in which the groundwater salinity, $g(z_i)$, jumped by 0.01increments of ppt from 0 to 20 ppt over the length of the transect. The critical disturbance duration, T, needed for a vegetation shift to occur was recorded for each point along the salinity gradient.

Figure 3.7 shows that the critical disturbance duration varies with position along the salinity gradient, for different values of the diffusion coefficients. It also shows, as in Figure 3.4, that the distance between the bifurcation points (g_1, g_2) shrinks from the original bifurcation points without diffusion (g_1^*, g_2^*), as the diffusion increases. Outside of the relevant range of bifurcation points, (g_1, g_2) for a given set of diffusion coefficients, only one boundary equilibrium is stable, so regime shift is impossible. Also, a regime shift occurs only when disturbance duration lies above the relevant critical curve in Figure 3.7. The areas below the curves are domains where ecological resilience is effective in resisting a regime shift, such that the system will always return to its original state after withdrawal of the disturbance. The value of critical disturbance duration, T, declines as groundwater salinity g increases, equivalent to regime shifts from N_1 to N_2 (E_1 to E_2) being more likely to occur at high groundwater salinity levels. With diffusion, the

critical value declines sharply as g approaches g_2, where resilience of E_1 decreases to zero. I expect T to approach infinity when g approaches g_1 from above, because regime shift is impossible when $g < g_1$. There was a limit to what I could demonstrate numerically, because the finite (0.01) size of my salinity grid scale did not allow us to let g approach g_1 indefinitely. As diffusion rate increases, potential regime shift zone shrinks, as indicated in Figure 3.4. Overall critical disturbance duration, T, also decreases with diffusion rate.

Figure 3.7 also implies that each patch along the groundwater salinity gradient between the bifurcation points shifts to an alternative stable state at a different value of the disturbance duration. Therefore, the response of the ecosystem to disturbances along the whole gradient might be patchy rather than involving the whole gradient simultaneously. I further find that the response is not straightforwardly linear. In the case of vegetation diffusion between patches, as disturbance duration gradually increases, the ecosystem as a whole does not change until it reaches a critical value; patches close to g_2^* begin to shift first, and for the shift to occur at lower values of g, more time is required (Figure 3.7).

Discussion

This research studied the ecotone between two vegetation types along an environmental gradient. The vegetation types can occur as alternative stable states along part of the gradient on either side of the ecotone. The specific system that I studied, the ecotone between halophytic and glycophytic vegetation along a groundwater salinity gradient, is highly vulnerable to disturbances, such salinity pulses from storm surge overwash, so it was important to estimate the resilience of the ecotone to disturbances of

various magnitudes and durations. I believe this sort of estimation of resilience of an ecotone to a disturbance is relatively novel.

Analogous to other ecotones sharpened by positive feedback switches (e.g., Wilson and Agnew, 1992), in the ecotone considered here each vegetation type promotes local soil salinity levels that favor itself in competition with the other type. I found that, because of these positive feedbacks, there is a range of values of groundwater salinity bounded by two bifurcation points, $g_1^* < g < g_2^*$, for which two alternative equilibria exist. This range was shown to depend sensitively on parameters such as β_0, the rate at which evaporation from soil can cause upward infiltration of salinity from groundwater into the soil. I showed also that increasing diffusion rates of vegetation can lead to shrinkage of the range between the two bifurcation points. The usual pattern of vegetation caused by these interactions is a sharp ecotone between salt-tolerant vegetation (mangroves) near the coastline and salt-intolerant vegetation inland, although the underlying elevation and groundwater salinity may change only slightly along the ecotone. A disturbance such as an input of salinity from a storm surge could upset this stable boundary, leading to a regime shift of salt-tolerant vegetation inland. I showed, however, that, for the parameters of my model as least, a simple pulse disturbance is not sufficient; the salinity has to be held at high levels for some time. Howewer, my model probably overestimates the critical disturbance duration needed for regime shift. This is because I assumed groundwater salinity as a gradient was not increased by the assumed storm surge overwash disturbance, although hydrologic models indicate that groundwater salinity may be increased for years after such a disturbance (personal communication, Eric Swain, U. S. Geological Survey). In addition, direct mortality of SI vegetation and increasing

floating dispersal of mangrove propagules due to storm surge were not considered, both of which could increase the likelihood of a regime shift.

My model considered competition of vegetation types along a gradient in which each vegetation type could modify its local environmental conditions, where the conditions are factors that act as inhibitors of one of the species (salinity in this case, but low temperature, drought, fire, soil pH, allelopathy, etc., in others). This includes a large class of situations. But it should be noted that there is another class of models, structurally similar, that considers competition for a resource (e.g., nutrient) whose rate of input has a spatial gradient. The situation that is analogous to mine is the case in which one species is more efficient and can suppress resource concentration lower than the second species can survive. If the second species is a better competitor for another resource, light, then a stable boundary could occur with the second species occupying the part of the gradient with a higher rate of resource input. Therefore, I expect connections to exist between my study and studies of resource competition along gradients (see, e.g., Grover, 1997).

The Lotka-Volterra competition equations have long provided insights about the possibility of coexistence of two species. The LV equations demonstrated, in particular, that the coexistence of two stable states is impossible when strength of interspecific competition is stronger than strength of intraspecific competition. My analyses were also based on this special case of LV competition. Research has indicated that interspecific competition plays an important role in halophytic species distribution, and it suggests that halophytic species are usually excluded from areas of low salinity by competitive

exclusion, although they do well in monocultures (Kenkel et al., 1991; La Peyre et al., 2001; Silander and Antonovics, 1982).

Two alternative non-coexistence stable states indicate a discontinuous transition from one species to another species can occur as a consequence of a continuous change in the value of some parameter. My results indicate that an ecotone would be formed with a distinct boundary line if groundwater salinity has a spatial gradient. Yamamura (1976) confirmed this property of LV competition equations with mathematical proof. In a non-mathematical context, Shugart et al. (1980) simulated beech-yellow poplar transition along a temperature gradient using an individual-based model. More recently, ecotone models, such as treeline models (Wiegand et al., 2006), have simulated complex positive feedback along smooth environmental gradients, but they all implicitly include competition. In all cases, two competitors form a simple positive feedback loop, which can explain many of sharp species boundaries (DeAngelis et al., 1986).

The rates of diffusion that I consider in this model do not lead to mixing of individuals of the two vegetation types. Instead, in my case there were still sharp boundaries. This is not too surprising, first because positive feedback, which is explicitly connected by salinity dynamics, is strong enough to overcome small diffusional mixing effects. Second, my model simulates gradients instead of homogeneous space, and the gradient narrows the ecotone width. Fagan et al. (1999) suggested that sharp edges can be described by stipulating either zero flux (Neumann boundary) or mortality on a boundary (Dirichlet boundary). The boundary between the two vegetation types in my model corresponds to Dirichlet conditions, because propagules of each species encounter high mortality rates if they happen to land on the other side of the boundary. Mangrove

propagules are outcompeted when their neighbors are mostly glycophytic types, and the glycophytic propagules are not able to survive, given the high salinity of the soil in the zone dominated by mangroves. This corresponds to my mechanism of positive feedback that overcomes diffusion near boundary and increases mortality outside the boundary. Reaction-diffusion systems are classical examples where positive feedback interacts with diffusion to form patterns (Koch and Meinhardt, 1994).

My results are consistent with theoretical studies showing that spatial heterogeneity may weaken the tendency for large-scale catastrophic regime shifts, either if dispersion is unimportant or if local environmental characteristics vary along a smooth gradient (van Nes and Scheffer, 2005). If dispersion between patches is negligible, each patch along a gradient shifts to alternative stable state at different values of overall disturbance duration. Therefore, the response of the ecosystem as a whole is gradual.

These findings all have implications for possible changes in the vegetation of low-lying coastal regions, such as southern Florida, where rising sea level is leading to greater vulnerability of coastal vegetation to storm surges from hurricanes. While the model results here are hypothetical, changes towards salinity-tolerant vegetation have been noted in experimental studies on salinity inundation (Baldwin and Mendelssohn, 1998). Also, observations of coastal areas of Louisiana following hurricanes Katrina and Rita in 2005, which created storm surges affecting the coastal areas of Louisiana, have identified changes towards more salinity-tolerant vegetation(Steyer et al., 2010). Therefore, modeling is needed to anticipate future changes.

Table 3.1 A list of the parameters and their values, estimated to be consistent with conditions of a coastal Florida ecosystem.

Parameter	Definition	Value used	Units
ρ_i	Intrinsic growth rate of species *i*	0.1	$year^{-1}$
α_{ij}	Competition coefficient of species j to species i	$\alpha_{11} = \alpha_{22} = 0.03$	$kg\ m^{-2}\ year^{-1}$
		$\alpha_{12} = 0.02$	
		$\alpha_{21} = 0.06$	
β_0	Salinity increase coefficient by groundwater salinity	0.3	$year^{-1}$
β_1	Salinity increase coefficient by ST species, N_2	1.0	$year^{-1}$
μ	half attenuation coefficient	3.14	ppt
k	Monod coefficient	1.2	kg
ε	Salinity washout rate by precipitation	1.5	$year^{-1}$
g	Groundwater salinity	0~20	ppt
D_1 , D_2 , D_s	Diffusion coefficients	Can be varied	m^2/year

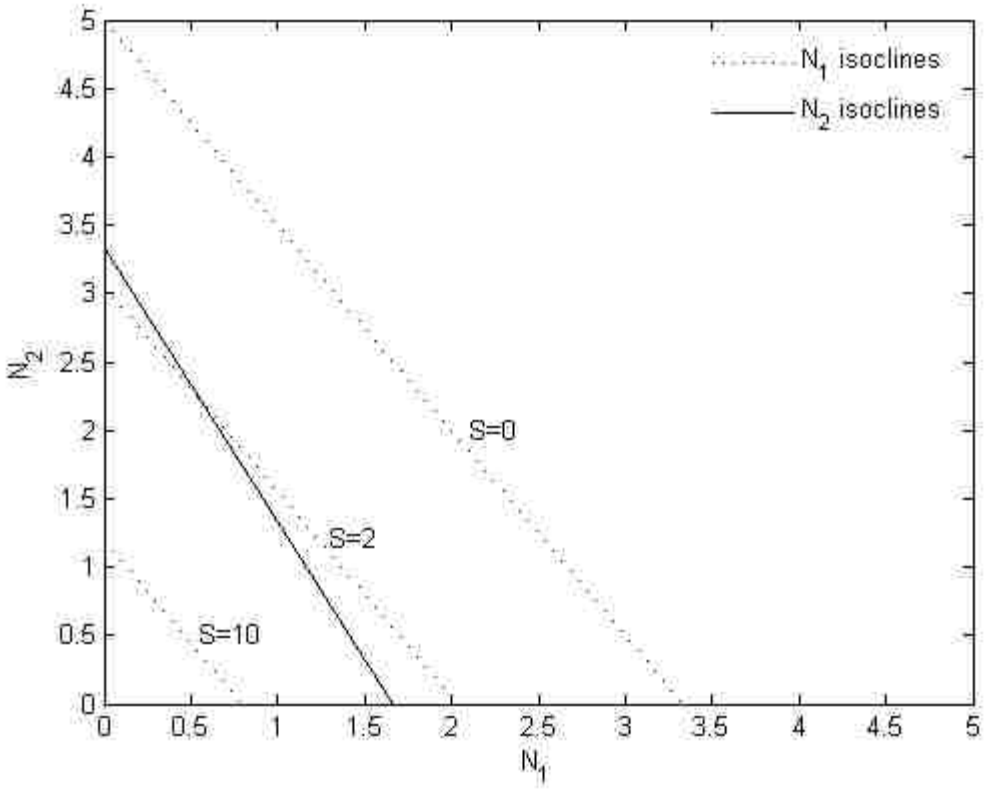

Figure 3.1: Zero-growth isoclines of N_1 (dash line) at condition of S=0, 2 and 10, respectively, and N_2 (solid line).

(a)

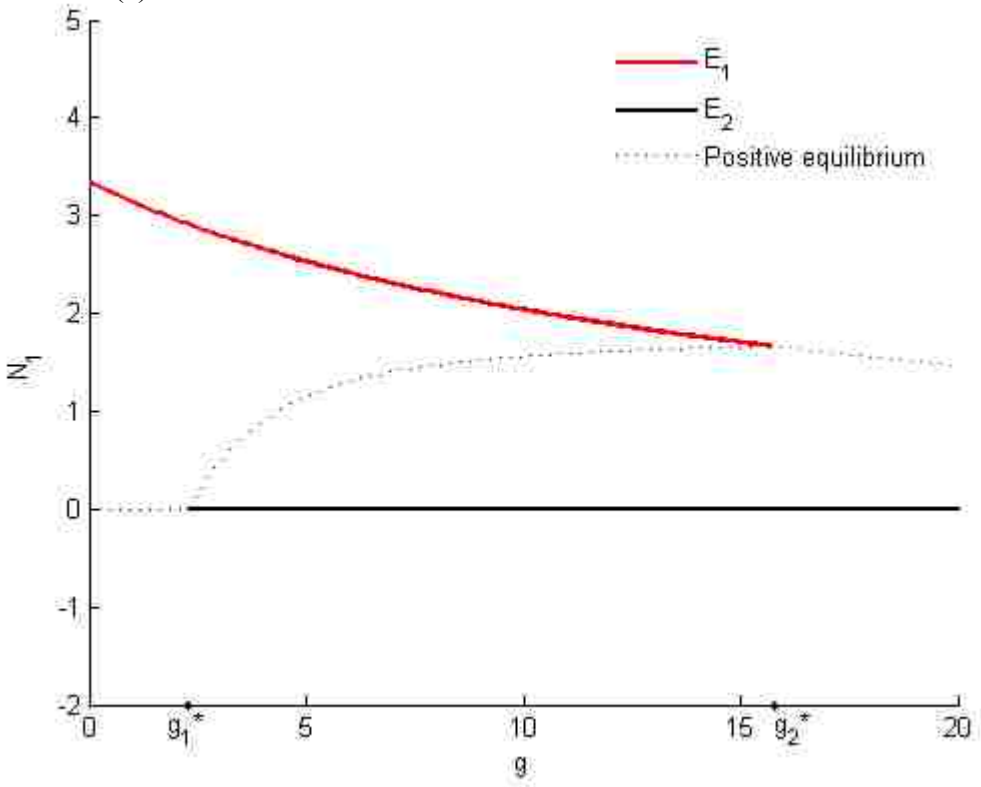

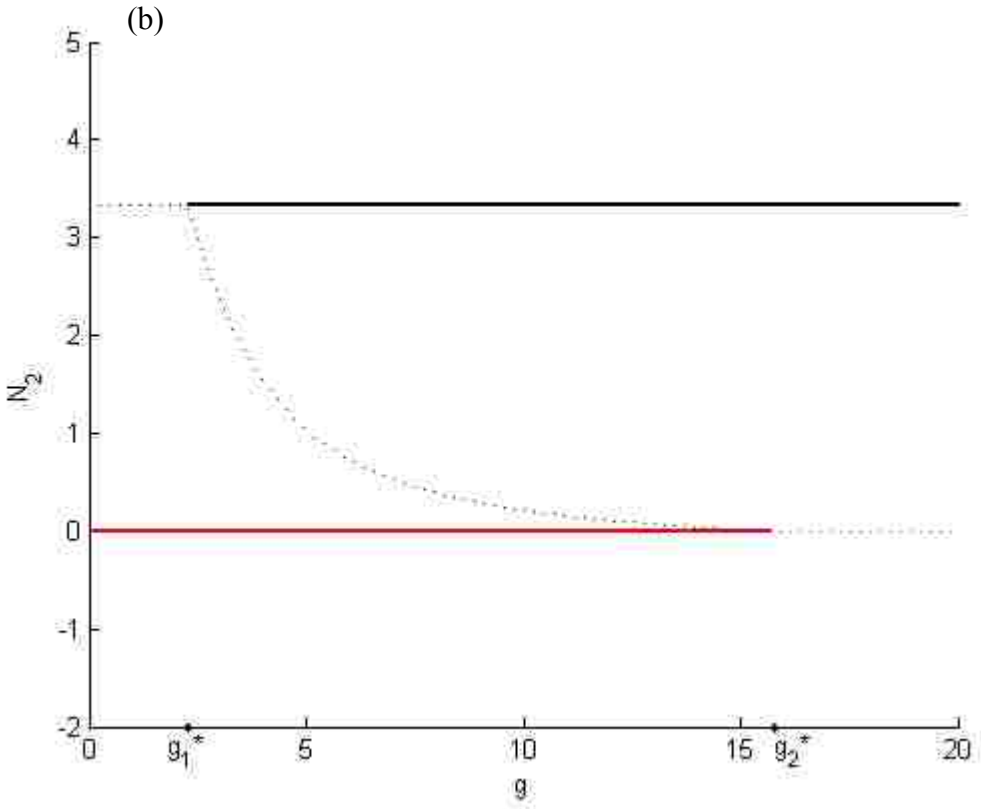

Figure 3.2: Bifurcation diagram showing the values of N_1 and N_2 at the stable equilibria E_1 (red), E_2 (black) (solid lines) and at the unstable equilibrium (dashed blue line) as groundwater salinity, g, is varied. The top panel shows the value of N_1 at E_1 decreasing from a maximum value as g is increased from zero and disappearing at $g = g_2^*$. It also shows N_1 at E_1 remaining at zero as g is decreased from very large values, and disappearing at $g = g_1^*$. In the overlap region between the stable equilibria for N_1, there is an unstable equilibrium denoted by the dashed line. The lower panel shows the analogous pattern for N_2.

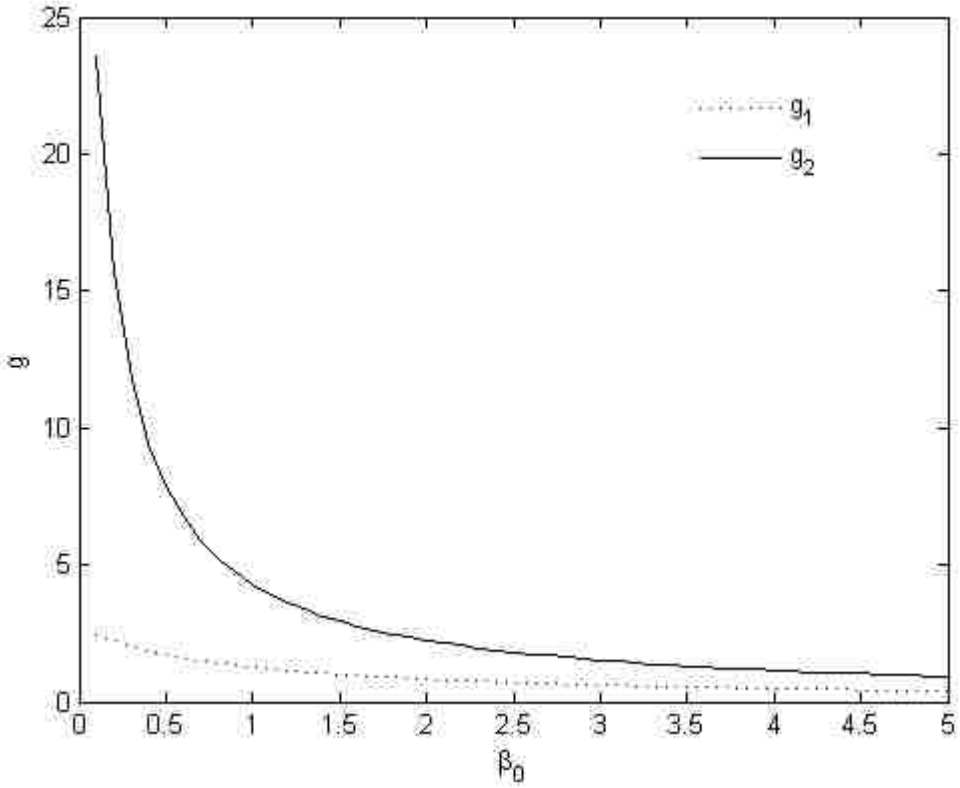

Figure 3.3: Changes of g_1^* and g_2^* as functions of the coefficient, β_0, for the rate of upward capillary movement.

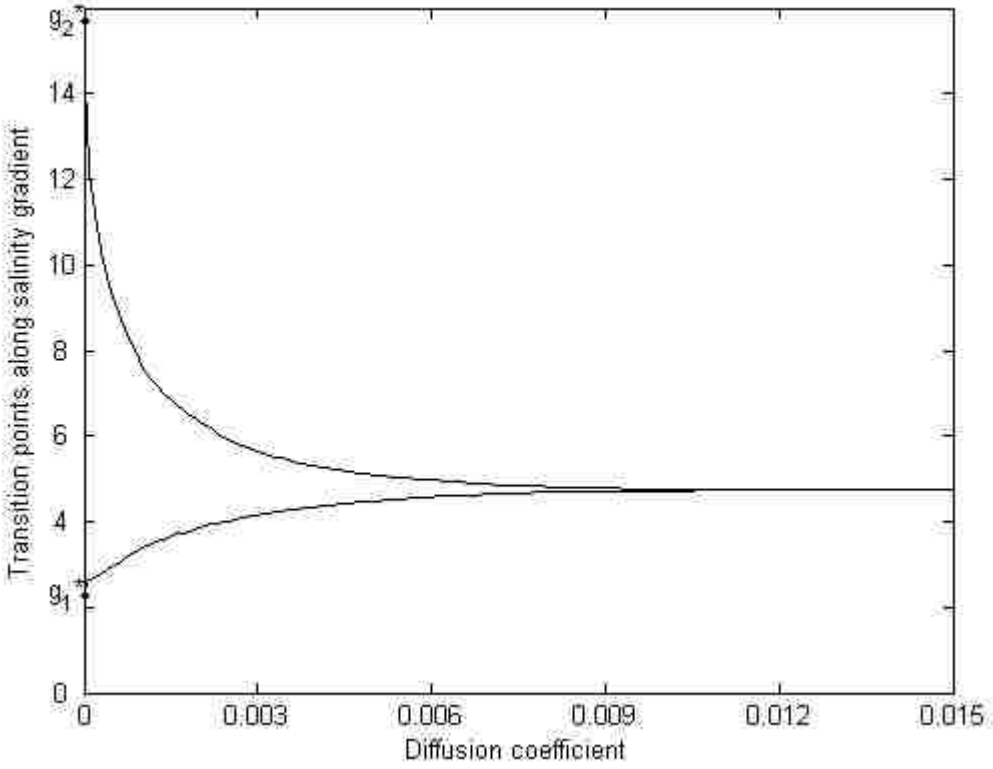

Figure 3.4: Bifurcation points vary with diffusion coefficients of the vegetation. It is assumed that $D_1=D_2$, and that they change together. g_1^* and g_2^* are the bifurcation points when diffusion coefficients equal zero.

(a)

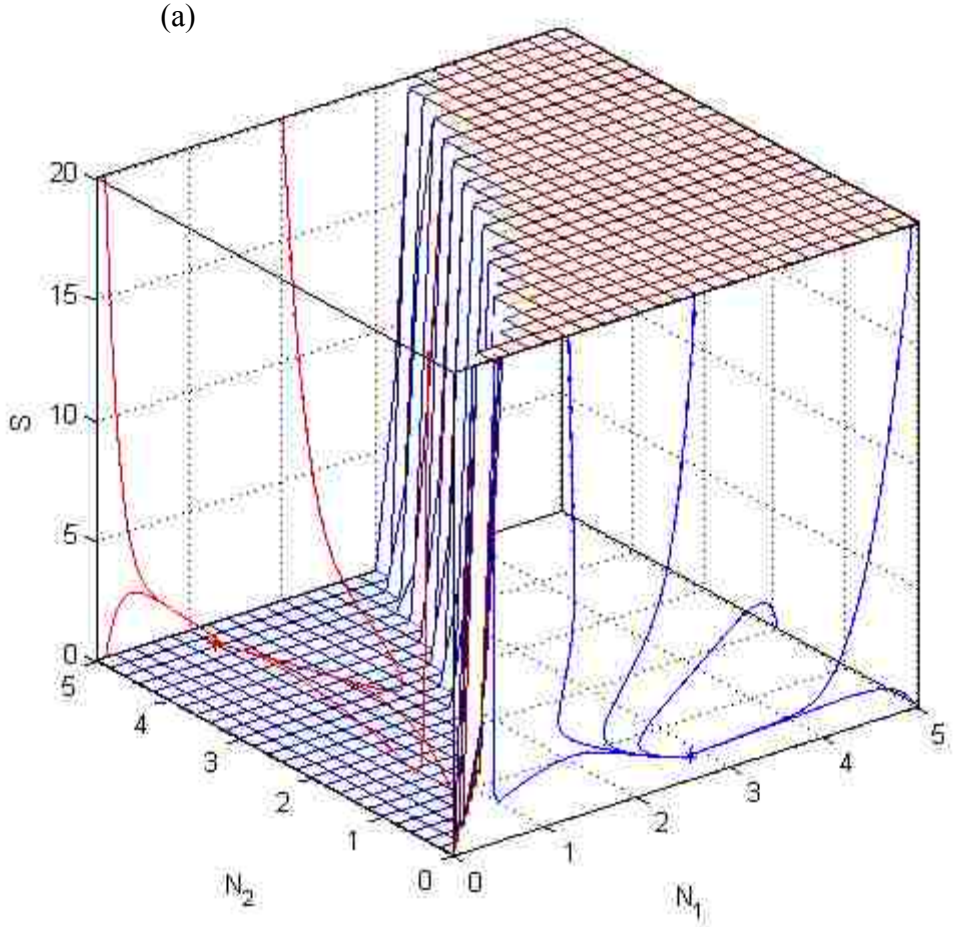

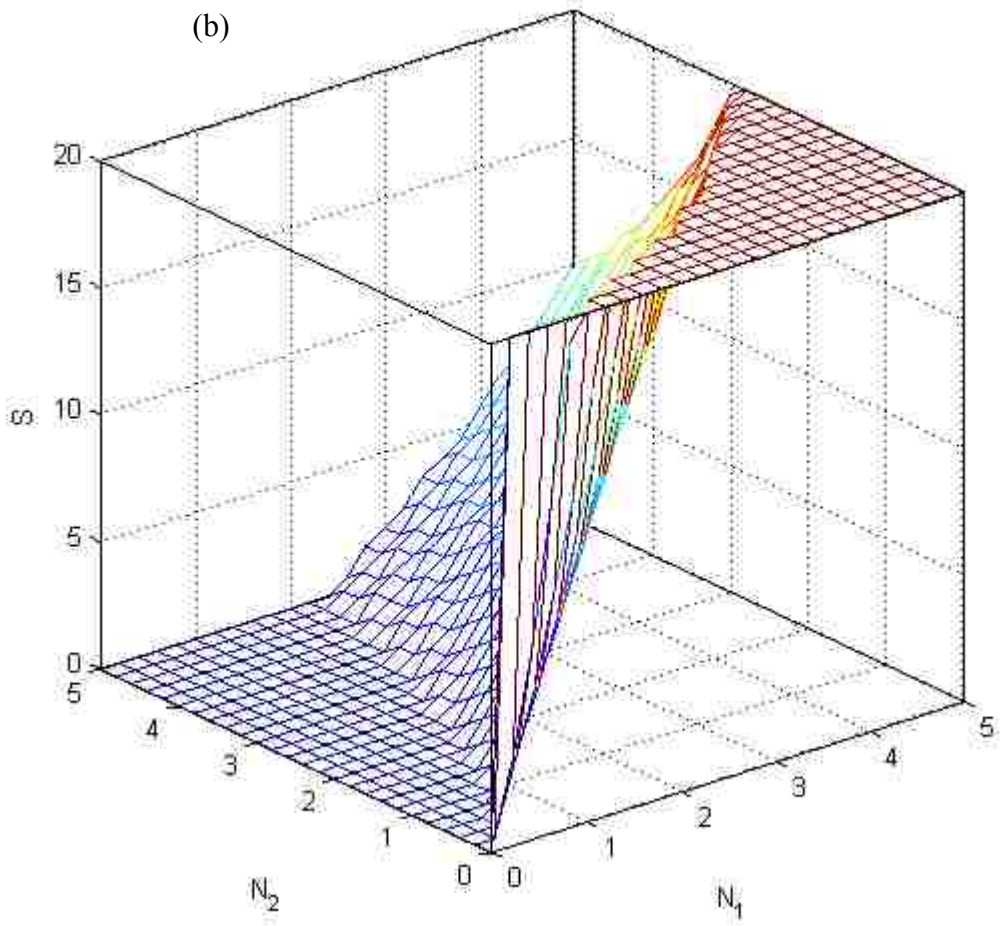

Figure 3.5: Basins of attraction separated by a boundary between E_1 and E_2 for g=5.0 based on (a) parameter values from Table 1, and (b) the case in which salinity dynamics are slowed by 20-fold. Red lines with arrows show the trajectories of different initial points that go to E_2, blue lines with arrows show the trajectories of different initial points that go towards E_1.

(a)

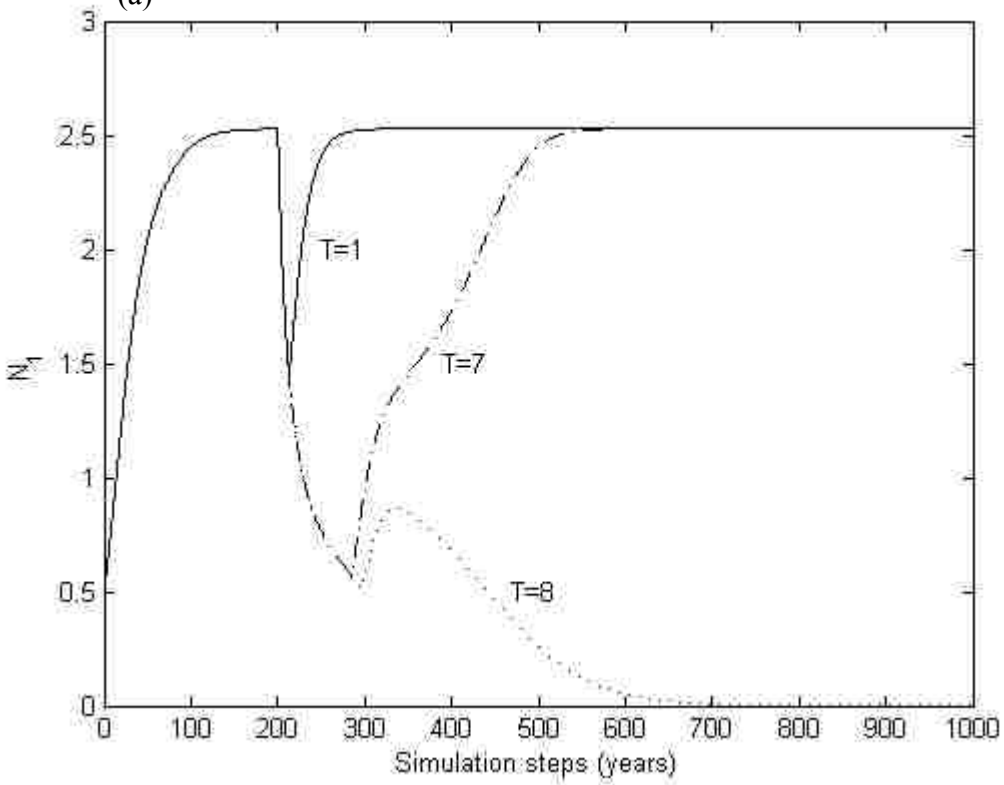
3
2.5
2
1.5
1
0.5
0
0
100
200
300
400
500
600
700
800
900
1000
T=1
T=7
T=8
Simulation steps (years)

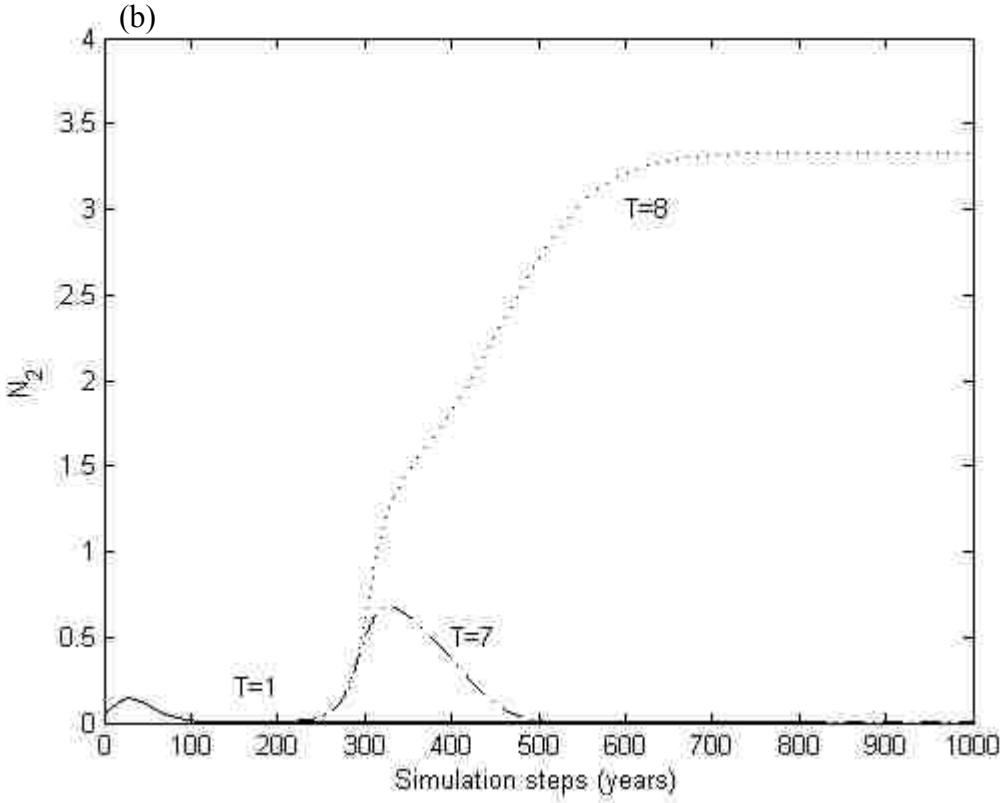

Figure 3.6: Numerical evaluation of (a) N_1 and (b) N_2, g=5.0. The disturbance starts at year 200, and the duration are T=1, 7 and 8 years, respectively.

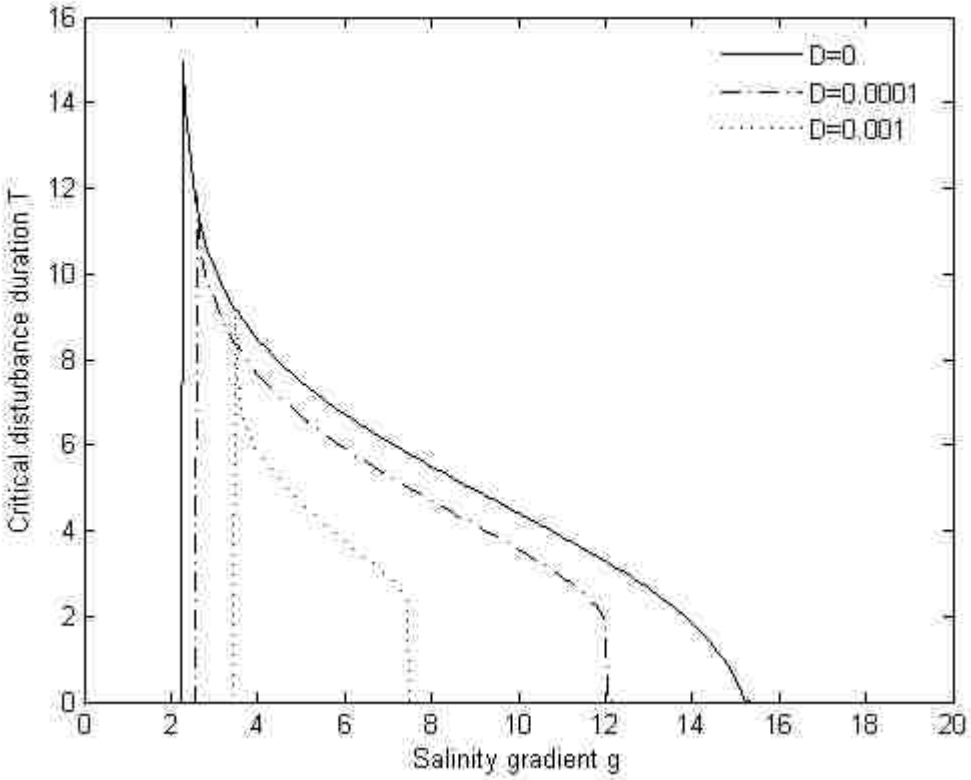

Figure 3.7: Simulation outputs of critical disturbance duration against salinity gradient at different diffusion rate level. Note that the two bifurcation points converge as *D* increases. For convenience, I assumed the same diffusion rates for both vegetation types.

Chapter 4

ANALYSIS AND SIMULATION OF STORM SURGE EFFECTS ON MANGROVE-MARSH ECOTONE

Summary

Mangrove-freshwater marsh ecotones of the Everglades represent transitions between halophytic and glycophytic communities. Although the ecotones appear to be relatively stable, they are likely to be vulnerable to regime shifts from storm surge events that push the ecoteones large distances inland. Using a coupled vegetation and hydrology model, I investigated two factors closely related to storm surge effects on vegetation. One of these factors is salinity intrusion, which has been proposed to be a major disturbance to freshwater wetlands. The other is passive transport of mangrove seedlings, which has rarely been reported as driver for ecotone position changes. The model simulation results indicate that the possibility of a regime shift from freshwater marsh to mangroves is more sensitive to the density of mangrove seedlings transported into the marsh than to the intensity of the storm surge overwash of the marsh end of the ecotone. The observed high salinities after a vegetation regime shift are not a result of the salinity intrusion alone. Once mangrove seedling establish successfully, high salinity will be maintained because of their continued high evapotranspiration, even as salinity builds up in the soil. However, initial salinity intrusion is important, as it helps mangrove prapagules compete with dense freshwater marsh. I applied the model to an Everglades site during the period 2000-2010. Hydrology dynamics were investigated during that period. Empirical data show that hydrological properties recovered rapidly after the impact of Hurricane Wilma in 2005, and the model indicates that changes in the mangrove-freshwater marsh ecotone were unlikely to have resulted from that hurricane.

Background

Mangroves along the Gulf Coast of southwest Florida are valued for their ability to protect freshwater landward habitats, such as freshwater marsh and tree islands, from the impact of erosion due to sea level rise and storm surge events. Field experiments and simulations have shown that mangroves can attenuate storm surge height by 40-50 cm/km by dampening incoming wave energy (Zhang et al., In press). Empirical data indicate that, although the immediate effects of a hurricane winds and waves on a mangrove forest can cause severe structural damage, post-hurricane regeneration usually takes only a short time period to return to a pre-hurricane state (Baldwin et al., 2001; Ross et al., 2006). However, low salinity landward wetlands, despite some protection from the mangroves between them and the sea, are still vulnerable to ocean water intrusion and may suffer long-term changes from the salinity overwash of storm surges (Howes et al., 2010).

The spatial distribution of the mangroves and freshwater marshes in the coastal Everglades is characterized by a sharp transition between the halophytic mangroves and freshwater (glycophytic) marshes along the gradual underlying groundwater salinity gradient from the coast inland. This type of pattern between halophytic and glycophytic vegetation has been noted before (Ungar, 1998) and is analogous to another sharp ecotone that occurs in low-lying coastal habitat between mangrove trees and hardwood hammock trees. The mechanisms for that sharp ecotone were hypothesized by Sternberg et al. (2007) and have been studied in more detail recently by simulation modeling (Jiang et al., 2012). The sharp mangrove-marsh ecotone appears to be ecologically resilient against small disturbances in soil porewater salinity. However, freshwater marshes have

been lost due to salt-water encroachment, at an estimated migration rate of mangroves into freshwater vegetation at 3.1 m/year for the last 70 years in parts of coastal South Florida (Gaiser et al., 2006). Sea level rise is thought to be the primary driver of the changes (Krauss et al., 2011; Saha et al., 2011), with a more than 20cm rise since 1930 (Maul and Martin, 1993). Historical aerial images show that major landward expansion of mangroves at the expense of freshwater marshes occurred between the late 1920s and early 1940s (Ball, 1980; Foster and Smith III, 2001). This indicates that vegetation changes are not a simple linear response to sea level rise, which has led to studies of storm surge effect on mangrove-marsh ecotones, as a possible explanation.

Ocean water intrusion through storm surges may affect large areas on a short time scale; e.g., cause a short-term salinity increase in the soil and groundwater of an inundated area. Whether such short-term pulses can feasibly lead to long-term effects on vegetation depends on many factors; the physiological and competitive properties of local vegetation, precipitation, overland freshwater flow, elevation gradient, and depth and salinity of groundwater (Jiang et al., In press; White and Falkland, 2010). To my knowledge, however, there are no reports of long-term effects on mangrove-marsh ecotones stemming from the salinity overwash from storm surges. That may simply be a result of ecologists not specifically looking for long-term changes from such short-term pulse events. Gradual vegetation changes are not likely to be detected before they become obvious, at which point the possible connection to an earlier storm surge might be forgotten.

I also do not know of any modeling that has predicted changes on mangrove-marsh ecotones due to storm surges. However, it has been hypothesized that large-scale

pulsed disturbance like storm surge event might cause the shifts in the position of other ecotones between halophytic and glycophytic vegetation (Ross et al., 2009; Teh et al., 2008). For example, in tropical and subtropical coastal areas increase in salinities of the unsaturated soil, or vadose zone, induced by salinity overwash events have been known to reduce or eradicate the salinity-intolerant species and promote landward migration of mangroves (see references in Teh et al., 2008). A simulation model of the mangrove-hardwood hammock ecotone in southern Florida indicated that a single large pulse of salinity on freshwater vegetation in the proximity of seed sources of halophytic vegetation might result in a regime change toward the halophytic mangrove vegetation at the expense of the glycophytic hardwood hammock vegetation (Teh et al., 2008). The mechanisms by which storm surge might 'tip' glycophytic vegetation towards halophytic vegetation involve modifications of the local environment by plants, which in turn change the relative competitive advantages of different vegetation types. The processes are discussed in detail in Jiang et al. (2012).

The hypothesis of a regime shift requires two prerequisites; an increase in salinity and an invasion of mangrove seedlings following a storm surge, but other factors are involved as well. In this study, I aim to analyze, using a model based on a regime shift theory, how long-term changes in the mangrove-marsh ecotone could occur after storm surge events, and whether, on the basis of empirical data, they are likely to have occurred in a region of the Everglades affected by a hurricane. First, hydrology and salinity dynamics are investigated from 2000-2010, a period during which Hurricane Wilma passed northwest of Everglades (2005). Second, vegetation dynamics are simulated based on hydrology data from Hurricane Wilma. Finally, long-term vegetation changes

under given scenarios of salinity intrusion and amount of mangrove seedling dispersal to freshwater marsh sites by hypothetical storm surge are simulated.

Method

Study site

The mangrove-marsh ecotone I studied is adjacent to the Harney River estuary (25°25' N, 81°03' W), which is a tributary of the Everglades Shark River slough into the Gulf of Mexico. At US Geology Survey gauging stations SH4 and SH5 there are permanent north-south transects across a 300 m fringe mangrove into the freshwater marsh. The SH4-SH5 transition is approximately 9.5 km upstream on the Harney River. SH4 is a mangrove (*Rhizophora mangle*) dominated site, 40 m inland from the Harney River. SH5 is freshwater marsh (*Cladium jamaicense*) dominated site, 350 m inland from the Harney River.

Water budget and salinity

The water budget was computed as a water balance on a daily basis. Root zone salinity in a given spatial cell is determined by infiltration rate, which is the difference between the precipitation, P, tidal input, T, and evapotranspiration, E. Groundwater salinity in the same given spatial cell is determined by the difference between the infiltration rate and daily groundwater level change. Infiltration rate (I_{NF}) is calculated as follows,

$$I_{NF} = E - P - T.$$

The dynamics of salinity in the root zone are given by Sternberg et al (2007),

$$\rho z \frac{dS_V}{dt} = I_{NF} S_{GW} \qquad for\ I_{NF} > 0 \tag{4.1}$$

$$\rho z \frac{dS_V}{dt} = I_{NF} S_V \qquad for\ I_{NF} < 0 \tag{4.2}$$

where ρ is the porosity, z is root zone height, and S_V and S_{GW} are the salinities of the pore water in the root zone and of the underlying groundwater, respectively and I_{NF} has unit of distance per unit time. Positive values of infiltration indicate capillary rising from the groundwater to the root zone. Conversely, negative values of infiltration indicate percolating downward into the groundwater. The groundwater is the water lens sitting between root zone and underlying saline ocean water which is assumed to be 30 ppt (S_O). The dynamics of salinity in the groundwater are given by the equations,

$$\rho H_{GW} \frac{dS_{GW}}{dt} = \left(I_{NF} + \rho \frac{dH_{GW}}{dt} \right)\left(S_O - S_{GW}\right) \qquad for\ I_{NF} + \rho \frac{dH_{GW}}{dt} > 0, and\ I_{NF} > 0 \tag{4.3}$$

$$\rho H_{GW} \frac{dS_{GW}}{dt} = \left(I_{NF} + \rho \frac{dH_{GW}}{dt} \right)\left(S_O - S_V\right) \qquad for\ I_{NF} + \rho \frac{dH_{GW}}{dt} > 0, and\ I_{NF} < 0 \tag{4.4}$$

$$\rho H_{GW} \frac{dS_{GW}}{dt} = 0 \qquad for\ I_{NF} + \rho \frac{dH_{GW}}{dt} < 0, and\ I_{NF} > 0 \tag{4.5}$$

$$\rho H_{GW} \frac{dS_{GW}}{dt} = I_{NF}\left(S_{GW} - S_V\right) \qquad for\ I_{NF} + \rho \frac{dH_{GW}}{dt} < 0, and\ I_{NF} < 0 \tag{4.6}$$

where H_{GW} is groundwater level. When the balance of groundwater level change compensating infiltration lost to root zone ($I_{NF} + \rho \frac{dH_{GW}}{dt}$) is positive, additional water from underlying saline ocean water will go into groundwater. Otherwise, groundwater salinity doesn't affect by underlying saline water.

To parameterize the model, water level or stage data were obtained from US Geology Survey gages at SH4 and SH5. Daily water level changes were calculated as the difference from 1 day to the next. Daily rainfall data were obtained from the Everglades

Depth Network website (http://sofia.usgs.gov/eden/). Monthly averages and standard deviations were used to generate precipitation input for model. Tidal height and tidal salinity data were obtained from Everglades National Park gauging station on the Harney River (HR). The evapotranspiration, E, I used in the model is calculated by multiplying potential evapotranspiration (PET) by salinity affect (f_S). Daily potential evapotranspiration (PET) data were obtained from the Everglades Depth Network website. Evapotranspiration deductions due to salinity affect (f_S) are significantly different between salt-tolerant (halophytic) and salt-intolerant (glycophytic) species. Glycophytic species decrease transpiration when salinity begins to reach levels the plants cannot tolerate, while halophytic species can continue to transpire at relatively high salinity. To represent the differences in halophytic and glycophytic vegetation, I modified two equations for the salinity affect (f_S) from Sternberg et al (2007).

$$f_{S1} = \frac{3.14}{3.14 + S_V} \tag{4.7}$$

$$f_{S2} = 1.5\left(\frac{60 - S_V}{90 - S_V}\right) \tag{4.8}$$

where f_{S1} is the salinity affect for freshwater marsh, and f_{S2} is the salinity affect for mangroves.

Vegetation dynamics

Competition between mangrove and freshwater marsh was simulated by extending an existing individual based model, the Spatially Explicit Hammocks and Mangroves (SEHM) model (Jiang et al., 2012). Although the SEHM model was developed for two forest tree types, the mechanisms by which sharp ecotones are formed through the interactions of environmental gradients and self-reinforcement of soil

porewater salinity are hypothesized to be the same as those that function in the mangrove-marsh ecotone case. However, direct vegetation competition might be different; e.g., mangroves are superior at competition for light compared with the understory of marsh, whereas the mangroves are less tolerant than marsh to long periods of flooding. I use the Overview, Design Concepts, and Details protocol (Grimm et al., 2006; Grimm et al., 2010) to describe my model. A complete description of the model is available in Appendix C in the supplementary material, as well as in Jiang et al. (2012). Here, I provide only an overview of vegetation dynamics.

I simulated competition between mangroves and freshwater marshes, including the effects of the underlying hydroperiod, soil porewater and ground water salinity. Since freshwater marsh (sawgrass) is relatively spatially homogeneous at a scale of 10 m by 10 m, I do not model individual sawgrass plants. Biomass of sawgrass in a given cell is determined by monthly gains from photosynthesis and losses due to respiration or mortality. Photosynthesis is modeled as the maximum possible rate multiplied by limitation factors, including salinity, light, hydroperiod and mangrove biomass in the given cell. Similar to SEHM (Jiang et al. 2012), mangrove dynamics are modeled as individual-based. During each monthly time step, every tree can have a growth increment that is a function of light, hydroperiod, and the salinity of the particular spatial cell. Then, after a mangrove tree reaches maturity, new seedlings are produced at monthly intervals by the tree. The probability of each of these seedlings producing a successful new recruit depends on the salinity of the soil porewater. At the end of the monthly time step, the probability of death to trees is related to size-dependent factors, such as low d.b.h.

(diameter at breast height of tree), or from reduced growth rate caused by competition or salinity.

Analysis and simulation

Model simulations were performed on a 30 X 30 grid of cells, where each cell was assumed to be 10 X 10 m^2. Elevation of the cells was assumed to be 8 cm to NAVD88. Tidal signal inputs are a maximum at the riverward edge of the simulation landscape, and decrease exponentially inland. At the daily time scale, the hydrodynamics submodel updates salinities of the soil porewater and groundwater. Monthly average values of salinity in each cell, which affect tree growth and seedling establishment, are then returned to vegetation dynamics submodels.

Hydrology data from January 1st 2000 to January 1st 2010 were analyzed to investigate storm surge effects. A major event during that period was the occurrence of Hurricane Wilma, which approached south Florida from the southwest and made landfall near Everglades City, about 50 km north of the Harney River transition as a Category 3 hurricane on October 2005. Elevation of SH4 (river side) and SH5 (inland side) are 11.2 cm and 4.9 cm to datum NAVD88, respectively. Salinity and water level changes after Hurricane Wilma were input to the simulation model and test storm surge effects.

The study sites I investigated are 9.5 km upstream on the Harney River. Salinities of Harney River around my study sites are usually less than 5ppt during wet season. To further investigate how salinity intrusion and mangrove dispersal affect long-term ecotone movement, I simulated vegetation dynamics under given scenarios of both different levels of salinity disturbance duration and different amounts of mangrove propagules carried by the storm surge into original freshwater marsh sites. Due to lack of

studies on mangrove seedling dispersal after the storm surge, I assumed pulse dispersal input to freshwater marsh sites with Poisson distribution on the spatial grid. Three levels of propagule densities, 0, 500 and 1000 seedlings/ha, respectively, were tested. Long-term vegetation dynamics were also simulated under given scenarios of salinity disturbance duration caused by storm surge salinity intrusion. Three levels of salinity intrusion duration, 0, 1 and 2 years respectively, were tested at high salinity of 30 ppt.

Results:

Water budget and salinity:

Precipitation data from 2002 to 2010 show a seasonal pattern (Figure 4.1a), with high rainfall occurring in the wet season (May-November), and also show inter-annual variation. Monthly rainfall amounts in October and November of 2005 (Hurricane Wilma made landfall on October 24, 2005) were within the normal range and the trend compares well to other years of October and November. Potential evapotranspiration for my study site estimated by USGS shows a seasonal pattern with peak occurring between June and August (Figure 4.1b), corresponding to the solar cycle. Hurricane Wilma did not affect potential evapotranspiration. Groundwater level daily data for SH4 and SH5 show a seasonal pattern, with highest levels around September and lowest around April of each year (Figure 4.1c). Water level in SH4 varied slightly less than in SH5 on a seasonal basis. Groundwater level increased significantly on the day Wilma made landfall and the following few days. Groundwater level returned to its usual trajectory of seasonal variation soon after the storm surge.

The groundwater salinity patterns of SH4 and SH5 are different (Figure 4.1d). Groundwater salinity at SH4 increases during dry season, and declines sharply when the

relatively fresher Harney River high tides combine with precipitation to wash out salt during wet season. However, groundwater salinity at SH5 is relatively stable due to its distance away from the riverbank. At SH4, groundwater salinity increased a little bit after Hurricane Wilma due to the storm surge from the ocean side, but still stayed much lower than dry season salinity. Surface water of SH5 is lower than SH4 and followed the same pattern. I still did not find any long lasting salinity increase followed by storm surge for either SH4 or SH5.

Simulations of the soil porewater salinity capture the seasonal signal pattern of surface water from SH4, which is dominated mostly by mangroves (Figure 4.2). While freshwater marsh dominated cells show a damped seasonal pattern similar to mangrove sites, the model does not fit SH5 surface water data very well (Figure 4.2). Soil porewater salinity from mangrove dominated cells increased dramatically in the model during the late dry season due to strong evapotranspiration and little precipitation. Overall salinities of freshwater marsh sites were lower than mangrove sites, especially during dry season. The reason is that at freshwater marsh sites, evapotranspiration slows down if soil porewater salinity starts to increase, thus damping infiltration of underlying saline water.

Vegetation dynamics:

Using the 10-year average hydrology data in the simulation model, the vegetation distribution that is produced shows a clear boundary between mangroves and freshwater marsh, resembling field observations of the coastal Everglades (Figure 4.3). As shown in Figure 1, Hurricane Wilma did not cause significant changes in precipitation, evaporation, or groundwater salinity. Only the water level increased for several days, but then decreased again. My simulations, which include pulse increases of water level and

surface water salinity without any direct mortality to the original vegetation, do not show any long-term effects on freshwater marsh dynamics from Hurricane Wilma stemming from salinity intrusion. It has been reported, however, that direct hurricane wind damage to the mangrove forest can be 30-80% depending on intensity of hurricane and distance to hurricane eye (Armentano et al., 1995; Harcombe et al., 2009; Milbrandt et al., 2006). Figure 4.4 shows the recovery of basal area of mangroves projected by the model following 30%, 50% and 80% mortality, respectively, due to hurricane damage. Mangrove forest recovered in all three cases, without any expansion of freshwater marsh into the mangrove zone.

Effects of salinity intrusion and mangrove dispersal

I combined three levels of salinity intrusion duration and three levels of mangrove seedling density passively dispersed to freshwater marsh sites to further analyze storm surge effects on ecotone dynamics. Results show that in the absence of dispersal of mangrove seedlings by the storm pulse, the ecotone between mangroves and freshwater marsh is, as might be expected, relatively stable, even when the duration of the saltwater intrusion is increased in the model (Figure 4.5 bottom panels). The only inputs of mangrove seedlings in that case were short range dispersal from mangrove trees along the ecotone. In the absence of significant transport of mangrove seedlings by the storm surge, theoretical duration thresholds of high soil salinity necessary to cause a shift must be as high as 8 years, much longer than what would be expected to actually occur (Jiang et al, in press). As more mangrove seedlings are carried by storm surge into freshwater marsh habitats, more marsh habitats change to mangrove permanently (Figure 4.5 top and middle panels). In these cases, salinity intrusion duration strengthens the mangrove

invasion processes. The results correspond to Jiang et al (In press), in which a mathematical model shows that only a "press" disturbance of salinity for a long period of time might cause regime shift. Figure 6 shows an example of a typical cell that was originally occupied by freshwater marsh. A salinity disturbance occurred at year 80 and lasted for 1 year with a moderate amount of transport of mangrove seedlings into the marsh. However, the regime shift of salinity occurred only around year 120, 40 years after the disturbance, by which time the mangrove seedlings had successfully produced adult mangroves, which then accumulate salt in the rooting zone.

Discussion

This research studied regime shift mechanisms of the mangrove-freshwater marsh ecotone caused by storm surge event at southern Florida. I explicitly investigated different levels of two significant factors, salinity intrusion and mangrove seedling transport, associate with the storm surge. This separation of these two factors differs from the studies in the preceding two chapters, in which seedling transport was not explicitly taken into account. These two factors are prerequisites for triggering vegetation changes, in which positive feedback between plants and soil porewater salinity is necessary to cause the regime shift. I discovered that the spatial extent of the regime shift responded more sensitively to the number of mangrove seedlings transported into the marsh area than to the salinity intrusion itself. Once the mangrove seedlings were successfully established, the soil porewater salinity increased due to continuing evapotranspiration by the mangroves, even as soil porewater salinity increased to high levels.

Hurricane Wilma did not cause significant hydrology changes at my study sites for several reasons. First, the ecotone transition is 9.5 km upstream on the Harney River.

Intrusion of water from Harney River by Hurricane Wilma was much fresher than ocean water, and even less saline than groundwater of SH4. In addition, saline water intrusion after Wilma was washed out by heavy rainfall during wet season. Furthermore, the slightly lower elevation of SH5 helped in the accumulation of freshwater from upstream. However, hurricanes might cause severe hydrology changes at other locations. For example, high groundwater salinities could last for three years in certain areas where drainage of surface water is slow, as shown from a hindcast hydrology model of the Great Miami Hurricane at 1926 (Eric Swain, personal communication).

Although sea level rise and storm surges have been considered to be primary drivers of coastal vegetation changes, the mechanisms by which they trigger vegetation changes are different. On the one hand, sea level rise is a gradual change that can eventually push environmental conditions (e.g., groundwater salinity) past a threshold, beyond which a regime shift of an affected vegetation zone from glycophytic to halophytic vegetation. On the other hand, a regime shift caused by storm surge is a large disturbance that pushes the system beyond the threshold all at once, such that it cannot return to the original vegetation state (glycophytic), but moves to the alternative state (halophytic). If the disturbance is not so large that it pushes the system outside its domain of ecological resilience, the ecosystem can return to its original state following a disturbance. Evapotranspiration is the process causing the largest water output from the Everglades ecosystem (Saha et al., 2012), and it tends to increase soil salinity by leaving salt in the soil. Plants can adjust their transpiration in response to changing soil salinity conditions and therefore modify local salinity conditions. If an external salinity disturbance lasts for enough time, mangroves can invade freshwater marsh habitats and

then maintain high salinity via evapotranspiration. If mangroves do not invade the marsh habitats and establish successfully during the disturbance time window, the following wet season would wash out salt and whole system would return to original state.

My analysis from hydrology-related processes indicates that the storm surge disturbance from Hurricane Wilma did not trigger regime shift at the site for which I have data. Instead the hydrologic system returned to its original state following the storm surge. I do not have direct data on mangrove seedling transport at my study site following Hurricane Wilma. Although there are rare reports of mangrove seedling dispersal after the storm surge (Rathcke and Landry, 2003), lots of experiments on long-distance mangrove dispersal indicate that pulse dispersal after storm surge is possible (Rabinowitz, 1978a; Rabinowitz, 1978b; Sousa et al., 2007). My research may inspire empirical studies to investigate mangrove dispersal and establishment after a storm surge.

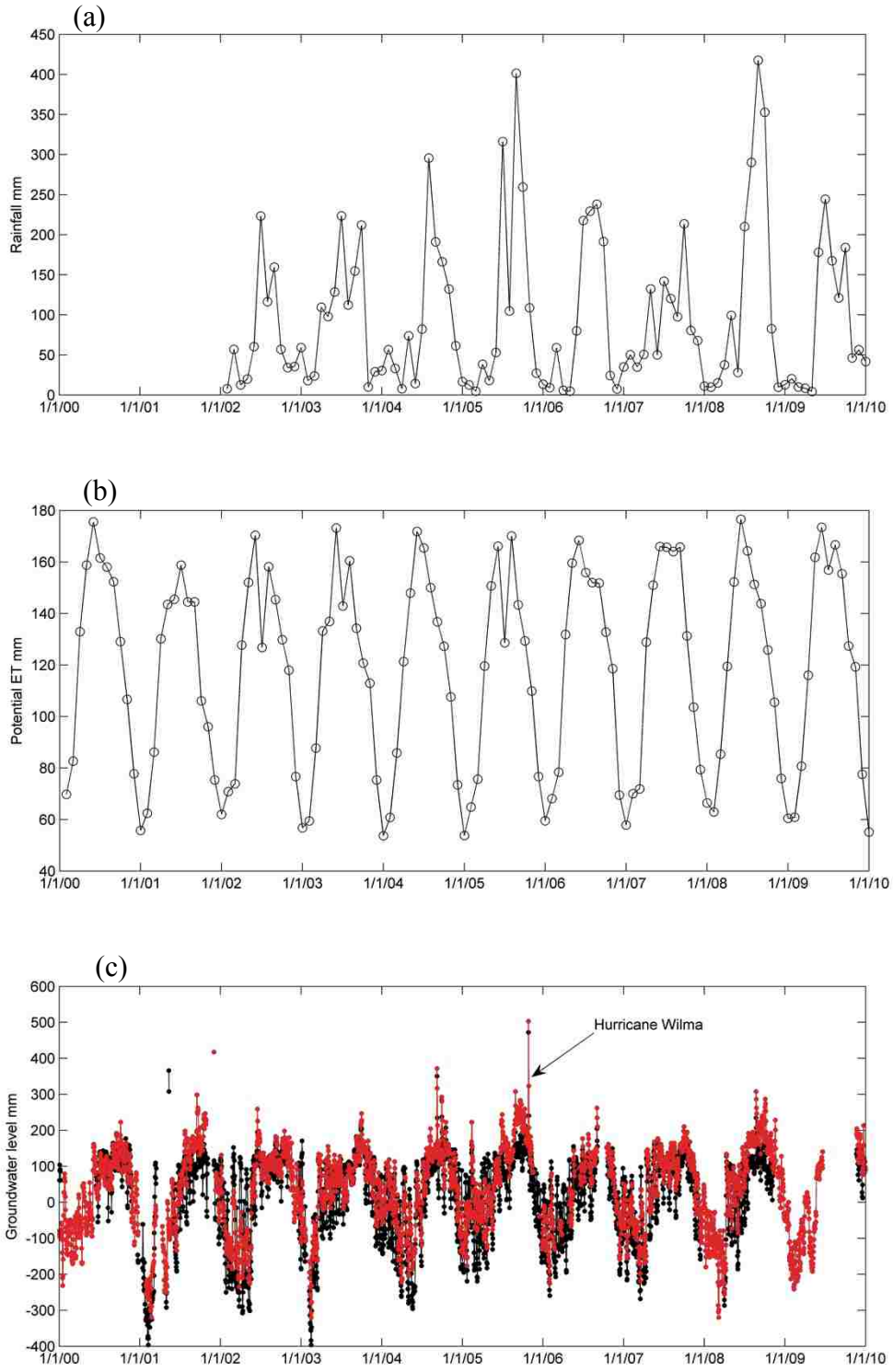
(a)
Rainfall mm
450
400
350
300
250
200
150
100
50
0
1/1/00
1/1/01
1/1/02
1/1/03
1/1/04
1/1/05
1/1/06
1/1/07
1/1/08
1/1/09
1/1/10
(b)
Potential ET mm
180
160
140
120
100
80
60
40
1/1/00
1/1/01
1/1/02
1/1/03
1/1/04
1/1/05
1/1/06
1/1/07
1/1/08
1/1/09
1/1/10
(c)
Groundwater level mm
600
500
400
300
200
100
0
-100
-200
-300
-400
Hurricane Wilma
1/1/00
1/1/01
1/1/02
1/1/03
1/1/04
1/1/05
1/1/06
1/1/07
1/1/08
1/1/09
1/1/10

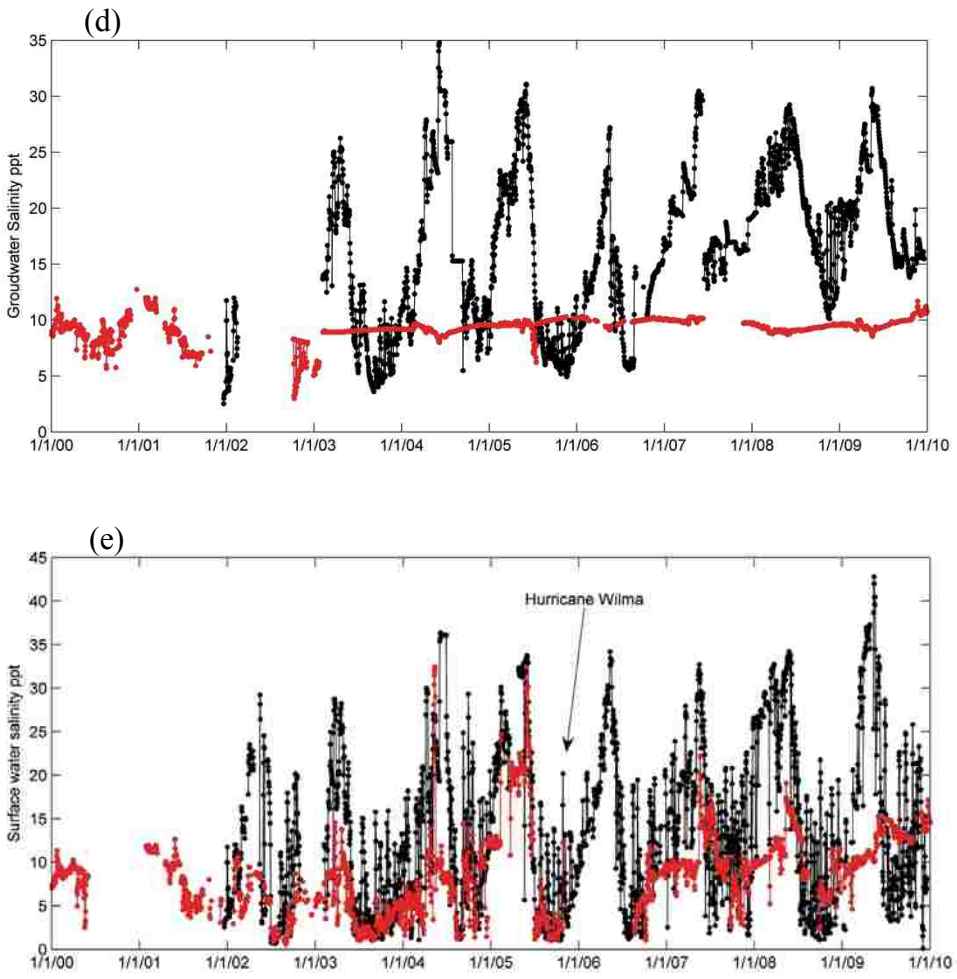

Figure 4.1 Raw data for (a) precipitation, (b) potential evapotranspiration, (c) groundwater level, (d) groundwater salinity, (e) surface water salinity; over study site SH4 (black lines) and SH5 (red lines).

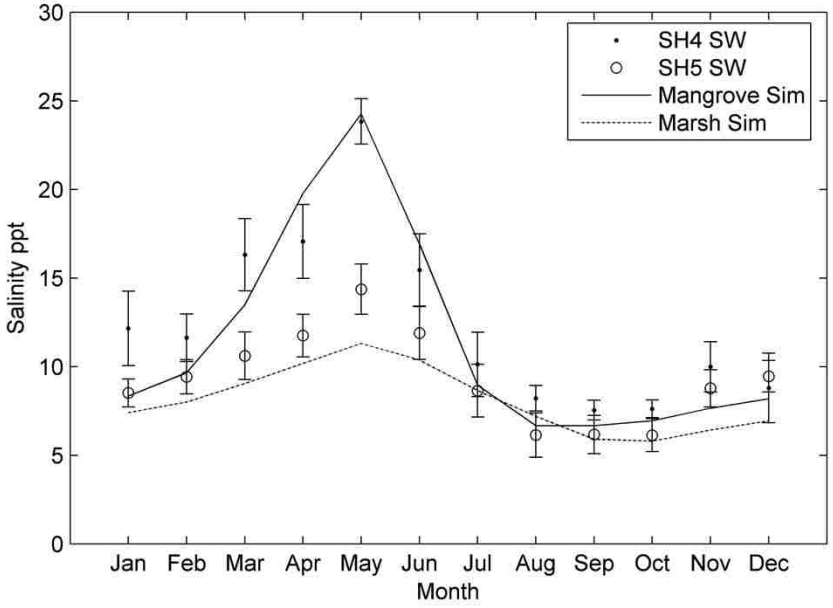

Figure 4.2 Simulation of soil porewater salinities averaging mangrove sites and marsh sites, respectively, compared to monthly average with standard error of surface water salinities from SH4 and SH5, respectively.

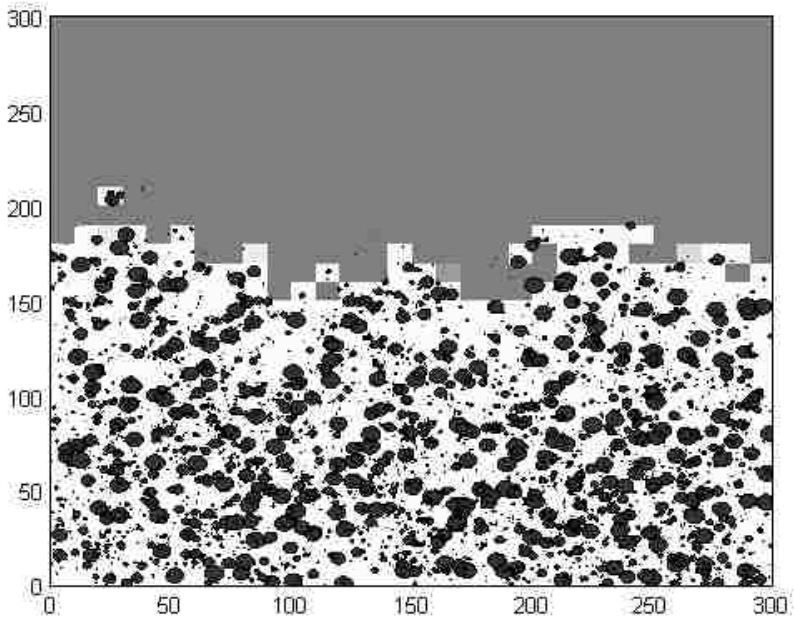

Figure 4.3 Spatial distribution of individual mangroves (dark circles) and freshwater marsh (gray cells) output from simulation model

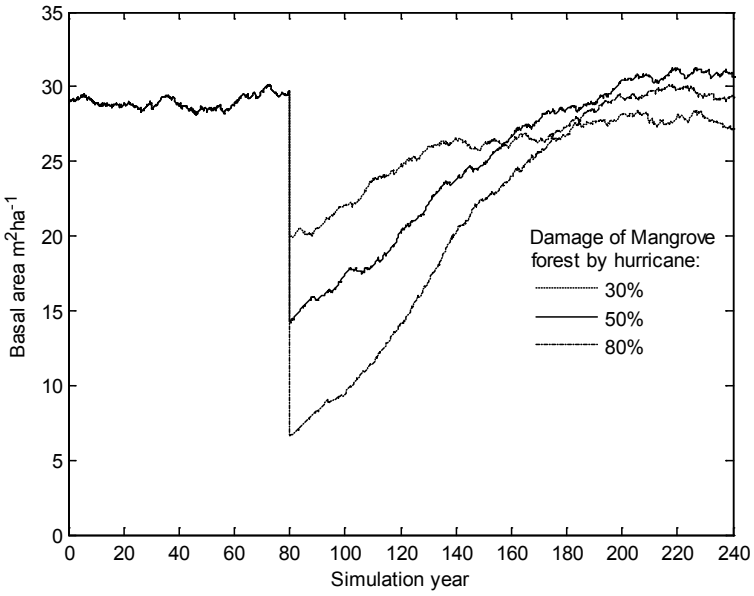

Figure 4.4 Model-projected basal areas of mangroves following 30%, 50% and 80% destruction by hurricane, respectively, at year 80.

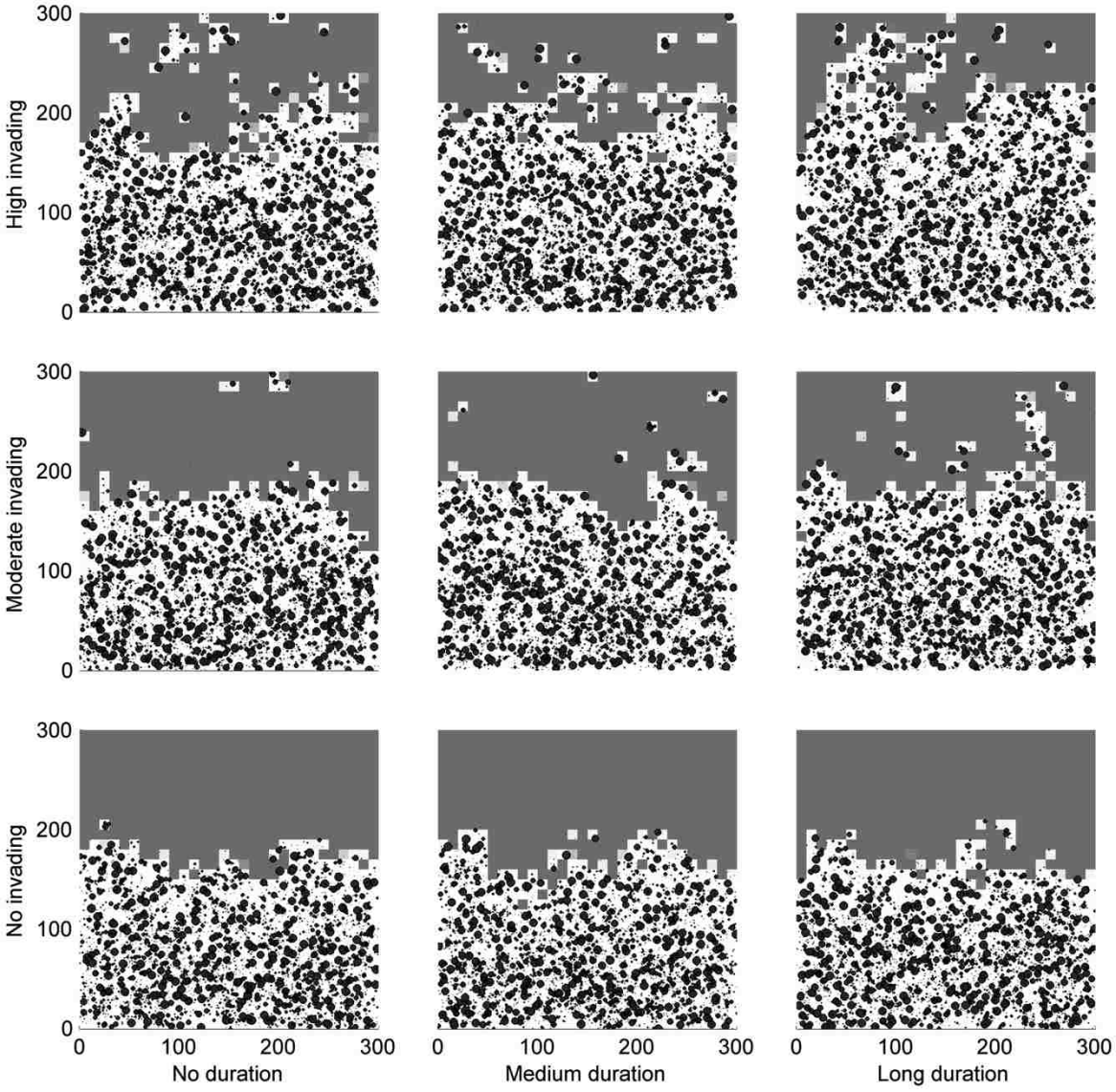

Figure 4.5 Spatial distribution between freshwater marsh (gray cells) and individual mangrove trees (black circles) under 9 different scenarios, which are combinations of 3 levels of mangrove seedlings transported into the marsh (none transported, a moderate number transported, and a large number transported) and 3 levels of salinity intrusion duration (zero duration, medium duration and long duration).

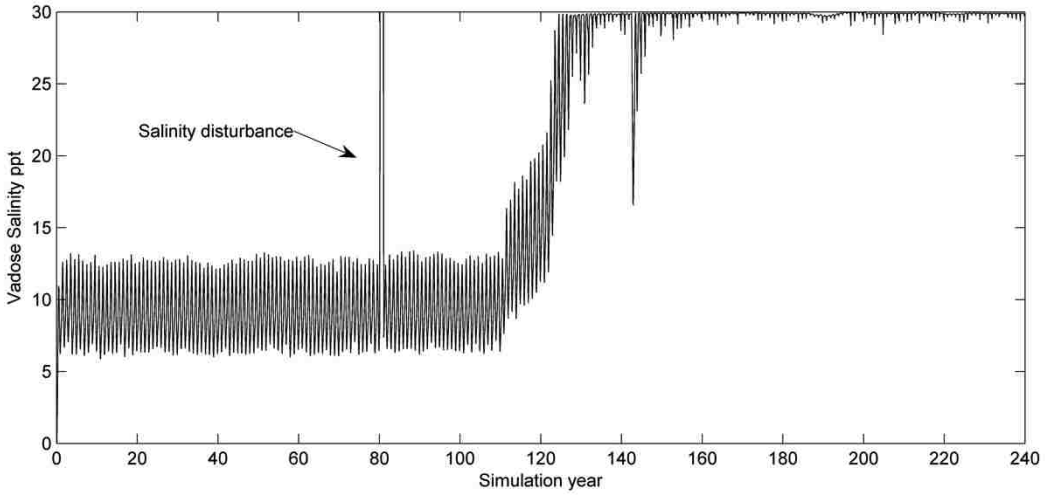

Figure 4.6 Output of soil porewater salinity dynamics for a former freshwater marsh occupied cell change to mangroves. Salinity disturbance with 1-year high salinity duration and mangrove seedling invasion occurring at year 80.

Chapter 5

OVERALL CONCLUSIONS

The research in this dissertation examined mechanisms of storm surge effects on coastal vegetation. First, I developed a computer simulation model, SEHM, to investigate mechanisms of spatial pattern formation of coastal vegetation in response to external gradients and positive feedbacks affecting soil porewater salinity. Second, I estimated the resilience of the ecotone of coastal vegetation to potential salinity disturbance. And finally, I applied the simulation model to a southern Florida mangrove-freshwater marsh ecotone and tested the possible effects of Hurricane Wilma on long-term coastal vegetation changes. Here I summarize the results of each section and discuss how my research succeeded in addressing the challenges in regime shift theory of coastal communities.

An earlier model, MANHAM (Sternberg et al. 2007, Teh et al. 2008), proposed a positive feedback mechanism to explain sharp boundaries between halophyte and glycophytic vegetations, even though there is only a gradual change in the physicochemical environment (Ungar, 1998). However, the relative contributions of positive feedback and the externally imposed environmental gradients on the formation of the sharp ecotone are hard to discern. I asked the following questions: Will the sharp boundary still exist if the self reinforcing feedback is taken out of the model? Could the self-reinforcing feedback alone cause sharp boundaries between vegetation types under completely uniform environmental conditions? The challenge was that the hypothesized self -reinforcing feedback mechanism is an intrinsic property of my study system, and it is impossible to do field experiments to control the self- reinforcing feedback, since it is

not possible to manipulate the plants' functional response of evapotranspiration . In Chapter 2, I succeeded in distinguishing the effects of the positive feedback mechanism and external environmental gradient by doing sort of a "Gedanken-experiment" based on the simulation model.

The model simulation results indicate that stability of ecotones of coastal vegetation are more complex than previously suggested, involving interactions of environmental gradients and self-reinforcement of vadose zone salinity. A combination of a high water table and high salinity of the water table underlying vegetation of both types creates conditions under which a storm surge might 'tip' glycophytic vegetation towards halophytic vegetation. Investigation of effects of precipitation on positive feedback indicates that the dry season, with its low precipitation, is the period of strongest positive feedback, and has a strong effect on the precise location of the ecotone.

Another challenge I addressed was that of estimating the resilience of the ecotone between coastal halophytic and glycophytic vegetation along a salinity gradient. Regime shift theory implies that the ecotone resists change until the change in the environment is great enough to overcome the self-reinforcing feedbacks of the vegetation. That resistance is termed "resilience". However, how to estimate and quantify ecotone resilience is still elusive. The methods I developed in Chapter 3 are able to estimate how strong of disturbance is needed to cause a regime shift. In the case studied, each vegetation type, through soil feedback loops, promoted local soil salinity levels that favored itself in competition with the other type. Alternative stable equilibria, one for salinity-tolerant and one for salinity intolerant vegetation, were shown to exist over a region of the groundwater salinity gradient, bounded by two bifurcation points. This

region was shown to depend sensitively on parameters such as the rate of upward infiltration of salinity from groundwater into the soil due to evaporation. I showed also that increasing diffusion rates of vegetation can lead to shrinkage of the range between the two bifurcation points. A disturbance such as an input of salinity to the soil from a storm surge could upset this stable boundary, leading to a regime shift of salinity-tolerant vegetation inland. I showed, however, that, for my model as least, a simple pulse disturbance would not be sufficient; the salinity would have to be held at a high level, as a 'press,' for some time. The approach used here should be generalizable to study the resilience of a variety of ecotones to disturbances.

In Chapter 4, I applied the coupled hydrological-ecological simulation model to study mangrove-freshwater marsh ecotone changes at the coastal edge of Florida Everglades. I analyzed how long-term changes in the mangrove-marsh ecotone could occur after storm surge events, and whether, on the basis of empirical data, they are likely to have occurred in a region of the Everglades affected by a hurricane. By using the simulation model, I was able to investigate both salinity intrusion and passive transport of mangrove seedlings due to storm surge event. Salinity intrusion has been proposed to be a major disturbance to freshwater wetlands. The mangrove invasion, however, has rarely been reported as driver for ecotone position changes, regardless the fact that mangrove propagules can float and disperse over wide areas (Rabinowitz, 1978a; Sousa et al., 2007). The model simulation results indicate that the possibility of a regime shift from freshwater marsh to mangroves is more sensitive to the density of mangrove seedlings transported into the marsh than to the intensity of the storm surge overwash of the marsh end of the ecotone.

Another major contribution of my dissertation work is the individual (or agent)-based model I developed in Chapter 2 and Chapter 4. I succeeded in addressing the modeling challenge of linking agent-based model of two tree types (halophytic and glycophytic) to model of hydrology and salinity in the vadose zone. This required using two coordinate systems, a continuous one for individual trees and a grid-based one for hydrology and salinity. That was a major step in linking hydrology with realistic vegetation. The future development is to link the model with more realistic hydrology, such as USGS's Saturated-Unsaturated TRAnsport (SUTRA) model. My research focused on theoretical studies, but its application to empirical researches is significant.

Appendix A: **Model description for Chapter 2**

I use the Overview, Design Concepts, and Details protocol (Grimm et al., 2006; 2010) to describe my model.

Purpose

My objective is to determine the relative influences of environmental gradients and positive feedbacks between vegetation and vadose zone salinity on the sharpness of the ecotone between salinity-tolerant and salinity-intolerant vegetation, and, in addition, to show an example of using an individual- or agent-based vegetation submodel in a model to simulate water fluxes in an ecohydrological system. This is addressed by simulating intra- and inter- specific competition between mangroves and hammocks, including the effects of the underlying hydrodynamics of tides, soil porewater and ground water.

State variables and scales

The model includes two basic types of variables: individual trees, both mangrove and hammock trees, which are agents, and abiotic variables, water and salinity. Individual trees are variables defined by the following state variables: age, diameter at breast height (dbh) and spatial location. A seedling bigger than a defined dbh threshold is considered to be successfully established and is defined as an "individual." Seedlings or propagules that are smaller than the dbh threshold are recorded only as numbers. Trees are discrete individuals that are distributed continuously over the two-dimensional area covered by the model. But the model also keeps track of the cells occupied by each individual tree, in order to link tree growth with water and salinity dynamics, which are described on cells.

The spatial framework for the abiotic variables, water and salinity, consists of discrete spatial cells, in a 100 x 100 array of cells where each cell is 1 x 1 m. One end of the area (seaward side) is at zero elevation, and elevation increases 10 mm per cell moving inland. The water content and salinity in each cell are tracked in sub-daily time steps. In order for individual trees to interact with the abiotic variables, the model keeps track of the fraction of root biomass of each individual tree in one or more cells.

SEHM utilizes two computational time steps: a daily time scale for physiological processes of water uptake by plants, which changes soil salinity, and a monthly time scale for vegetation dynamics. During each monthly time step, every tree can have a growth increment that is a function of light availability and neighborhood competition, and is weighted by the salinity of cells occupied by the tree's roots. Then, after a tree reaches maturity, new recruits are produced at monthly intervals by the tree. Successful establishment of new recruits depends, in part, on the salinity of the soil porewater and also on neighborhood competition. At the end of the monthly time step, death may occur due to size-dependent factors (low d.b.h.) and also from reduced growth rate caused by competition or salinity. Information on the total amount of root biomass distributed in each cell is passed to the salinity dynamics submodel (described later), which updates water and salinity on daily time steps. Monthly average values of salinity in each cell, which affect tree growth and seedling establishment, are then returned to the submodel for vegetation dynamics (described later).

Process overview and scheduling

My vegetation model is based on the individual-based stochastic dynamics of plants in a spatio-temporally varying coastal environment. The behaviors of individuals,

including growth, reproduction, dispersal and mortality, etc., are represented by empirical rules based on ecological mechanisms. The basic processes of every individual tree are started from the seedling stage. These are growth, evapotranspiration, seed dispersal, and mortality. The abiotic variables, water and salinity, undergo processes of movement within and between cells because of a combination of tidal input, precipitation, capillary movement upwards from groundwater, evapotranspiration, and horizontal diffusion of water and solute between cells.

Design Concepts

Basic principles. The theoretical ideas being tested in this model are whether indirect positive feedbacks between vegetation types and their environment have a tendency to produce and maintain sharp boundaries between different vegetation types.

Emergence. The key output of the model is the development of ecotones between vegetation types. These emerge from an interaction of abiotic and biotic processes.

Adaptation. The two woody plant types, hardwood hammock trees and mangroves, have different levels of adaptation to salinity. Mangroves continue to evapotranspire, even under conditions of highly saline soil porewater, while hammock trees diminish evapotranspiration as salinity increases (see submodels).

Interaction. Individual mangrove and hammock trees interact with members of both their own and the other type, described by the Field of Neighborhood approach (Berger and Hildenbrandt, 2000). They also interact indirectly through their influences on soil porewater salinity caused by their evapotranspiration.

Initialization

Trees are initialized in each model simulation run by assuming some initial distribution that is random in the spatial distribution of both mangrove and hammock trees and in the ages of mature trees ready to produce new recruits. Salinity of cells is initialized at zero.

Input Data

Precipitation, tides, water table salinity and distance to water table are external conditions that are set at different values, depending on specific simulation experiments. These might be set at constant levels in some of the treatments that are part of the model studies described below. For the full version of the model simulation, precipitation and effects of tides are prescribed as cosine functions. Mean precipitation and tidal height in the simulated area was 2.75 mm/day and 175 mm, respectively. Water table salinities and distance to water table are gradual linear functions of distance to the shoreline.

Vegetation growth submodel

Vegetation is modeled using a variation on the well known individual-based forest simulation models, such as the FORET model (Shugart and West, 1977). FORET assumes that the growth equation for a tree is represented by the optimal growth rate multiplied by relevant depression factors:

$$\frac{dD}{dt} = \frac{GD\left(1 - DH / D_{\max} H_{\max}\right)}{274 + 3b_2 D - 4b_3 D^2} neib \cdot sal \quad ,$$

where D is d.b.h. of the tree (cm), H is tree height (cm) and D_{max} and H_{max} are maximum values of diameters and heights for a given tree species. See table 1 for the detailed parameters. The two multiplicative factors on the right represent corrections of the 'optimal growth'. The first factor, *neib*, is shading and nutrient competition from

neighboring trees, and the second factor, *sal*, represents depression in growth because of salinity in the soil porewater.

Neighborhood multiplier

Tree-to-tree competition, including neighborhood shading and nutrient competition, can be expressed as,

$$neib = \frac{K_{FA}}{K_{FA} + \alpha_{ii} FA_i + \alpha_{ij} FA_j},$$

where *neib* is the neighborhood multiplier. FA_i is stress factor of intra-specific competition, either mangroves or hammocks. α_{ii} is strength of intra-specific competition. FA_j is stress factor of inter-specific competition. α_{ij} is strength of the effect of species *j* on species *i*. I assume the strength of intra-specific competition equals 1, and that inter-specific competition is measured in proportion to intra-specific competition. Salinity is not taken into account in this multiplier. If the combined stress factor equals the half-saturation coefficient, K_{FA}, growth is reduced by half. If the tree has no competing neighbors, then, *neib* = 1.0, but *neib* decreases as competition increases. The stress factor, *FA*, for the *k*th of *N* trees is given by the Field of Neighborhood (FON) approach (Berger and Hildenbrandt, 2000):

$$FA^k = \frac{1}{A} \sum_{n \neq k} \int_{A'} FON_n(x, y) da' .$$

$FON_n(x,y)$ is the field strength of the n^{th} tree at location (*x,y*) and the integral is over the area of zone of influence (*A*) around the tree. *A'* is the overlapping area of the focal FON (tree k) and the neighboring tree (tree n). The field strength for an individual tree is assumed to be 1 at the stem (R_{Basal}), and to decrease exponentially with increasing

distance to a minimum value (FON_{Min}) at the borderline of the zone of influence (R_{FON}), as follows:

$$FON(r) = 1 \qquad 0 \le r < R_{Basal}$$

$$FON(r) = \exp\left[-\frac{\left|\ln\left(FON_{Min}\right)\right|}{R_{FON} - R_{Basal}}\left(r - R_{Basal}\right) \right] \qquad R_{Basal} \le r \le R_{FON}$$

$$FON(r) = 0 \qquad r > R_{FON}$$

where r is distance to the center of tree stem.

Salinity multiplier

I assume the effect of salinity on growth occurs through its effect on the water uptake rate, normalized by the maximum possible rate. The uptake by a specific tree is summed over the spatial cells that the tree's roots occupy, weighted by the amount of biomass of the tree in each particular cell, which may differ in soil salinity.

$$sal = \sum \frac{f_{(x,y)} T\left(Sv\right)}{T\left(0\right)}$$

where, *sal* is salinity multiplier effect on growth rate, $f_{(x,y)}$ is the fraction of root biomass in each of the cells that an individual tree's roots can reach. *T(0)* is the water uptake rate when salinity is zero, *T(Sv)* is the water uptake rate when salinity is *Sv*, estimated by empirical relationships. I use the same equation for water uptake as in Sternberg et al. (2007).

An individual tree's root system can reach several cells when the tree reaches a sufficiently large size, and takes up water from these cells. Salinity within each cell is assumed to be homogeneous. If enough water is taken up from the cell, saline groundwater will infiltrate by capillary action into the cell and increase its salinity.

Salinity diffusion horizontally between cells also is possible. The fraction of root biomass per cell, *f(x,y)*, is root biomass at one cell divided by total root biomass. The root biomass in each cell is average of biomass at four corner points of cell, which is integrated from the root lateral distribution.

$$f_{(x,y)} = \frac{1}{4}\sum_{i=1}^{4} B_l^i \Big/ B_{root}$$

Root lateral distribution B_l can be expressed as an exponential function of distance from the tree base (l):

$$B_l = B_0 e^{-\beta l}$$

where, β is the attenuation rate of root density, and B_0 stands for the initial root density at the tree base. B_0 is calculated from (Komiyama et al., 2000; Komiyama et al., 1987),

$$B_0 = \frac{B_{root}}{2\pi\beta^{-2}\left(1 - e^{-\beta Max\_l}\left(\beta Max\_l + 1\right)\right)}$$

where Max_l is the maximum extension of the roots of a tree,

$Max\_l = D^2 \big/ (a_{HL} + b_{HL} D^2)$,

and where a_{HL} and b_{HL} are constants of the allometric relationship between maximum root extension and tree diameter.

The relationship between root biomass and tree diameter is given by an allometric equation (Komiyama et al., 2008).

$$B_{root} = \eta c_{AB} D^{b_{AB}}$$

where, B_{root} is total biomass of the root system and η is the ratio of below-ground biomass to above-ground biomass. The mangroves of Florida have been recorded as accumulating large amounts of biomass in their roots (Castaneda, 2010) , so this ratio is high compared

to that of upland forests. c_{AB} and b_{AB} are constants of the allometric relationship between tree diameter and root biomass.

Death submodel

Each individual plant, once it is old enough to have status as an individual, is assumed to have some constant intrinsic mortality rate, m_c. Because of environmental stress, such as high salinity, growth is slowed, which eventually can lead to an enhanced probability of mortality. It is assumed that growth rates below a specified threshold will expose trees to insect and disease attacks or severe weather event damage, and could result in negative carbon balances (Keane et al., 2001). Because I already have included stress factors in the growth function, I only need a relationship between mortality and growth rate. I use a diameter-dependent mortality equation as in SORTIE (Pacala et al., 1996) :

$$mor = m_c + m_s e^{-(uD+v\overline{g})}$$

where *mor* is the probability of monthly mortality, *u* and *v* are species-specific constants, *D* is the diameter, $\overline{g}$ is the average relative diameter growth rate against optimal growth rate without stress for the previous 24 months, and m_s is a stress-dependent coefficient.

Regeneration and dispersal

A tree reaches reproductive maturity if it reaches a threshold d. b. h. An adult tree produces a number of propagules, P_{max}, each month, but only a few survive to reach my defined state of being an "individual". The percentage of seedlings that survive and become "individuals" depends on soil porewater salinity (*Sv*) and field strength ($FS_{(x,y)}$) at their location, defined from FON as

$$br_{(x,y)} = \frac{P_{\max}\varepsilon}{1+e^{-\theta(K_{sv}-Sv)}} \frac{K_{FS}}{K_{FS}+\alpha_{ii}FS^{i}_{(x,y)}+\alpha_{ij}FS^{j}_{(x,y)}}$$

where, $br_{(x,y)}$ is monthly recruitment rate at location *(x,y)*, which in my model actually means 'successful establishment rate'; ε is the baseline fraction that survive; the birth rate is reduced by half, if salinity equals the half-saturation point, K_{sv}; θ is the coefficient of salinity effect on birth rate; field strength, $FS^{i}_{(x,y)}$, is the accumulated *FON* value resulting from the sum over all of the species *i* having an effect at location *(x,y)*; and K_{FS} is the half-saturation coefficient of field strength on birth rate.

Mangrove propagules float on the water surface of the intertidal area, and are affected by the hydrodynamics of tides and currents (Stieglitz and Ridd, 2001). I simulated micro-site closed vegetation dynamics, and ignored vegetation dispersal from outside of system. Thus long distance dispersal, in which propagules typically are carried by river or flood, was not considered. The probability of a propagule being dispersed within the closed system is as follows;

$$dis(d) = \frac{f_L \times e^{-f_L d}}{1-e^{-Max\_d \times f_L}},$$

where, *dis* is the probability distribution of the dispersal distance, *d* is the distance away from the parent tree, f_L is the coefficient of dispersal probability with distance, and *Max_d* is the maximum dispersal distance. In consideration of short-distance dispersal, most of the mangrove propagules stick near the mother tree in the mud. So I assumed mangrove maximum dispersal distance to be shorter than hardwood hammocks.

Hydrology and salinity dynamics

The salinity in a given spatial cell is updated in daily time step following (Sternberg et al., 2007; Teh et al., 2008). The opposing processes of infiltration and

capillary rise of water depend on the difference between the precipitation, evaporation and plant uptake of water. Salinity change rate depends on infiltration rate or capillary rise rate over the depth of vadose zone. All spatial cells at elevations lower than tidal height were allowed to have their water mixed with the salinity of tides, which is assumed to be 30 ppt.

Appendix B: Mathematical analysis for Chapter 3

1.1 The model without diffusion

$$\begin{aligned}
\frac{dN_1}{dt} &= N_1(\rho_1 h(S) - \alpha_{11}N_1 - \alpha_{12}N_2),\\
\frac{dN_2}{dt} &= N_2(\rho_2 m(S) - \alpha_{21}N_1 - \alpha_{22}N_2),\\
\frac{dS}{dt} &= \beta_0 g + \beta_1 \frac{N_2}{k+N_2} g - \epsilon S
\end{aligned} \tag{B.1}$$

with non-negative initial conditions $(N_1(0), N_2(0), S(0)) \in \mathbb{R}^3_+ = \{(x_1, x_2, x_3) \in \mathbb{R}^3 : x_1 \geq 0, x_2 \geq 0, x_3 \geq 0\}$. We have the following assumptions:

(1) $h(S) = \dfrac{\mu}{\mu + S}$ and $m(S) = 1$, where $\mu > 0$;

(2) all parameters are positive;

(3) $\alpha_{12}\alpha_{21} - \alpha_{11}\alpha_{22} > 0$.

1.2 Elementary analysis

The Jacobian matrix of (B.1) at $(N_1, N_2, S) \in \mathbb{R}^3_+$ is $J((N_1, N_2, S)) =$

$$\begin{pmatrix}
(\rho_1 h(S) - \alpha_{11}N_1 - \alpha_{12}N_2) - \alpha_{11}N_1 & -\alpha_{12}N_1 & \rho_1 N_1 h'(S)\\
-\alpha_{21}N_2 & (\rho_2 m(S) - \alpha_{21}N_1 - \alpha_{22}N_2) - \alpha_{22}N_2 & \rho_2 N_2 m'(S)\\
0 & \beta_1 kg/(k+N_2)^2 & -\epsilon
\end{pmatrix}.$$

In particular, if $h(S) = \dfrac{\mu}{\mu + S}$ and $m(S) = 1$, then $J((N_1, N_2, S)) =$

$$\begin{pmatrix} (\rho_1 h(S) - \alpha_{11}N_1 - \alpha_{12}N_2) - \alpha_{11}N_1 & -\alpha_{12}N_1 & -\rho_1 N_1 h^2(S)/\mu \\ -\alpha_{21}N_2 & (\rho_2 - \alpha_{21}N_1 - \alpha_{22}N_2) - \alpha_{22}N_2 & 0 \\ 0 & \beta_1 kg/(k+N_2)^2 & -\epsilon \end{pmatrix}.$$

Using the theory of monotone dynamical systems (Smith, 1995) and an approach similar to that of Jiang and Tang (2008), we prove that

Theorem 1.1. *Each non-negative solution of* (B.1) *converges to an equilibrium point.*

1.3 Equilibria and their stabilities

Direct calculation yields that system (B.1) has three boundary equilibria, namely,

$$E_0 = (0, 0, \frac{\beta_0 g}{\epsilon}), E_1 = (0, \frac{\rho_2}{\alpha_{22}}, (\beta_0 + \beta_1 \frac{\rho_2}{k\alpha_{22} + \rho_2})\frac{g}{\epsilon}) \text{ and } E_2 = (\frac{\rho_1 \mu}{\alpha_{11}(\mu + \beta_0 g/\epsilon)}, 0, \frac{\beta_0 g}{\epsilon}).$$

Proposition 1.2. *Let*

$$g_1 = \frac{\epsilon\mu\Big(\frac{\rho_1\alpha_{22}}{\rho_2\alpha_{12}} - 1\Big)(k\alpha_{22} + \rho_2)}{k\beta_0\alpha_{22} + (\beta_0 + \beta_1)\rho_2} \text{ and } g_2 = \Big(\frac{\rho_1\alpha_{21}}{\rho_2\alpha_{11}} - 1\Big)\frac{\epsilon\mu}{\beta_0}.$$

Then

(1) E_0 *is unstable and* $W^s(E_0) \cap \mathbb{R}^3_+ = \{(N_1, N_2, S) \in \mathbb{R}^3_+ : N_1 = N_2 = 0, S \geq 0\}$;

(2) E_1 *is unstable if* $g < g_1$, *stable if* $g > g_1$;

(3) E_2 *is unstable if* $g > g_2$, *stable if* $g < g_2$.

In addition, if E_1 is unstable, then $W^s(E_1) \cap \mathbb{R}^3_+ = \{(N_1, N_2, S) \in \mathbb{R}^3_+ : N_2 > 0, S \geq 0\}$; if E_2 is unstable, then $W^s(E_2) \cap \mathbb{R}^3_+ = \{(N_1, N_2, S) \in \mathbb{R}^3_+ : N_1 > 0, S \geq 0\}$. Here $W^s(E)$ denote the stable manifold of an equilibrium E.

Proof. The Jacobian matrices at the three boundary equilibria E_0, E_1 and E_2 are

$$J(E_0) = \begin{pmatrix} \dfrac{\rho_1\mu}{\mu + \beta_0 g/\epsilon} & 0 & 0 \\ 0 & \rho_2 & 0 \\ 0 & \beta_1 g/k & -\epsilon \end{pmatrix},$$

$$J(E_1) = \begin{pmatrix} \dfrac{\rho_1\mu}{\mu + \left(\beta_0 + \beta_1 \dfrac{\rho_2}{k\alpha_{22} + \rho_2}\right)\dfrac{g}{\epsilon}} - \dfrac{\rho_2\alpha_{12}}{\alpha_{22}} & 0 & 0 \\ -\rho_2\alpha_{21}/\alpha_{22} & -\rho_2 & 0 \\ 0 & \beta_1 gk/(k + \rho_2/\alpha_{22})^2 & -\epsilon \end{pmatrix}$$

and

$$J(E_2) = \begin{pmatrix} -\dfrac{\rho_1\mu}{\mu + \beta_0 g/\epsilon} & -\dfrac{\rho_1\alpha_{12}\mu}{\alpha_{11}(\mu + \beta_0 g/\epsilon)} & -\dfrac{\rho_1^2\mu^2}{\alpha_{11}(\mu + \beta_0 g/\epsilon)^3} \\ 0 & \rho_2 - \dfrac{\rho_1\alpha_{21}\mu}{\alpha_{11}(\mu + \beta_0 g/\epsilon)} & 0 \\ 0 & \beta_1 g/k & -\epsilon \end{pmatrix}.$$

The proposition is immediately proved. □

Remark 1.3. If $g_2 > 0$, that is, $\dfrac{\rho_1\alpha_{21}}{\rho_2\alpha_{11}} - 1 > 0$, then $g_1 < g_2$ and $\dfrac{\partial(g_2 - g_1)}{\partial\beta_0} < 0$. In fact,

$$\alpha_{12}\alpha_{21} > \alpha_{11}\alpha_{22} \Leftrightarrow \frac{\rho_1\alpha_{21}}{\rho_2\alpha_{11}} - 1 > \frac{\rho_1\alpha_{22}}{\rho_2\alpha_{12}} - 1 \Leftrightarrow \left(\frac{\rho_1\alpha_{21}}{\rho_2\alpha_{11}} - 1\right)\frac{\epsilon\mu}{\beta_0} > \left(\frac{\rho_1\alpha_{22}}{\rho_2\alpha_{12}} - 1\right)\frac{\epsilon\mu}{\beta_0}$$

$$\Rightarrow g_2 = \Big(\frac{\rho_1\alpha_{21}}{\rho_2\alpha_{11}} - 1\Big)\frac{\epsilon\mu}{\beta_0} > g_1 = \frac{\epsilon\mu\Big(\frac{\rho_1\alpha_{22}}{\rho_2\alpha_{12}} - 1\Big)(k\alpha_{22} + \rho_2)}{k\beta_0\alpha_{22} + (\beta_0 + \beta_1)\rho_2}$$

$$\Rightarrow \Big(\frac{\rho_1\alpha_{21}}{\rho_2\alpha_{11}} - 1\Big)\frac{\epsilon\mu}{\beta_0} > \frac{\epsilon\mu\Big(\frac{\rho_1\alpha_{22}}{\rho_2\alpha_{12}} - 1\Big)(k\alpha_{22} + \rho_2)}{k\beta_0\alpha_{22} + (\beta_0 + \beta_1)\rho_2} \times \frac{\beta_0(k\alpha_{22} + \rho_2)}{k\beta_0\alpha_{22} + (\beta_0 + \beta_1)\rho_2}$$

$$\Leftrightarrow \frac{\partial g_2}{\partial \beta_0} = -\Big(\frac{\rho_1\alpha_{21}}{\rho_2\alpha_{11}} - 1\Big)\frac{\epsilon\mu}{\beta_0^2} < \frac{\partial g_1}{\partial \beta_0} = -\frac{\epsilon\mu\Big(\frac{\rho_1\alpha_{22}}{\rho_2\alpha_{12}} - 1\Big)(k\alpha_{22} + \rho_2)^2}{(k\beta_0\alpha_{22} + (\beta_0 + \beta_1)\rho_2)^2}.$$

Let $K = \{(x_1, x_2, x_3) \in \mathbb{R}^3 : x_1 \geq 0, x_2 \leq 0, x_3 \leq 0\}$ and $\mathrm{Int}K = \{(x_1, x_2, x_3) \in K : x_1 > 0, x_2 < 0, x_3 < 0\}$. For $x, y \in \mathbb{R}^3_+$, we define $x \leq_K y$ if $y - x \in K$, $x <_K y$ if $x \leq_K y$ and $x \neq y$, and $x \ll_K y$ if $y - x \in \mathrm{Int}K$. When $x, y \in \mathbb{R}^3_+$ and $x \leq_K (\ll_K) y$, let $[x, y]_K = \{w \in \mathbb{R}^3_+ : x \leq_K w \leq_K y\}$ ($(x, y)_K = \{w \in \mathbb{R}^3_+ : x \ll_K w \ll_K y\}$).

Remark 1.4. Note that $E_1 \leq_K E_0 \leq_K E_2$ and all orbits starting in $\mathbb{R}^3_+$ are attracted to the set $[E_1, E_2]_K$ (see Gao and Liang, 2007). The set of all positive equilibria, denoted by E^+, is a subset of $(E_1, E_2)_K$ and it is totally strongly ordered with respect to $\ll_K$, i.e., either $E^* \ll_K \tilde{E}^*$ or $\tilde{E}^* \ll_K E^*$ for any two points E^* and $\tilde{E}^*$ in E^+ satisfying $E^* \neq \tilde{E}^*$.

Theorem 1.5. *For system* (B.1)*, both E_1 and E_2 are stable if and only if there exists a positive equilibrium E^*. Moreover, it is unique and unstable when E^* exists.*

Proof. Suppose that both E_1 and E_2 are stable, then $g_1 < g < g_2$.

If $E^* = (N_1^*, N_2^*, S^*)$ is a positive equilibrium of (B.1), then it satisfies the following three equations

$$\begin{aligned} &\rho_1\frac{\mu}{\mu + S} - \alpha_{11}N_1 - \alpha_{12}N_2 = 0, \\ &\rho_2 - \alpha_{21}N_1 - \alpha_{22}N_2 = 0, \\ &\beta_0 g + \beta_1\frac{N_2}{k + N_2}g - \epsilon S = 0. \end{aligned} \tag{B.2}$$

Let $\omega = \alpha_{12}\alpha_{21} - \alpha_{11}\alpha_{22} > 0$. After solving N_1 and S in terms of N_2 from the last two equations of (B.2), and substituting them into the first equation, we get

$$\rho_1 \frac{\mu}{\mu + (\beta_0 g + \beta_1 \frac{N_2}{k+N_2} g)/\epsilon} - \alpha_{11}\frac{\rho_2 - \alpha_{22}N_2}{\alpha_{21}} - \alpha_{12}N_2 = 0,$$

which can be simplified to a quadratic equation

$$F(N_2) \equiv AN_2^2 + BN_2 + C = 0, \tag{B.3}$$

where $A = (\beta_0 + \beta_1 + \frac{\epsilon\mu}{g})\omega > 0$, $B = (\beta_0 + \frac{\epsilon\mu}{g})k\omega + (\beta_0 + \beta_1 + \frac{\epsilon\mu}{g})\rho_2\alpha_{11} - \frac{\epsilon\mu}{g}\rho_1\alpha_{21}$ and $C = (\beta_0 + \frac{\epsilon\mu}{g})k\rho_2\alpha_{11} - \frac{\epsilon\mu}{g}k\rho_1\alpha_{21}$.

Since $g < g_2$ implies $C < 0$, (B.3) has exactly one positive root, N_2^*. To establish the existence of E^*, we need verify the positivity of

$$N_1^* = (\rho_2 - \alpha_{22}N_2^*)/\alpha_{21} \text{ and } S^* = (\beta_0 g + \beta_1 \frac{N_2^*}{k+N_2^*} g)/\epsilon,$$

respectively. Obviously, it suffices to show that $N_2^* < \rho_2/\alpha_{22}$ or $F(\rho_2/\alpha_{22}) > 0$. In

fact,

$$
\begin{aligned}
&F(\frac{\rho_2}{\alpha_{22}}) = A(\frac{\rho_2}{\alpha_{22}})^2 + B\frac{\rho_2}{\alpha_{22}} + C \\
=&(\beta_0+\beta_1+\frac{\epsilon\mu}{g})(\omega\frac{\rho_2^2}{\alpha_{22}^2}+\rho_2\alpha_{11}\frac{\rho_2}{\alpha_{22}}) + (\beta_0+\frac{\epsilon\mu}{g})(k\omega\frac{\rho_2}{\alpha_{22}}+k\rho_2\alpha_{11}) - \frac{\epsilon\mu}{g}(\rho_1\alpha_{21}\frac{\rho_2}{\alpha_{22}}+k\rho_1\alpha_{21}) \\
=&(\beta_0+\beta_1+\frac{\epsilon\mu}{g})\frac{\rho_2^2}{\alpha_{22}^2}(\omega+\alpha_{11}\alpha_{22}) + (\beta_0+\frac{\epsilon\mu}{g})k\frac{\rho_2}{\alpha_{22}}(\omega+\alpha_{11}\alpha_{22}) - \frac{\epsilon\mu}{g}\rho_1\alpha_{21}(\frac{\rho_2}{\alpha_{22}}+k) \\
=&(\beta_0+\beta_1+\frac{\epsilon\mu}{g})\frac{\rho_2^2}{\alpha_{22}^2}\alpha_{12}\alpha_{21} + (\beta_0+\frac{\epsilon\mu}{g})k\frac{\rho_2}{\alpha_{22}}\alpha_{12}\alpha_{21} - \frac{\epsilon\mu}{g}\rho_1\alpha_{21}(\frac{\rho_2}{\alpha_{22}}+k) \\
=&(\beta_0+\beta_1)\frac{\rho_2^2}{\alpha_{22}^2}\alpha_{12}\alpha_{21} + \beta_0 k\frac{\rho_2}{\alpha_{22}}\alpha_{12}\alpha_{21} - \frac{\epsilon\mu}{g}\big(\rho_1\alpha_{21}(\frac{\rho_2}{\alpha_{22}}+k) - \frac{\rho_2^2}{\alpha_{22}^2}\alpha_{12}\alpha_{21} - k\frac{\rho_2}{\alpha_{22}}\alpha_{12}\alpha_{21}\big) \\
=&(\beta_0+\beta_1)\frac{\rho_2^2}{\alpha_{22}^2}\alpha_{12}\alpha_{21} + \beta_0 k\frac{\rho_2}{\alpha_{22}}\alpha_{12}\alpha_{21} - \frac{\epsilon\mu}{g}(\rho_2+k\alpha_{22})(\frac{\rho_1\alpha_{22}}{\rho_2\alpha_{12}}-1)\frac{\rho_2}{\alpha_{22}^2}\alpha_{12}\alpha_{21} > 0
\end{aligned}
$$

is equivalent to $g > g_1$. Thus the proof of the necessity is complete.

Conversely, suppose that there is a positive equilibrium $E^* = (N_1^*, N_2^*, S^*)$. From the first two equations of (B.2), we can solve N_1 and N_2 in terms of S, i.e.,

$$N_1^* = (\rho_2\alpha_{12} - \rho_1 h(S^*)\alpha_{22})/\omega > 0 \text{ and } N_2^* = (\rho_1 h(S^*)\alpha_{21} - \rho_2\alpha_{11})/\omega > 0,$$

which imply that $\frac{\rho_2\alpha_{11}}{\rho_1\alpha_{21}} < h(S^*) < \frac{\rho_2\alpha_{12}}{\rho_1\alpha_{22}}$. Note that $E^* \in (E_1, E_2)_K$ and therefore $S_1 \equiv \frac{\beta_0 g}{\epsilon} < S^* < S_2 \equiv (\beta_0 + \beta_1\frac{\rho_2}{k\alpha_{22}+\rho_2})\frac{g}{\epsilon}$, then $h(S_2) < h(S^*) < h(S_1)$. Hence $h(S_2) < \frac{\rho_2\alpha_{12}}{\rho_1\alpha_{22}}$ and $h(S_1) > \frac{\rho_2\alpha_{11}}{\rho_1\alpha_{21}}$ which mean that both E_1 and E_2 are stable.

When E^* exists, the Jacobian matrix of (B.1) at $E^* = (N_1^*, N_2^*, S^*)$ is

$$J(E^*) = \begin{pmatrix} -\alpha_{11}N_1^* & -\alpha_{12}N_1^* & -\rho_1 N_1^* h^2(S^*)/\mu \\ -\alpha_{21}N_2^* & -\alpha_{22}N_2^* & 0 \\ 0 & \beta_1 kg/(k+N_2^*)^2 & -\epsilon \end{pmatrix}$$

and its determinant $\det(J(E^*)) > \epsilon(\alpha_{12}\alpha_{21} - \alpha_{11}\alpha_{22})N_1^*N_2^* = \epsilon\omega N_1^*N_2^* > 0$. Therefore, E^* must have a positive eigenvalue and it is unstable. By the theory of connecting orbits in Hess (1991), system (B.1) can have at most one positive equilibrium. Otherwise, there must exist a further positive equilibrium which contradicts to (B.3). □

Remark 1.6. From (B.3), we can obtain an explicit expression for the positive equilibrium when it exists. Since $\mathrm{tr}(J(E^*)) = -(\alpha_{11}N_1^* + \alpha_{22}N_2^* + \epsilon) < 0$, $J(E^*)$ has one positive eigenvalue and two eigenvalues with negative real parts. Therefore, the stable manifold $W^s(E^*)$ of E^* is a two-dimensional smooth surface which separates $\mathrm{Int}\mathbb{R}^3_+$ into two parts: the lower one in the order $\leq_K$ is the basin of attraction for E_1 and the upper one is the basin of attraction for E_2. This result is consistent with the competition exclusion principle in two-species Lotka-Volterra competition model.

1.4 The model with diffusion

Now, we develop a spatial model for the interaction between salt-tolerant and salt-intolerant vegetation types by including species diffusion and salt distribution. Thus, we have the following reaction-diffusion equations (Murray, 2003),

$$\begin{aligned}
&\frac{\partial N_1}{\partial t} = N_1(\rho_1 h(S) - \alpha_{11}N_1 - \alpha_{12}N_2) + D_1\frac{\partial^2 N_1}{\partial z^2} \text{ in } (0,\infty)\times(0,\infty),\\
&\frac{\partial N_2}{\partial t} = N_2(\rho_2 m(S) - \alpha_{21}N_1 - \alpha_{22}N_2) + D_2\frac{\partial^2 N_2}{\partial z^2} \text{ in } (0,\infty)\times(0,\infty),\\
&\frac{\partial S}{\partial t} = \beta_0 g(z) + \beta_1\frac{N_2}{k+N_2}g(z) - \epsilon S + D_S\frac{\partial^2 S}{\partial z^2} \text{ in } (0,\infty)\times(0,\infty),\\
&\frac{\partial N_1}{\partial \nu} = \frac{\partial N_2}{\partial \nu} = \frac{\partial S}{\partial \nu} = 0 \text{ on } \{0\}\times(0,\infty),\\
&N_1(\cdot,0), N_2(\cdot,0) \text{ and } S(\cdot,0) \geq 0 \text{ in } (0,\infty),
\end{aligned} \tag{B.4}$$

where $N_1(z,t), N_2(z,t)$ and $S(z,t)$ are the population density/concentration of N_1, N_2 and S in altitude z at time t. The diffusion rates D_1, D_2 and D_S are assumed to be positive constants and $g(z)$ is a positive decreasing function of z.

To investigate the dynamics of (B.4), we first study its corresponding steady state problem

$$\begin{aligned}
&N_1(\rho_1 h(S) - \alpha_{11}N_1 - \alpha_{12}N_2) + D_1\frac{\partial^2 N_1}{\partial z^2} = 0 \text{ in } (0,\infty),\\
&N_2(\rho_2 m(S) - \alpha_{21}N_1 - \alpha_{22}N_2) + D_2\frac{\partial^2 N_2}{\partial z^2} = 0 \text{ in } (0,\infty),\\
&\beta_0 g(z) + \beta_1\frac{N_2}{k+N_2}g(z) - \epsilon S + D_S\frac{\partial^2 S}{\partial z^2} = 0 \text{ in } (0,\infty),\\
&\frac{\partial N_1}{\partial \nu} = \frac{\partial N_2}{\partial \nu} = \frac{\partial S}{\partial \nu} = 0 \text{ at } z = 0, N_1, N_2 \text{ and } S \geq 0 \text{ in } (0,\infty),
\end{aligned} \tag{B.5}$$

Let $X_1 = \dfrac{\partial N_1}{\partial z}, X_2 = \dfrac{\partial N_2}{\partial z}$ and $T = \dfrac{\partial S}{\partial z}$. Then (B.6) can be transferred to a non-autonomous ordinary differential equations

$$\begin{aligned}
&N_1' = X_1, N_2' = X_2, S' = T,\\
&X_1' = -(N_1(\rho_1 h(S) - \alpha_{11}N_1 - \alpha_{12}N_2))/D_1,\\
&X_2' = -(N_2(\rho_2 m(S) - \alpha_{21}N_1 - \alpha_{22}N_2))/D_2,\\
&S' = -(\beta_0 g(z) + \beta_1\frac{N_2}{k+N_2}g(z) - \epsilon S)/D_S.
\end{aligned} \tag{B.6}$$

Appendix C: **Model description for Chapter 4**

I use the Overview, Design Concepts, and Details protocol (Grimm et al., 2006; 2010) to describe my model.

Purpose

My objective is to simulate the storm surge effects on coastal mangrove-freshwater marsh ecotone. Specifically, two factors closely related to storm surge disturbance, salinity intrusion and mangrove seedling dispersal are investigated using the vegetation competition model. This is addressed by simulating intra- and inter- specific competition between mangroves and freshwater marsh, including the coupling of vegetation with vadose zone salinity and the effects of tides, precipitation and groundwater salinity.

Entities, state variables and scales

The model includes two basic types of entities: individual mangrove trees, which are agents, and spatial cells, which have biotic variables of freshwater marsh biomass and abiotic of salinities. Individual trees are entities defined by the following state variables: age, diameter at breast height (d. b. h.) and spatial location. A seedling bigger than a defined d. b. h. threshold is considered to be successfully established and is defined as an "individual." Seedlings or propagules that are smaller than the d. b. h. threshold are recorded only as numbers. Trees are discrete individuals that are distributed continuously over the two-dimensional area covered by the model. Freshwater marsh is kept track as biomass of sawgrass in each cell.

The spatial framework for the abiotic variables, water and salinity, consists of discrete spatial cells, in a 30 x 30 cells where each cell is 10 x 10 m. Elevation of the cells was assumed to be 8 cm to NAVD88. The water level and salinity in each cell are tracked

in sub-daily time steps. In order for individual mangrove trees and freshwater marsh biomass in a given cell to interact with the abiotic variables, the model keeps track of the root biomass in the given cell.

The simulation model utilizes two computational time steps: a daily time scale for physiological processes of water uptake by plants, which changes soil salinity, and a monthly time scale for vegetation dynamics. During each monthly time step, biomass of freshwater marsh in a given cell is determined by monthly gains from photosynthesis and losses due to respiration or mortality. Similar to SEHM, mangrove dynamics are modeled as individual-based. During each monthly time step, every tree can have a growth increment that is a function of light, hydroperiod, and the salinity of the particular spatial cell. Then, after a mangrove tree reaches maturity, new seedlings are produced at monthly intervals by the tree. The probability of each of these seedlings producing a successful new recruit depends on the salinity of the soil porewater. At the end of the monthly time step, the probability of death to trees is related to size-dependent factors, such as low d.b.h. (diameter at breast height of tree), or from reduced growth rate caused by competition or salinity. Information on the total amount of root biomass distributed in each cell is passed to the salinity dynamics submodel (described in Chapter 4), which updates water and salinity on daily time steps. Monthly average values of salinity in each cell, which affect tree growth and seedling establishment, are then returned to the submodel for vegetation dynamics (described below).

Process overview and scheduling

My vegetation model combines the individual-based dynamics of mangrove trees and grid based dynamics of freshwater marsh in a spatio-temporally varying coastal

environment. Biomass of freshwater marsh in a given cell is determined by monthly gains from photosynthesis and losses due to respiration or mortality. Photosynthesis is modeled as the maximum possible rate, been multiplied by limitation factors, including salinity, light, hydroperiod and mangrove biomass in the given cell. The behaviors of individuals, including growth, reproduction, dispersal and mortality, etc., are represented by empirical rules based on ecological mechanisms. The basic processes of every individual tree are started from the seedling stage. These are growth, evapotranspiration, seed dispersal, and mortality. The abiotic variables, water and salinity, undergo processes of movement within and between cells because of a combination of tidal input, precipitation, capillary movement upwards from groundwater, evapotranspiration, and horizontal diffusion of water and solute between cells.

Design Concepts

Basic principles. The theoretical idea being addressed in this model is the assessment of the stability and possible regime shift of sharp ecotone between different vegetation types, and of the indirect competition through positive feedbacks between vegetation types and their environment.

Emergence. The key output of the model is the development of ecotones between vegetation types. These emerge from an interaction of abiotic and biotic processes.

Adaptation. The two vegetation types, mangrove trees and freshwater marsh, have different levels of adaptation to salinity and hydrology period. Mangroves continue to evapotranspire, even under conditions of highly saline soil porewater, while hammock trees diminish evapotranspiration as salinity increases (see submodels). In addition, mangroves have less tolerance than marsh for long periods of flooding.

Interaction. Individual mangrove trees interact with members of both their own and freshwater marsh biomass in a given cell. They also interact indirectly through their influences on soil porewater salinity caused by their evapotranspiration.

Initialization

Mangrove trees are initialized in each model simulation run by assuming some initial distribution that is random one the tidal influenced of the grid cells and in the ages of mature trees ready to produce new recruits. Freshwater marshes are initialized by assuming homogenous initial biomass in inland side of the grid cells. Salinity of cells is initialized at zero.

Input Data

Precipitation, tides, water table salinity and groundwater level are external conditions that are set at different values. Daily water level changes were calculated as the difference from 1 day to the next. Daily rainfall data were obtained from the Everglades Depth Network website (http://sofia.usgs.gov/eden/). Monthly averages and standard deviations were used to generate precipitation input for model. Tidal height and tidal salinity data were obtained from Everglades National Park gage Harney River (HR). Daily PET data were obtained from the Everglades Depth Network website.

Vegetation growth submodel

Individual mangrove tree is modeled using a variation on the well known individual-based forest simulation models, such as the FORET model (Shugart and West, 1977). FORET assumes that the growth equation for a tree is represented by the optimal growth rate multiplied by relevant depression factors:

$$\frac{dD}{dt} = \frac{GD\left(1 - DH / D_{\max} H_{\max}\right)}{274 + 3b_2 D - 4b_3 D^2} light \cdot sal \cdot hydro$$

,

where D is d.b.h. of the tree (cm), H is tree height (cm) and D_{max} and H_{max} are maximum values of diameters and heights for a given tree species. The two multiplicative factors on the right represent corrections of the 'optimal growth'. The first factor, *light*, is shading competition from neighboring trees, and the factors *sal* and *hydro* represents depression in growth because of salinity in the soil porewater and flooding period in the given cell, respectively.

Light multiplier

The growth rate effect by light depends on the fraction of light captured:

$$light = 1 - e^{-4.64*(AL-0.05)}$$

$$AL = e^{-0.5*LAI},$$

where AL is the available light to individual trees and LAI is the leaf area index of trees about the calculated tree.

Salinity multiplier

I assume the effect of salinity on growth occurs through its effect on the water uptake rate, normalized by the maximum possible rate. The uptake by a specific tree depends on soil salinity.

$$sal = \frac{T(Sv)}{T(0)},$$

where, *sal* is salinity multiplier effect on growth rate. *T(0)* is the water uptake rate when salinity is zero, *T(Sv)* is the water uptake rate when salinity is *Sv*, estimated by empirical relationships. I use the same equation for water uptake as in Sternberg et al. (2007).

Hydrology multiplier

Flooding stress is dependent on tree diameters. The tolerance of submergence, *LS*, in days increases as a mangrove tree grows, which is expressed in the model as,

$$LS = 30 + 150 * \frac{\mathrm{D}}{40 + D}$$

The hydrology multiplier is calculated as a declining coefficient when submergence greater than *LS* days (modified from Wu et al., 2003).

$$hydro = e^{0.016*(LS-WetDays)} \qquad if\ LS < WetDays$$

where *WetDays* is days of the cell submerged, which occupied by the tree.

Death submodel

Each individual plant, once it is old enough to have status as an individual, is assumed to have some constant intrinsic mortality rate, m_c. Because of environmental stress, such as high salinity, growth is slowed, which eventually can lead to an enhanced probability of mortality. It is assumed that growth rates below a specified threshold will expose trees to insect and disease attacks or severe weather event damage, and could result in negative carbon balances (Keane et al., 2001). Because I already have included stress factors in the growth function, I only need a relationship between mortality and growth rate. I use a diameter-dependent mortality equation as in SORTIE (Pacala et al., 1996) :

$$mor = m_c + m_s e^{-(uD+v\bar{g})}$$

where *mor* is the probability of monthly mortality, *u* and *v* are species-specific constants, *D* is the diameter, $\bar{g}$ is the average relative diameter growth rate against optimal growth rate without stress for the previous 24 months, and m_s is a stress-dependent coefficient.

Regeneration and dispersal

A tree reaches reproductive maturity if it reaches a threshold d. b. h. An adult tree produces a number of propagules, P_{max}, each month, but only a few survive to reach my defined state of being an "individual". The percentage of seedlings that survive and become "individuals" depends on soil porewater salinity (*Sv*) and freshwater marsh standing biomass (B_{stem}) at their location,

$$br_{(x,y)} = \frac{P_{\max}\varepsilon}{1+e^{-\theta(K_{sv}-Sv)}}\frac{K_{BS}}{K_{BS}+B_{stem}}$$

where, $br_{(x,y)}$ is monthly recruitment rate at location *(x,y)*, which in my model actually means 'successful establishment rate'; ε is the baseline fraction that survive; the birth rate is reduced by half, if salinity equals the half-saturation point, K_{sv}; θ is the coefficient of salinity effect on birth rate; and K_{BS} is the half-saturation coefficient of freshwater marsh standing biomass on mangrove seedling establishment rate.

Mangrove propagules float on the water surface of the intertidal area, and are affected by the hydrodynamics of tides and currents (Stieglitz and Ridd, 2001). I simulated micro-site closed vegetation dynamics, and ignored vegetation dispersal from outside of system. Thus long distance dispersal, in which propagules typically are carried by river or flood, was not considered. The probability of a propagule being dispersed is as follows,

$$dis(d) = \frac{f_L \times e^{-f_L d}}{1-e^{-Max\_d \times f_L}},$$

where, *dis* is probability distribution of the dispersal distance, *d* is distance away from the parent tree, f_L is coefficient of dispersal probability with distance, and *Max_d* is the maximum dispersal distance. In consideration of short-distance dispersal, most of

mangrove propagules stick near the mother tree in the mud. So I assumed mangrove maximum dispersal distance to be shorter than hardwood hammocks.

Freshwater marsh dynamics

The net primary production of the freshwater marsh in a given cell is expressed as photosynthetic production of the standing biomass, minus respiration and mortality. Therefore, the net primary production is mathematically expressed as follows,

$$\frac{dB}{dt} = P_{\max} \cdot light \cdot sal \cdot hydro - resp - mort$$

where, P_{max} is the optimal photosynthesis without limitation, which multiplied by relevant depression factors. The multipliers follow the same concepts as for mangrove trees, except that leaf area index *(LAI)* in light multiplier are calculated for all mangrove trees above marsh height; and that tolerance of submergence (*LS*) is assumed to be constant 180 days.

REFERENCES

Accatino, F., De Michele, C., Vezzoli, R., Donzelli, D., Scholes, R. J., 2010. Tree–grass co-existence in savanna: Interactions of rain and fire. Journal of Theoretical Biology. 267 (2), 235-242.

Adema, E. B., Grootjans, A. P., 2003. Possible positive-feedback mechanisms: plants change abiotic soil parameters in wet calcareous dune slacks. Plant Ecology. 167 (1), 141-149.

Agnew, A. D. Q., Wilson, J. B., Sykes, M. T., 1993. A vegetation switch as the cause of a forest/mire ecotone in New Zealand. Journal of Vegetation Science. 4 (2), 273-278.

Alexander, T. R., Crook, A. G., Recent vegetational changes in Southern Florida. In: P. J. Gleason, (Ed.), Environments of South Florida: Past/ Present/ Future. Miami Geological Society, Miami, 1974, pp. 61-72.

Anderson, G. H., Smith III, T. J., Teague, P. D., Variations in mangrove peat salinity from April 1997 to April 2003: A spatial analysis. Harney River Estuary, Everglades National Park., Annual Technical Presentations Meeting - SFWMD/USGS Cooperative Program, West Palm Beach, FL, 2003.

Anderson, K. J., 2007. Temporal patterns in rates of community change during succession. American Naturalist. 169 (6), 780-793.

Armentano, T. V., Doren, R. F., Platt, W. J., Mullins, T., 1995. Effects of hurricane Andrew on coastal and interior forests of Southern Florida: Overview and synthesis. Journal of Coastal Research. (21), 111-144.

Bader, M., Rietkerk, M., Bregt, A., 2008. A simple spatial model exploring positive feedbacks at tropical alpine treelines. Arctic, Antarctic, and Alpine Research. 40 (2), 269-278.

Baldwin, A., Egnotovich, M., Ford, M., Platt, W., 2001. Regeneration in fringe mangrove forests damaged by Hurricane Andrew. Plant Ecology. 157 (2), 151-164.

Baldwin, A. H., Mendelssohn, I. A., 1998. Effects of salinity and water level on coastal marshes: an experimental test of disturbance as a catalyst for vegetation change. Aquatic Botany. 61 (4), 255-268.

Ball, M. C., 1980. Patterns of secondary succession in a mangrove forest of Southern Florida. Oecologia. 44 (2), 226-235.

Ball, M. C., 2002. Interactive effects of salinity and irradiance on growth: implications for mangrove forest structure along salinity gradients. Trees-Structure and Function. 16 (2-3), 126-139.

Beisner, B. E., Haydon, D. T., Cuddington, K., 2003. Alternative stable states in ecology. Frontiers in Ecology and the Environment. 1 (7), 376-382.

Bekker, M. F., 2005. Positive feedback between tree establishment and patterns of subalpine forest advancement, Glacier National Park, Montana, U.S.A. Arctic, Antarctic, and Alpine Research. 37 (1), 97-107.

Berger, U., Hildenbrandt, H., 2000. A new approach to spatially explicit modelling of forest dynamics: Spacing, ageing and neighbourhood competition of mangrove trees. Ecological Modelling. 132 (3), 287-302.

Berger, U., Rivera-Monroy, V. H., Doyle, T. W., Dahdouh-Guebas, F., Duke, N. C., Fontalvo-Herazo, M. L., Hildenbrandt, H., Koedam, N., Mehlig, U., Piou, C., Twilley, R. R., 2008. Advances and limitations of individual-based models to analyze and predict dynamics of mangrove forests: A review. Aquatic Botany. 89 (2), 260-274.

Boughton, E. A., Quintana-Ascencio, A. F., Menges, E. S., Boughton, R. K., 2006. Association of ecotones with relative elevation and fire in an upland Florida landscape. Journal of Vegetation Science. 17 (3), 361-368.

Briske, D. D., Bestelmeyer, B. T., Stringham, T. K., Shaver, P. L., 2008. Recommendations for development of resilience-based state-and-transition models. Rangeland Ecology & Management. 61 (4), 359-367.

Briske, D. D., Washington-Allen, R. A., Johnson, C. R., Lockwood, J. A., Lockwood, D. R., Stringham, T. K., Shugart, H. H., 2010. Catastrophic thresholds: A synthesis of concepts, perspectives, and applications. Ecology and Society. 15 (3), 37.

Carpenter, S. R., Ludwig, D., Brock, W. A., 1999. Management of eutrophication for lakes subject to potentially irreversible change. Ecological Applications. 9 (3), 751-771.

Castaneda, E., Landscape patterns of community structure, biomass, and net primary productivity of mangrove forests in the Florida coastal Everglades as a function of resources, regulators, hydroperiod, and hurricane disturbance. Department of Oceanography and Coastal Sciences, Vol. Ph.D. Louisiana State University, Eunice, 2010, pp. 171.

Chen, R. G., Twilley, R. R., 1998. A gap dynamic model of mangrove forest development along gradients of soil salinity and nutrient resources. Journal of Ecology. 86 (1), 37-51.

Churkina, G., Svirezhev, Y., 1995. Dynamics and forms of ecotone of under the impact of climatic change: Mathematical approach. Journal of Biogeography. 22 (2/3), 565-569.

Clements, F. E., 1907. Plant physiology and ecology. Henry Holt, New York.

Clymo, R. S., Hayward, P. M., The ecology of Sphagnum. In: A. J. E. Smith, (Ed.), Bryophyte Ecology. Chapman and Hall, London, 1982, pp. 229-289.

Cutini, M., Agostinelli, E., Acosta, T. R. A., Molina, J. A., 2010. Coastal salt-marsh zonation in Tyrrhenian central Italy and its relationship with other Mediterranean wetlands. Plant Biosystems. 144 (1), 1-11.

D'Odorico, P., Engel, V., Carr, J., Oberbauer, S., Ross, M., Sah, J., 2011. Tree–grass coexistence in the Everglades freshwater system. Ecosystems. 14 (2), 298-310.

DeAngelis, D. L., Post, W. M., Travis, C. C., 1986. Positive feedback in natural systems. Springer-Verlag, Berlin.

Doyle, T. W., Girod, G. F., The frequency and intensity of Atlantic hurricanes and their influence on the structure of South Florida Mangrove communities. In: H. F. Diaz, R. S. Pulwarty, Eds.), Hurricane, Climate and Socioeconomic Impact. Springer Verlag, New York, New York, USA, 1997, pp. 55-65.

Doyle, T. W., Girod, G. F., Brooks, M. A., Modeling mangrove forest migration along the southwest coast of Florida under climate change. In: Z. H. Ning, R. E. Turner, T. W. Doyle, K. Abdollahi, Eds.), Integrated Assessment of the Climate Change Impacts on the Gulf Coast Region. GRCCC and LSU Graphic Services, Baton Rouge, LA, 2003, pp. 211-221.

Ehrenfeld, J. G., Ravit, B., Elgersma, K., 2005. Feedback in the plant-soil system. Annual Review of Environment and Resources. 30 (1), 75-115.

Eppinga, M., Rietkerk, M., Wassen, M., De Ruiter, P., 2009. Linking habitat modification to catastrophic shifts and vegetation patterns in bogs. Plant Ecology. 200 (1), 53-68.

Fagan, W. F., Cantrell, R. S., Cosner, C., 1999. How habitat edges change species interactions. The American Naturalist. 153 (2), 165-182.

Folke, C., Carpenter, S., Walker, B., Scheffer, M., Elmqvist, T., Gunderson, L., Holling, C. S., 2004. Regime shifts, resilience, and biodiversity in ecosystem management. Annual Review of Ecology, Evolution, and Systematics. 35, 557-581.

Foster, A. M., Smith III, T. J., Changes in the mangrove/marsh ecotones of the Florida Everglades. 16th Biennial Conference of the Estuarine Research Federation, St. Petersburg, FL, 2001.

Gaiser, E. E., Zafiris, A., Ruiz, P. L., Tobias, F. A. C., Ross, M. S., 2006. Tracking rates of ecotone migration due to salt-water encroachment using fossil mollusks in coastal South Florida. Hydrobiologia. 569, 237-257.

Gao, D., Liang, X., 2007. A competition-diffusion system with a refuge. Discrete Contin. Dyn. Syst. Ser. B, 8, 435-454.

Genkai-Kato, M., Carpenter, S. R., 2005. Eutrophication due to phosphorus recycling in relation to lake morphometry, temperature, and macrophytes. Ecology. 86 (1), 210-219.

Gentle, C. B., Duggin, J. A., 1997. Allelopathy as a competitive strategy in persistent thickets of Lantana camara L. in three Australian forest communities. Plant Ecology. 132 (1), 85-95.

Gilad, E., Shachak, M., Meron, E., 2007. Dynamics and spatial organization of plant communities in water-limited systems. Theoretical Population Biology. 72 (2), 214-230.

Grimm, V., Berger, U., Bastiansen, F., Eliassen, S., Ginot, V., Giske, J., Goss-Custard, J., Grand, T., Heinz, S. K., Huse, G., Huth, A., Jepsen, J. U., Jorgensen, C., Mooij, W. M., Muller, B., Pe'er, G., Piou, C., Railsback, S. F., Robbins, A. M., Robbins, M. M., Rossmanith, E., Ruger, N., Strand, E., Souissi, S., Stillman, R. A., Vabo, R., Visser, U., DeAngelis, D. L., 2006. A standard protocol for describing individual-based and agent-based models. Ecological Modelling. 198 (1-2), 115-126.

Grimm, V., Berger, U., DeAngelis, D. L., Polhill, J. G., Giske, J., Railsback, S. F., 2010. The ODD protocol: A review and first update. Ecological Modelling. 221 (23), 2760-2768.

Grimm, V., Revilla, E., Berger, U., Jeltsch, F., Mooij, W. M., Railsback, S. F., Thulke, H.-H., Weiner, J., Wiegand, T., DeAngelis, D. L., 2005. Pattern-oriented modeling of agent-based complex systems: Lessons from ecology. Science. 310 (5750), 987-991.

Grover, J. P., 1997. Resource competition. Chapman & Hall, London.

Harcombe, P. A., Mann Leipzig, L. E., Elsik, I. S., 2009. Effects of hurricane Rita on three long-term forest study plots in east Texas, USA. Wetlands. 29 (1), 88-100.

Hess, P., 1991. Periodic-parabolic boundary value problems and positivity. Notes in math 247, Longman Scientific and Technical, New York.

Holling, C. S., 1973. Resilience and Stability of Ecological Systems. Annual Review of Ecology and Systematics. 4, 1-23.

Hollins, S. E., Ridd, P. V., Read, W. W., 2000. Measurement of the diffusion coefficient for salt in salt flat and mangrove soils. Wetlands Ecology and Management. 8 (4), 257-262.

Hotes, S., Grootjans, A. P., Takahashi, H., Ekschmitt, K., Poschlod, P., 2010. Resilience and alternative equilibria in a mire plant community after experimental disturbance by volcanic ash. Oikos. 119 (6), 952-963.

Howes, N. C., FitzGerald, D. M., Hughes, Z. J., Georgiou, I. Y., Kulp, M. A., Miner, M. D., Smith, J. M., Barras, J. A., 2010. Hurricane-induced failure of low salinity wetlands. Proceedings of the National Academy of Sciences.

Jiang, J., DeAngelis, D., Smith, T., Teh, S., Koh, H.-L., 2012. Spatial pattern formation of coastal vegetation in response to external gradients and positive feedbacks affecting soil porewater salinity: a model study. Landscape Ecology. 27 (1), 109-119.

Jiang, J., Gao, D., DeAngelis, D. L., In press. Towards a theory of ecotone resilience: coastal vegetation on a salinity gradient. Theoretical Population Biology. In press.

Jiang, J., Tang, F., 2008. The complete classification on a model of two species competition with an inhibitor. Discrete Contin. Dyn. Syst. Ser. A, 20, 659-672.

Keane, R. E., Austin, M., Field, C., Huth, A., Lexer, M. J., Peters, D., Solomon, A., Wyckoff, P., 2001. Tree mortality in gap models: Application to climate change. Climatic Change. 51 (3-4), 509-540.

Kenkel, N. C., McIlraith, A. L., Burchill, C. A., Jones, G., 1991. Competition and the response of 3 plant-species to a salinity gradient. Canadian Journal of Botany. 69 (11), 2497-2502.

Koch, A. J., Meinhardt, H., 1994. Biological pattern formation: from basic mechanisms to complex structures. Reviews of Modern Physics. 66 (4), 1481.

Komiyama, A., Havanond, S., Srisawatt, W., Mochida, Y., Fujimoto, K., Ohnishi, T., Ishihara, S., Miyagi, T., 2000. Top/root biomass ratio of a secondary mangrove (Ceriops tagal (Perr.) C.B. Rob.) forest. Forest Ecology and Management. 139 (1-3), 127-134.

Komiyama, A., Ogino, K., Aksornkoae, S., Sabhasri, S., 1987. Root biomass of a mangrove forest in southern Thailand. 1. Estimation by the trench method and the zonal structure of root biomass. Journal of Tropical Ecology. 3 (02), 97-108.

Komiyama, A., Ong, J. E., Poungparn, S., 2008. Allometry, biomass, and productivity of mangrove forests: A review. Aquatic Botany. 89 (2), 128-137.

Krauss, K., From, A., Doyle, T., Doyle, T., Barry, M., 2011. Sea-level rise and landscape change influence mangrove encroachment onto marsh in the Ten Thousand Islands region of Florida, USA. Journal of Coastal Conservation. 15 (4), 629-638.

Krauss, K. W., Doyle, T. W., Doyle, T. J., Swarzenski, C. M., From, A. S., Day, R. H., Conner, W. H., 2009. Water level observations in mangrove swamps during two hurricanes in Florida. Wetlands. 29 (1), 142-149.

La Peyre, M. K. G., Grace, J. B., Hahn, E., Mendelssohn, I. A., 2001. The importance of competition in regulating plant species abundance along a salinity gradient. Ecology. 82 (1), 62-69.

Lara, R., Szlafsztein, C., Cohen, M., Berger, U., Marion, G., 2002. Implications of mangrove dynamics for private land use in Bragança, North Brazil: A case study. Journal of Coastal Conservation. 8 (1), 97-102.

Larsen, L. G., Harvey, J. W., 2010. How vegetation and sediment transport feedbacks drive landscape change in the Everglades and wetlands worldwide. American Naturalist. 176 (3), E66-E79.

Larsen, L. G., Harvey, J. W., Crimaldi, J. P., 2007. A delicate balance: Ecohydrological feedbacks governing landscape morphology in a lotic peatland. Ecological Monographs. 77, 591-614.

Levin, S. A., 1974. Dispersion and population interactions. The American Naturalist. 108 (960), 207-228.

Levine, J. M., Murrell, D. J., 2003. The community-level consequences of seed dispersal patterns. Annual Review of Ecology, Evolution, and Systematics. 34, 549-574.

Lin, G., Sternberg, L. D. L., 1992. Effect of Growth Form, Salinity, Nutrient and Sulfide on Photosynthesis, Carbon Isotope Discrimination and Growth of Red Mangrove (Rhizophora-Mangle L). Australian Journal of Plant Physiology. 19 (5), 509-517.

Lloyd, K. M., McQueen, A. A. M., Lee, B. J., Wilson, R. C. B., Walker, S., Wilson, J. B., 2000. Evidence on ecotone concepts from switch, environmental and anthropogenic ecotones. Journal of Vegetation Science. 11 (6), 903-910.

Lugo, A. E., 1981. The inland mangroves of Inagua. Journal of Natural History. 15 (5), 845-852.

Macchiato, M. F., Ragosta, M., Cosmi, C., Lo Porto, A., 1992. A method in multivariate statistics to analyze ecosystems starting from their species composition. Ecological Modelling. 62 (4), 295-310.

Malanson, G., 1997. Effects of feedbacks and seed rain on ecotone patterns. Landscape Ecology. 12 (1), 27-38.

Manson, F. J., Loneragan, N. R., Phinn, S. R., 2003. Spatial and temporal variation in distribution of mangroves in Moreton Bay, subtropical Australia: a comparison of pattern metrics and change detection analyses based on aerial photographs. Estuarine, Coastal and Shelf Science. 57 (4), 653-666.

Martin, P. H., Fahey, T. J., Sherman, R. E., 2011. Vegetation zonation in a neotropical montane forest: environment, disturbance and ecotones. Biotropica. DOI: 10.1111/j.1744-7429.2010.00735.x.

Maul, G. A., Martin, D. M., 1993. Sea-level rise at Key-West, Florida, 1846-1992 - america longest instrument record. Geophysical Research Letters. 20 (18), 1955-1958.

May, R. M., 1977. Thresholds and breakpoints in ecosystems with a multiplicity of stable states. Nature. 269 (5628), 471-477.

Milbrandt, E. C., Greenawalt-Boswell, J. M., Sokoloff, P. D., Bortone, S. A., 2006. Impact and response of southwest Florida mangroves to the 2004 hurricane season. Estuaries and Coasts. 29 (6), 979-984.

Murray, J.D., 2003. Mathematical biology II: Spatial models and biomedical applications. Springer-Verlag, Berlin.

Mutch, R. W., 1970. Wildland fires and ecosystems--A hypothesis. Ecology. 51 (6), 1046-1051.

Najjar, R. G., Walker, H. A., Anderson, P. J., Barron, E. J., Bord, R. J., Gibson, J. R., Kennedy, V. S., Knight, C. G., Megonigal, J. P., O'Connor, R. E., Polsky, C. D., Psuty, N. P., Richards, B. A., Sorenson, L. G., Steele, E. M., Swanson, R. S., 2000. The potential impacts of climate change on the mid-Atlantic coastal region. Climate Research. 14 (3), 219-233.

Nicholls, R. J., Cazenave, A., 2010. Sea-level rise and its impact on coastal zones. Science. 328 (5985), 1517-1520.

Nishimura, T. B., Kohyama, T., 2002. Formation and maintenance of community boundaries in a sub-alpine forest landscape in northern Japan. Journal of Vegetation Science. 13 (4), 555-564.

Odion, D. C., Moritz, M. A., DellaSala, D. A., 2010. Alternative community states maintained by fire in the Klamath Mountains, USA. Journal of Ecology. 98 (1), 96-105.

Oosting, H. J., 1955. The study of plant communities: An introduction to plant ecology. W. H. Freeman and Company, San Francisco, California.

Pacala, S. W., Canham, C. D., Saponara, J., Silander, J. A., Kobe, R. K., Ribbens, E., 1996. Forest models defined by field measurements: Estimation, error analysis and dynamics. Ecological Monographs. 66 (1), 1-43.

Passioura, J. B., Ball, M. C., Knight, J. H., 1992. Mangroves may salinize the soil and in so doing limit their transpiration rate. Functional Ecology. 6 (4), 476-481.

Perry, W., 2004. Elements of South Florida's comprehensive everglades restoration plan. Ecotoxicology. 13 (3), 185-193.

Petersen, J. K., Hansen, J. W., Laursen, M. B., Clausen, P., Carstensen, J., Conley, D. J., 2008. Regime shift in a coastal marine ecosystem. Ecological Applications. 18 (2), 497-510.

Pool, D. J., Snedaker, S. C., Lugo, A. E., 1977. Structure of mangrove forests in Florida, Puerto-Rico, Mexico, and Costa-Rica. Biotropica. 9 (3), 195-212.

Rabinowitz, D., 1978a. Dispersal properties of mangrove propagules. Biotropica. 10 (1), 47-57.

Rabinowitz, D., 1978b. Early growth of mangrove seedlings in Panama, and an hypothesis concerning relationship of dispersal and zonation. Journal of Biogeography. 5 (2), 113-133.

Rathcke, B. J., Landry, C. L., Dispersal and recruitment of white mangrove on San Salvador Island, Bahamas after Hurricane Floyd. In: D. L. Smith, S. Smith, Eds.), Proceedings of the ninth symposium on the natural history of the Bahamas, Gerace Research Center, San Salvador, Bahamas, 2003.

Ross, M. S., O'Brien, J. J., Flynn, L. J., 1992. Ecological site classification of Florida Keys terrestrial habitats. Biotropica. 24 (4), 488-502.

Ross, M. S., O'Brien, J. J., Ford, R. G., Zhang, K. Q., Morkill, A., 2009. Disturbance and the rising tide: the challenge of biodiversity management on low-island ecosystems. Frontiers in Ecology and the Environment. 7 (9), 471-478.

Ross, M. S., Ruiz, P. L., Sah, J. P., Reed, D. L., Walters, J., Meeder, J. F., 2006. Early post-hurricane stand development in Fringe mangrove forests of contrasting productivity. Plant Ecology. 185 (2), 283-297.

Saha, A., Moses, C., Price, R., Engel, V., Smith, T., III, Anderson, G., 2012. A hydrological budget (2002–2008) for a large subtropical wetland ecosystem indicates marine groundwater discharge accompanies diminished freshwater flow. Estuaries and Coasts. 35 (2), 459-474.

Saha, A., Saha, S., Sadle, J., Jiang, J., Ross, M., Price, R., Sternberg, L., Wendelberger, K., 2011. Sea level rise and South Florida coastal forests. Climatic Change. 107 (1), 81-108.

Scheffer, M., Carpenter, S., Foley, J. A., Folke, C., Walker, B., 2001. Catastrophic shifts in ecosystems. Nature. 413 (6856), 591-596.

Scheffer, M., Carpenter, S. R., 2003. Catastrophic regime shifts in ecosystems: linking theory to observation. Trends in Ecology & Evolution. 18 (12), 648-656.

Schmitz, N., Verheyden, A., Beeckman, H., Kairo, J. G., Koedam, N., 2006. Influence of a salinity gradient on the vessel characters of the mangrove species Rhizophora mucronata. Annals of Botany. 98 (6), 1321-1330.

Scholes, R. J., Archer, S. R., 1997. Tree-grass interactions in savannas. Annual Review of Ecology and Systematics. 28, 517-544.

Semeniuk, V., 1983. Mangrove distribution in northwestern Australia in relationship to regional and local fresh-water seepage. Vegetatio. 53 (1), 11-31.

Shannon, L. J., Field, J. G., Moloney, C. L., 2004. Simulating anchovy-sardine regime shifts in the southern Benguela ecosystem. Ecological Modelling. 172 (2-4), 269-281.

Shugart, H. H., Emanuel, W. R., West, D. C., DeAngelis, D. L., 1980. Environmental gradients in a simulation model of a beech-yellow-poplar stand. Mathematical Biosciences. 50 (3-4), 163-170.

Shugart, H. H., West, D. C., 1977. Development of an appalachian deciduous forest succession model and its application to assessment of the impact of the chestnut blight Journal of Environmental Management. 5 (2), 161-179.

Siccama, T. G., 1974. Vegetation, soil, and climate on the green mountains of Vermont. Ecological Monographs. 44 (3), 325-349.

Silander, J. A., Antonovics, J., 1982. Analysis of interspecific interactions in a coastal plant community - A perturbation approach. Nature. 298 (5874), 557-560.

Smith, H.L., 1995. Monotone dynamical systems: An introduction to the theory of competitive and cooperative systems. Mathematical surveys and monographs. Providence, RI.

Snyder, J. R., Herndon, A., Robertson, W. B. J., South Florida rockland. In: R. L. Myers, J. J. Ewel, Eds.), Ecosystems of Florida. The University of Central Florida Press, Orlando, 1990, pp. 230-279.

Sousa, W. P., Kennedy, P. G., Mitchell, B. J., Ordonez, B. M., 2007. Supply-side ecology in mangroves: Do propagule dispersal and seedling establishment explain forest structure? Ecological Monographs. 77 (1), 53-76.

Sternberg, L. D. L., Ishshalomgordon, N., Ross, M., Obrien, J., 1991. Water relations of coastal plant-communities near the ocean fresh-water boundary. Oecologia. 88 (3), 305-310.

Sternberg, L. D. L., Teh, S. Y., Ewe, S. M. L., Miralles-Wilhelm, F., DeAngelis, D. L., 2007. Competition between hardwood hammocks and mangroves. Ecosystems. 10 (4), 648-660.

Sternberg, L. D. S. L., 2001. Savanna-forest hysteresis in the tropics. Global Ecology and Biogeography. 10 (4), 369-378.

Sternberg, L. d. S. L., Swart, P. K., 1987. Utilization of freshwater and ocean water by coastal plants of Southern Florida. Ecology. 68 (6), 1898-1905.

Steyer, G. D., Cretini, K. F., Piazza, S., Sharp, L. A., Snedden, G. A., Sapkota, S., 2010. Hurricane influences on vegetation community change in coastal Louisiana. Open-File Report 2010-1105. U.S. Department of the Interior, U.S. Geological Survey.

Stieglitz, T., Ridd, P. V., 2001. Trapping of mangrove propagules due to density-driven secondary circulation in the Normanby River estuary, NE Australia. Marine Ecology-Progress Series. 211, 131-142.

Stoddart, D. R., Bryan, G. W., Gibbs, P. E., 1973. Inland mangroves and water chemistry, Barbuda, West Indies. Journal of Natural History. 7 (1), 33-46.

Stringham, T. K., Krueger, W. C., Shaver, P. L., 2003. State and transition modeling: An ecological process approach. Journal of Range Management. 56 (2), 106-113.

Swain, E. D., Wolfert, M. A., Bales, J. D., Goodwin, C. R., Two-dimensional hydrodynamic simulation of surface-water flow and transport to Florida bay

through the Southern Inland and Coastal Systems (SICS). U.S. Geological Survey Water-Resources Investigations Report 03-4287, 2003.

Teh, S. Y., DeAngelis, D. L., Sternberg, L. D. L., Miralles-Wilhelm, F. R., Smith, T. J., Koh, H. L., 2008. A simulation model for projecting changes in salinity concentrations and species dominance in the coastal margin habitats of the Everglades. Ecological Modelling. 213 (2), 245-256.

Transeau, E. N., 1935. The prairie peninsula. Ecology. 16 (3), 423-437.

Ukpong, I. E., 1991. The performance and distribution of species along soil-salinity gradients of mangrove swamps in southeastern Nigeria. Vegetatio. 95 (1), 63-70.

Ungar, I. A., 1998. Are biotic factors significant in influencing the distribution of halophytes in saline habitats? Botanical Review. 64 (2), 176-199.

Urrego, L. E., Polan, a, J., Buitrago, M. F., Cuartas, L. F., Lema, A., 2009. Distribution of mangroves along environmental gradients on San Andres Island (Colombian Caribbean). Bulletin of Marine Science. 85 (1), 27-43.

van Breemen, N., 1995. How sphagnum bogs down other plants. Trends in ecology & evolution (Personal edition). 10 (7), 270-275.

van Nes, E. H., Scheffer, M., 2005. Implications of spatial heterogeneity for catastrophic regime shifts in ecosystems. Ecology. 86 (7), 1797-1807.

Vilà, M., Lloret, F., Ogheri, E., Terradas, J., 2001. Positive fire–grass feedback in Mediterranean Basin woodlands. Forest Ecology and Management. 147 (1), 3-14.

Volkmar, K. M., Hu, Y., Steppuhn, H., 1998. Physiological responses of plants to salinity: A review. Canadian Journal of Plant Science. 78 (1), 19-27.

Voss, C. I., Provost, A. M., SUTRA, A model for saturated-unsaturated variable-density ground-water flow with solute or energy transport. U.S. Geological Survey Water-Resources Investigations Report 02-4231, 2010, pp. 291.

Walker, S., Wilson, J. B., Steel, J. B., Rapson, G. L., Smith, B., King, W. M., Cottam, Y. H., 2003. Properties of ecotones: Evidence from five ecotones objectively determined from a coastal vegetation gradient. Journal of Vegetation Science. 14 (4), 579-590.

White, I., Falkland, T., 2010. Management of freshwater lenses on small Pacific islands. Hydrogeology Journal. 18 (1), 227-246.

Wiegand, T., Camarero, J. J., Rüger, N., Gutiérrez, E., 2006. Abrupt population changes in treeline ecotones along smooth gradients. Journal of Ecology. 94 (4), 880-892.

Willard, D. A., Bernhardt, C. E., 2011. Impacts of past climate and sea level change on Everglades wetlands: placing a century of anthropogenic change into a late-Holocene context. Climatic Change. 107 (1-2), 59-80.

Williams, K., MacDonald, M., Sternberg, L. d. S. L., 2003. Interactions of storm, drought, and sea-level rise on coastal forest: A case study. Journal of Coastal Research. 19 (4), 1116-1121.

Wilson, A. M., 2005. Fresh and saline groundwater discharge to the ocean: A regional perspective. Water Resources Research. 41 (2), DOI 0.1029/2004wr003399.

Wilson, J. B., Agnew, D. Q., 1992. Positive-feedback switches in plant communities. Advances in Ecological Research. 23, 263-336.

Wu, Y., Rutchey, K., Guan, W., Vilchek, L., Sklar, F. H., Spatial simulations of tree islands for Everglades restoration. In: F. H. Sklar, A. Valk, Eds.), Tree islands of the everglades. Kluwer Academic Publishers, Netherlands, 2003, pp. 552.

Yamamura, N., 1976. A mathematical approach to spatial distribution and temporal succession in plant communities. Bulletin of Mathematical Biology. 38 (5), 517-526.

Zeng, Y., Malanson, G. P., 2006. Endogenous fractal dynamics at alpine treeline ecotones. Geographical Analysis. 38 (3), 271-287.

Zhang, K., Liu, H., Li, Y., Xu, H., Shen, J., Rhome, J., Smith III, T. J., In press. The role of mangroves in attenuating storm surges. Estuarine Coastal and Shelf Science. in press.